Chlamydiaceae and Chronic Diseases: Clinical Implications and Host-Cell Gene Expression in a Model of Interferon-γ-Induced Persistence

Thesis in partial fulfillment of the requirements for the
doctoral degree of the natural sciences
Dr. rer. nat.

Faculty of Biology, University of Hamburg

presented by
Dipl.-Biochem. Meike Eickhoff
born 27.08.1976 in Lübeck

Hamburg 2006

Genehmigt vom Department Biologie
der Fakultät für Mathematik, Informatik und Naturwissenschaften
an der Universität Hamburg
auf Antrag von Herrn Professor Dr. J. KRUPPA
Weiterer Gutachter der Dissertation:
Herr Professor Dr. U. WIENAND
Tag der Disputation: 05. Mai 2006

Hamburg, den 16. April 2006

Universität Hamburg
64
Fakultät
Mathematik, Informatik und Naturwissenschaften

Professor Dr. Reinhard Lieberei
Leiter des Departments

The doctoral thesis was conducted at the Department of Research and Development, QIAGEN Hamburg GmbH (formerly artus GmbH), Königstrasse 4a, 22767 Hamburg, Germany under the supervision of Thomas Laue.

Examiner:

1. **Prof. Dr. rer. nat. Joachim Kruppa**, Center of Experimental Medicine, Institute of Molecular Cell Biology, Universitätsklinikum Hamburg-Eppendorf, Martinistraße 52, 20246 Hamburg, Germany
2. **Prof. Dr. rer. nat. Udo Wienand**, Biocenter Klein Flottbek and Botanical Garden, Institute of Molecular Biology of the Plant, University of Hamburg, Ohnhorststrasse 18, 22609 Hamburg, Germany

Disputation: Hamburg, 05.05.2006

1. Contents

2. Acknowledgements

I would like to thank Professor Dr. Joachim Kruppa, Thomas Laue and Thomas Grewing for giving me the opportunity to carry out my thesis work at the Institute of Molecular Cell Biology (University of Hamburg) and the Department of Research and Development (QIAGEN Hamburg GmbH). It was a highly interesting and challenging task.

I also would like to express my gratitude to Professor Dr. Udo Wienand, who kindly agreed on being my co-examiner. Many thanks also to Dr. P. Scheinert and Dr. A. Hanne for the many helpful discussions about RNA amplification and Northern blot analysis to broaden my understanding of these techniques.

During my thesis work, I had the opportunity to do some research in cooperation with the Department of Medical Microbiology, Medical School Hannover. My deepest gratitude goes to Professor Dr. Andreas Klos for guiding me through the project with enthusiastic support and positive coaching.

Finally, I would like to thank my parents for their constant support and care throughout the years. I will always be grateful to them for their love, care and trust.

3. Key Words

Chlamydia, C. trachomatis, *C. pneumoniae*, real-time PCR, persistence, gamma interferon, gene expression, host-cell interaction, RNA amplification, microarray, aRNA

4. Abbreviations

Å	Ångstrom (10-8 cm)
ADP	adenosine diphosphate
AMP	adenosine monophosphate
aRNA	amplified antisense RNA
ATCC	American Type Culture Collection
ATP	adenosine triphosphate
ATPase	adenosine triphosphatase
bp	base pair
BSA	bovine serum albumin
C. pneumoniae	*Chlamydophila pneumoniae*
C. trachomatis	*Chlamydia trachomatis*
cAMP	cyclic AMP
cDNA	complementary DNA
CFU	colony-forming unit
Ci	curie(s)
cop/µl	copies per microliter
cop/ml	copies per milliliter
cpm	counts per minute
cps	counts per second
CTP	cytidine triphosphate
cycle/min	cycle(s) per minute
cycle/s	cycle(s) per second
D	Dalton
DEAE	diethylaminoethyl
dIVT	double *in vitro* transcription
DMEM	Dulbecco's modified Eagle's medium
DMSO	dimethyl sulfoxide
DNA	deoxyribonucleic acid
DNase	deoxyribonuclease
dNTP	deoxyribonucleoside triphosphate
dsDNA	double-stranded DNA
DTT	dithiothreitol
EB	Elementary body
EDTA	ethylenediaminetetraacetic acid
ELISA	enzyme-linked immunosorbent assay
EM	electron microscopy
FACS	fluorescent-activated cell sorter
FBS	fetal bovine serum
FCS	fetal calf serum
FITC	fluorescein isothiocyanate
GTP	guanosine triphosphate
GUS	β-glucuronidase
Hepes	N-2-hydroxyethylpiperazine-N'-ethane sulfonic acid
HPLC	high performance liquid chromatography
Hsp	heat shock protein

Ig	immunoglobulin
Inc	inclusion membrane protein
INF-γ	Interferon gamma, gamma interferon
IU	international unit(s)
IVT	*in vitro* transcription
kb	kilobase(s)
kbp	kilobase pair(s)
kD	kilodalton(s)
kIPS	kiloimpulse per second
LB medium	Luria-Bertani medium
LGV	Lymphogranuloma venerum
liter(s)	liter(s)
LPS	lipopolysaccharide
Mb	megabases
MEM	Eagle's minimum essential medium
MOI	multiplicity of infection
mol	mole(s)
mol wt	molecular weight
MOMP	major outer membrane protein, translation product of *ompA*
Mr	relative molecular mass
mRNA	messenger RNA
n	number in a study or group
NCBI	National Center for Biotechnology Information
ND	not determined
No.	number
NS	not significant
OD	optical density
Oligo	oligonucleotide
OMP	outer membrane proteins
ORF	open reading frame
P	probability
p.i.	post infection
PBS	phosphate-buffered saline
PCR	Polymerase chain reaction
PMPs	polymorphic outer membrane proteins
r	correlation coefficient
RB	Reticulate body
RFLP	Restriction Fragment Length Polymorphism
RNA	ribonucleic acid
RNase	ribonuclease
RNP	ribonucleic protein
rpm	revolutions per minute, rounds per minute
rRNA	ribosomal ribonucleic acid
RT	reverse transcription
s	second(s)
SD	standard deviation
SDS	sodium dodecyl sulfate

sec.	second(s)
SEM	standard error of the mean
ssDNA	single-stranded DNA
STD(s)	sexually transmitted disease(s)
TAE	Tris-Acetate-EDTA
Taq	Thermus aquaticus
TBP	TATA-Box binding protein
TBS	Tris buffered saline
TE	Tris-EDTA
Th1	T-helper lymphocyte, type 1
Tm	melting temperature
Tris	tris (hydroxymethyl) aminomethane
tRNA	transfer RNA
t-test	Student's t test
U	unit
UDP	uridine diphosphate
UV	ultraviolet
V	volt
Vers.	Version
vol	volume
W	watt

5. Summary

Bacteria of the family *Chlamydiaceae* are obligate intracellular parasites of eukaryotic cells. Coronary artery disease and cerebro-vascular stroke are the most common causes of death worldwide. Chronic diseases like adult-onset asthma or atherosclerosis and trachoma are increasingly attributed to *C. pneumoniae* and *C. trachomatis*, respectively. Persistence of these organisms in its respective host is suspected to be the cause of these chronic diseases. In its persistent form, *Chlamydiaceae* most probably remain in a viable but culture-negative state, in which chlamydicidal drugs are apparently not effective. An improved understanding of the persistence mechanisms will be critical for the development of innovative therapeutic strategies to effectively treat chlamydially induced chronic diseases.

In this thesis, the human pathogens *C. trachomatis* and *C. pneumoniae*, representing the two genera of the family *Chlamydiaceae*, were chosen to investigate their interrelationship with the host. To gain a better molecular understanding of the interaction between pathogen and host-cells, a comparative analysis of the gene expression pattern of HeLa-cells after active and IFN-γ-induced persistent infection with *C. pneumoniae* was performed using Affymetrix® microchips (HG-U133A). Over 360 human genes were identified with changes in their expression level after chlamydial infection. In 66 of these genes, the mRNA levels were in both experimental conditions up- and down regulated by at least a factor of 2.5. These results were verified by a detailed real-time PCR analysis of 19 selected genes. With one exception the pattern of expression was confirmed in all identified genes showing one group of permanently activated and another group of permanently down-regulated genes. In both cases, the alterations varied by factors from 2 to 10. The identified genes are involved in cell communication, response to biotic stimuli, host-cell metabolism, and apoptosis. It is assumed that similar changes might also take place in persistently infected host-cells *in situ* as part of the pathogenesis mechanism.

The step towards *in situ* monitoring is often impeded by too small amounts of sample material. Traditional RNA amplification methods, based on the Eberwine protocol, are often self-limiting due to 3'-biased amplified RNA. Therefore, a new technique to linearly amplify RNA was established for the persistence studies of *C. pneumoniae*. RNA from HeLa-cells, isolated 96h after IFN-γ-induced persistence, was analyzed by Affymetrix® microchips starting with 2.5 µg versus 10 ng of total RNA, which had been isolated by two different methods (IVT and dIVT). These results clearly indicate that the linear RNA amplification is the method of choice for *C. pneumoniae* gene expression studies *in vivo* in which sample amounts are limiting.

New diagnostic tools will be necessary for sensitively detecting *Chlamydiaceae* during all stages of their developmental cycle and for monitoring chlamydicidal drug therapy. In this thesis, quantitative as well as qualitative CE-marked real-time PCR assays, detecting *C. trachomatis* DNA from swab, urine and sperm samples, were developed. The quantitative assays are based on the specific amplification and detection of an *ompA* gene segment allowing for improved bacterial load monitoring. The up to 10-fold more sensitive qualitative assays combine both, detection of the genome and of the chlamydial cryptic plasmid. The qualitative assays greatly improve the ability to diagnose chlamydial infections, even in species lacking the cryptic plasmid.

The newly developed diagnostic tools and the establishment of an experimental design using linear RNA amplification technique permit the change from *in vitro* to *in vivo* chlamydial gene expression studies. The established technique will broaden our understanding of *Chlamydiaceae*'s persistence mechanism and advance our knowledge of how *Chlamydiaceae* participate in the pathogenesis of chronic diseases.

6. Zusammenfassung

Bakterien der Familie *Chlamydiaceae* sind obligat intrazelluläre Parasiten eukaryotischer Zellen. Die koronare Herzkranzgefässerkrankung (KHK) und der ischämische Schlaganfall gehören weltweit zu den häufigsten Todesursachen. Chlamydien werden zunehmend mit chronischen Erkrankungen wie Bronchialasthma bei Erwachsenen und Atherosklerose im Falle von *C. pneumoniae* oder dem Trachom bei *C. trachomatis* assoziiert. Dies verstärkt den Verdacht, dass Chlamydien für mehrere Jahre in ihrem Wirt persistieren können und dadurch chronische Erkrankungen auslösen. Im Status der Persistenz liegen die Bakterien metabolisch und morphologisch verändert vor, sind nicht kultivierbar und scheinen mit heutigen Medikamenten nicht therapierbar zu sein. Um durch Chlamydien hervorgerufene chronische Erkrankungen behandeln und heilen zu können, wird die Entwicklung eines tieferen Verständnisses für den Ablauf und die Mechanismen der Persistenz erforderlich sein. In dieser Arbeit wurden die beiden human-pathogenen Erreger *Chlamydia trachomatis* und *Chlamydophila pneumoniae* stellvertretend für die beiden Genera (*Chlamydia* und *Chlamydophila*) der Familie der *Chlamydiaceae* untersucht.

Um die Pathogenese besser zu verstehen und um Ansatzpunkte für mögliche Therapien chlamydialer Erkrankungen zu schaffen, wurden in dieser Arbeit Affymetrix® Microarrays (HG-U133A) verwendet und die Genexpression von epithelialen HeLa-Zellen nach Infektion mit *C. pneumoniae* vergleichend analysiert. Es konnten dabei über 360 Wirtszell-Gene gefunden werden, deren Expression sich nach chlamydialer Infektion veränderte. Bei 66 davon kam es zu einer mittleren oder starken Regulation (Faktor 2 bis 10-fach). Zusätzlich wurde für eine Überprüfung der in den Arrays gewonnen Ergebnissen eine Auswahl von 19 Genen durch real-time PCR detailliert analysiert. Bis auf eine Ausnahme konnten alle gefundenen Genregulationen bestätigt werden. Diese ließen sich in zwei Hauptgruppen einordnen: permanent aktivierte und permanent herunterregulierte Gene. Ähnliche Änderungen in der Wirtszell-Genexpression sind auch als Teil der Pathogenese bei persistierenden Chlamydieninfektion *in situ* denkbar.

Der Wechsel von *in vitro* zu *in vivo* Modellen gestaltet sich jedoch schwierig, da für Microarray Untersuchungen nicht genügend Untersuchungsmaterial zur Verfügung steht. Herkömmliche RNA Amplifikationsmethoden, die auf dem James Eberwine Verfahren basieren, sind oft selbstlimitierend durch unvollständig amplifizierte RNA. Ein Teilprojekt dieser Arbeit war es deshalb, den Einsatz einer neuen linearen RNA Amplifikationstechnik für *C. pneumoniae* Persistenz-Studien zu überprüfen. Dafür wurde RNA aus HeLa-Zellen nach 96h INF-γ Persistenzinduktion mit Affymetrix® Microarrays analysiert. Bei dem

Versuchsansatz wurden zwei RNA Ausgangskonzentrationen (2,5 µg und 10 ng) und zwei verschiedene Präparationsverfahren (IVT und dIVT) miteinander verglichen. Das Ergebnis unterstreicht den Einsatz von linearen Amplifikationsverfahren bei *C. pneumoniae* Genexpressionsstudien *in vivo*, da zwischen hohen und niedrigen RNA Konzentrationen, wie sie den Ausgangskonzentrationen in Zellkultur-Experimenten im Vergleich zu *in vivo* Modellen entsprechen, hervorragende Korrelationen erzielt werden konnten (im Mittel 95%).
Zusätzlich sind neue diagnostische Anwendungsverfahren notwendig, die es erlauben, Chlamydien während ihres gesamten Entwicklungszyklus hoch sensitiv nachzuweisen und damit den Therapieverlauf zu überwachen. Im Rahmen dieser Arbeit wurden CE-markierte qualitative und quantitative real-time PCR Assays für den Nachweis von *C. trachomatis* DNA aus Abstrich-, Urin- und Sperma-Proben entwickelt. Die quantitativen Assays basieren auf der spezifischen Amplifikation und Detektion eines Abschnitts des chlamydialen Genoms (*ompA* Gen). Sie ermöglichen eine genaue und sensitive Messung der Bakterienlast während der Therapie. Die qualitativen Assays verbinden die hohe Sensitivität eines Nachweises basierend auf dem kryptischen Plasmid mit der hohen Spezifität einer Genom-basierenden PCR. Aus diesem Grund eignen sich die bis zu zehnfach sensitiveren qualitativen Assays für routinemäßige Vorsorgeuntersuchungen, die es erlauben, chlamydiale Infektionen, einschliesslich Plasmid-freier Varianten, schon im Frühstadium zu diagnostizieren.
Neu entwickelte Nachweisverfahren und die Etablierung einer Methodik zur Nutzung linearer RNA Amplifikation für chlamydiale Genexpressionsstudien ermöglichen den Wechsel von *in vitro* zu *in vivo* Modellen. Dieser Wechsel wird helfen, die heutigen Kenntnisse über Persistenzmechanismen und den Anteil der *Chlamydiaceae* an chronischen Erkrankungen deutlich zu erweitern.

7. Introduction

Interactions between bacteria of the family of *Chlamydiaceae* and their human host-cells were examined. Since Henle-Koch's postulate in 1884 (refined and published by Robert Koch in 1890) a causal relationship between a parasite and a disease was established. Scientists began to examine and to fight these parasites. New techniques including targeted genetic changes of parasites have improved the analysis of bacteria host-cell interaction and the caused diseases in recent years. For example, by knocking-out and switching-on of specific parasite genes, the gene function can be determined. For *Chlamydiaceae*, scientific genetic changes fail because of the unique chlamydial biphasic developmental cycle. To obtain a better understanding of chlamydial host-cell interactions *Chlamydia*-induced altered host-cell gene expression were analyzed by microarray screening and real-time PCR.

Bacteria of the family *Chlamydiaceae* are obligate intracellular parasites of eukaryotic cells. The family *Chlamydiaceae* includes two human pathogens: *Chlamydia* (*C.*) *trachomatis* and *C. pneumoniae*. *C. abortus* and *C. psittaci* can also cause infections in humans but true hosts are ruminants for *C. abortus* and birds, muskrats and cattle for *C. psittaci*. Therefore, *C. trachomatis* and *C. pneumonia*e were chosen as representatives for the family *Chlamydiaceae*.

Chlamydiaceae can be associated with chronic diseases such as atherosclerosis where *Chlamydia* is seemingly present in a persistent form in which this organism remains in a viable but culture-negative state. The improved understanding of persistence mechanisms underlying chlamydial diseases will be critical for the development of more targeted therapeutic strategies using chlamydicidal drugs even effective against persistent infection. Taking this importance of persistence into account analysis of *Chlamydia*-induced altered host-cell gene expression was carried out using acute and persistently infected human cells.

Currently, cells used in microarray studies often come from cell cultures with addition of persistence inducing agents like gamma interferon (IFN-γ). *In vivo* models have great potential for advancing our knowledge of persistence processes, but are often complicated by small amounts of sample material. To allow changing from *in vitro* to *in vivo* models part of this thesis was devoted to prove the usage of linear amplification technique of small sample RNA (10 ng), for subsequent use in microarray analysis.

7.1 HISTORY

Between 1929 and 1930, widespread outbreaks of an atypical and severe pneumonia, termed psittacosis, occurred. These outbreaks, acquired from psittacine birds (parrots etc), led to the description of minute basophilic particles in Giemsa stained blood and tissue from the infected birds and human patients. Bedson et al. proved the etiological relationship of these particles to psittacosis (Bedson, 1950) and went on to characterize the developmental cycle that defines all members of the order *Chlamydiales* (Bedson and Gostling, 1954).

That *Chlamydiaceae* were not viruses became evident in 1965 with the advent of tissue culture techniques and electron microscopy. Shortly after Moulder (Moulder, 1966) definitively reported the bacterial nature of *Chlamydiae* in 1966, the genus *Chlamydia* was established (Page, 1966) and divided into two species, *Chlamydia trachomatis* and *Chlamydia psittaci* (Page, 1968). *Chlamydia pneumoniae* (Grayston, 1989b) and *Chlamydia pecorum* (Fukushi and Hirai, 1992), formerly known as strains of *C. psittaci*, were designated as distinct species in 1989 and 1992, respectively. More recently, new molecular diagnostic methods based on nucleic acid amplification led to the association of *Chlamydia* with diseases of previously unknown etiology (arthritis, Alzheimer disease, coronary artery disease, etc.). More than 40 chlamydial strains were deposited in the American Type Culture Collection (ATCC). New environmental *Chlamydiae* were also discovered across a wide range of animal phyla. The new molecular knowledge led to a new taxonomy (Figure 1) that added three new Non-*Chlamydiaceae* families (*Parachlamydiaceae*, *Waddliaceae* and *Simkaniaceae*), increased the number of species in the family *Chlamydiaceae* to nine, and groups these species into two genera, *Chlamydia* and *Chlamydophila* (Everett *et al.*, 1999). However, this issues continues to be heavily debated (Schachter *et al.*, 2001). In this thesis (except introduction), the old nomenclature is used for *Chlamydia trachomatis* and *Chlamydia pneumoniae*.

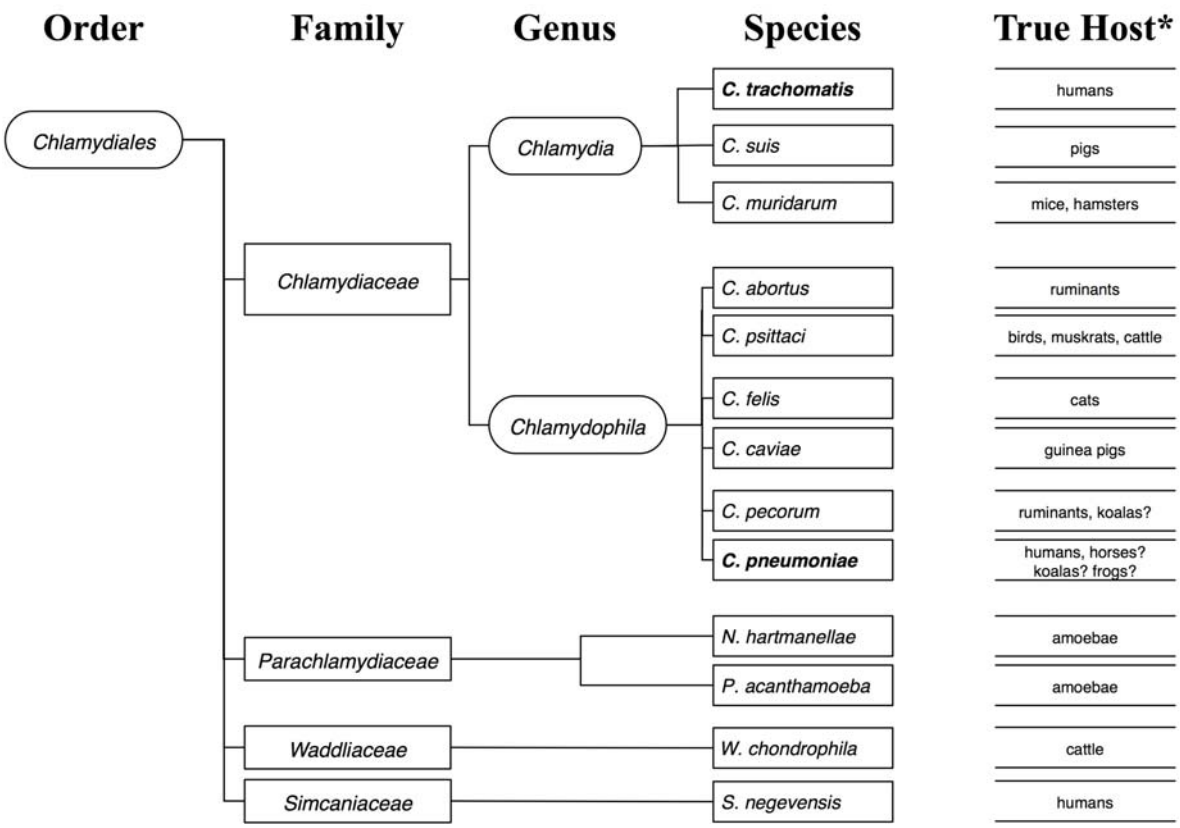

*A true host is infected in nature, supports multiplication of the pathogen and releases its progeny to infect more individuals of the same host species.

Figure 1: Taxonomy of the order *Chlamydiales*. The classification of Everett *et al*. is used (Everett *et al.*, 1999).

7.2 TAXONOMY AND PATHOGENESIS OF THE *CHLAMYDIACEAE*

Many *Chlamydiaceae* coexist in an apparently asymptomatic state within host-cells, which probably act as a natural reservoir for them. *Chlamydiaceae* are found within the cells of vertebrates, while similar particles have been reported in invertebrate species including coelenterates, arthropods and mollusks. Members of the *Chlamydiales* share greater than 80% sequence identity for the 16S ribosomal rRNA (ribosomal ribonucleic acid) gene and/or greater than 80% identity for the gene encoding their 23S rRNA (Everett *et al.*, 1999). Based on these findings, five new species were validated in April 1999: *C. suis*, *C. muridarum* (formerly *C. trachomatis*), *C. caviae*, *C. felis* and *C. abortus* (formerly *C. psittaci*). In addition, *C. pneumoniae*, *C. pecorum* and *C. psittaci* were moved from the genus *Chlamydia* to the genus *Chlamydophila*.

The genus *Chlamydophila* shows genetic and protein sequence differences with the genus *Chlamydia*, does not produce detectable glycogen, and only has one ribosomal operon (*Chlamydia* spp. have two). Chlamydial strains and species have varying inclusion morphology and variable probabilities of having an extrachromosomal plasmid or

sulfadiazine resistance. All species of the *Chlamydiaceae* are Gram-negative and express the family-specific lipopolysaccharide epitope. The *Chlamydiaceae* have a distinctive, biphasic developmental cycle for their replication (see chapter **Life cycle)**. A complex of disulfide-crosslinked envelope proteins that include the 40-kDa major outer membrane protein (MOMP, a translation product of *ompA*), a hydrophilic cysteine-rich 60-kDa protein and a low-molecular mass cysteine-rich lipoprotein maintain the extracellular osmotic stability of the *Chlamydiaceae* elementary bodies (EBs). During chlamydial infection, the disulfide-crosslinks within and among these envelope proteins become chemically reduced, allowing transformation of EBs into intracellular reticulate bodies (RBs). *Chlamydiaceae* have little or no detectable peptidoglycan and no transfer RNA (tRNA) in the 16S-23S-rRNA intergenic spacer.

7.2.1 Genus *Chlamydia*

7.2.1.1 Chlamydia trachomatis

Chlamydia trachomatis is an intracellular bacterial pathogen that functions as an etiologic agens of important human diseases. Depending on transmission route and age of the patient, *Chlamydia trachomatis* causes infections of the eyes, lungs, or urogenital (urinary-genital) area, as well as chronic arthritis in both sexes (for a review, see reference Inman *et al.*, 2000). It remains a significant cause of infectious, preventable blindness (trachoma) in the developing world (Weinstock *et al.*, 1994) and is one of the most common causes of sexually transmitted diseases (STDs), although the majority of infected persons are not aware of it because *Chlamydia* infections are often asymptomatic. *C. trachomatis* infections may spread to the upper reproductive tract, including the uterus, fallopian tubes and ovaries. Scarring of the fallopian tubes may cause permanent damage to the reproductive system, resulting in infertility or life-threatening tubal pregnancy (Weinstock *et al.*, 1994).

The first indication of chlamydial genital tract infections was reported in 1910, when Heyman claimed to have observed in genital tract material the trachoma inclusions that described Halberstaedter and von Prowazek in trachoma 1907 (Halberstaedter and Prowazek, 1907). The first isolation of *Chlamydia* from the genital tract was reported by Jones et al. (Jones *et al.*, 1959), using the embryonated hen's egg, a technique which had been first used by T'ang et al. (T'ang *et al.*, 1957) for trachoma. *C. trachomatis* strains are generally sensitive to sulfadiazine and tetracyclines.

C. trachomatis is comprised of two human biovars: the trachoma and lymphogranuloma venereum (LGV). The trachoma biovar currently has 14 serovars A to K, including Ba, Da and Ia, and one genovariant Ja. The infection is limited primarily to epithelial cells of mucous membranes. It has also been detected in posterior bilaminar tissue removed from patients with disease of the temporomandibular joint. Chlamydial strains belonging to the serovars A, B, Ba or C are usually called ocular serovars. They cause trachoma, a chronic conjunctivitis. Trachoma is one of the world's leading causes of preventable blindness. Another eye infection caused by *C. trachomatis* is neonatal conjunctivitis. Usually the infection is derived from the mother's genital tract at birth, in which case the causative organism are the genital serovars D to K of *C. trachomatis*.

The LGV biovar consists of four serovars, L1, L2, L2a and L3, which can invade lymphatic tissue and cause systemic diseases. The LGV serovars are the causative agents of Lymphogranuloma venereum (LGV), an uncommon form of sexually transmitted disease. The distribution of LGV is worldwide, but most notably in India, Africa and South East Asia. Strains in the LGV biovar are characterized in the laboratory by their ability to grow in cell culture without the need for centrifuge-assisted infection or for pre-treatment of host-cells with polycations. They also show faster and more vigorous growth in cell culture.

C. trachomatis strains have a high degree of sequence conservation in the genes that have been characterized (e.g. 16S rRNA genes differ by < 0.65%). The genome of *C. trachomatis* consists of a circular chromosome of 1.045 Mb and a conserved cryptic plasmid, which is approximately 7.5 kb in size and is present in multiple copies (5-10) in the organism. The complete gene sequences of two strains have been sequenced: D/UW-3/CX (1,042,519 bp) and L2/434/BU (1,038,680 bp). Complete sequences of D/UW-3/CX and L2/434/BU as well as partial sequence information of other strains can be found at the homepage of the "Chlamydia Genome Project" (http://chlamydia-www.berkeley.edu:4231/index.html). *Chlamydia* species are readily identified and distinguished from other species by comparison of ribosomal gene sequences that have been designated as 'signature sequences' (Everett *et al.*, 1999) or by inspection of the 16S–23S rRNA intergenic spacer (Everett and Andersen, 1997).

The gene for the major outer membrane protein (MOMP), *ompA* or *omp1*, is widely used to distinguish *C. trachomatis* strains by both DNA amplification techniques and serotyping. The cryptic plasmid has practical importance as the favored target for nucleic acid amplification technologies, since the use of this multi-copy gene improves the possibility to detect infected patients. However, a few isolates of *C. trachomatis* have been described that do not contain

the plasmid. In addition, it was shown that the cryptic plasmid is not necessary for the survival and the replication of *Chlamydia* (Miyashita *et al.*, 2001; Matsumoto *et al.*, 1998; Stothard *et al.*, 1998; Farencena *et al.*, 1997; An and Olive, 1994). All plasmids from human *C. trachomatis* isolates are extremely similar, with less than 1% nucleotide sequence variation. All are about 7,500 nucleotides in size, with eight open reading frames computer-predicted to code for proteins of more than 100 amino acids, with short non-coding sequences between some of them only. All chlamydial plasmids have four 22 base pair tandem repeats in the intergenic region between ORFs 1 and 8, plus AT rich clusters upstream of this region and an inverted repeat. Part of this thesis was the developing of an accurate, reliable and easy-to-use diagnostic assay using real-time PCR, capable of detecting all *C. trachomatis* strains, including those that do not express the cryptic plasmid.

7.2.1.2 Chlamydia suis

In 1994 a chlamydial isolate named S45 was identified in apparently healthy pigs. It had characteristics resembling *Chlamydia trachomatis* like sulfadiazine sensitivity (Storz *et al.*, 1994), although some strains were resistant to sulfadiazine and/or tetracycline. Therefore, it was classified as *C. trachomatis*. Sequencing studies on *ompA* indicated that this isolate was closer to *C. muridarum* than to *C. trachomatis*. Given differences in host tropism and in the sequence of the gene encoding 16S rRNA, S45 has in 1999 officially reclassified as *Chlamydia suis* (Everett *et al.*, 1999). Several strains of *C. suis* are known to have an extrachromosomal plasmid, pCS.

Up to now *C. suis* has only been isolated from swine, where it causes conjunctivitis, enteritis, pneumonia and asymptomatic infection. DNA hybridization, RFLP and nucleotide sequence studies on porcine lung and intestine samples showed a high prevalence of mixed infections with *Chlamydophila abortus* and *Chlamydia suis (Hoelzle et al., 2000)*. Considering the close relationship of *C. suis* to *C. trachomatis*, it is alarming that tetracycline resistant *C. suis* strains have emerged (Lennart J. *et al.*, 2001). The resistant strains could grow in tetracycline concentrations up to 4 μg/ml, whereas sensitive *C. suis* strains and most human *C. trachomatis* strains are sensitive to about 0.1 μg/ml. Both *C. suis* and *C. trachomatis* were capable of growing together in the same inclusion. To discover new targets for drug therapy before emerging of tetracycline resistant *C. trachomatis* strains is still a major focus in chlamydial science. The analysis of chlamydial life cycle including persistence state seems to be the best way to fit this needs.

7.2.1.3 Chlamydia muridarum

C. muridarum is a species reclassified in 1999 out of the former mouse pneumonitis biovar of *C. trachomatis* (Everett *et al.*, 1999). Two strains of *C. muridarum*, MoPn and SFPD have been isolated from mice and hamsters. MoPn infection produces pneumonia in mice and is sensitive to sulfadiazine. It has an extrachromosomal plasmid, pMoPn. SFPD is an enteric isolate. *C. muridarum* is used to establish experimental infections in mice that mimic *C. trachomatis* infections in humans.

7.2.2 Genus *Chlamydophila*

7.2.2.1 Chlamydophila abortus

Chlamydophila abortus (formerly *Chlamydia psittaci*) is one of the most important causes of abortion and weak neonates with isolates found in sheep, cattle and goats (e.g. strains B577, EBA, OSP, S26/3 and A22). Chlamydial abortion has been described worldwide for sheep (Storz, 1971) as well as for goats (Appleyard *et al.*, 1983; Jain *et al.*, 1975; McCauley and Tieken, 1968). Chlamydial strains causing abortion in goats are thought to be similar to abortion strains in sheep. The first report of enzootic abortion in sheep was 1936 by Grieg (Grieg, 1936). The etiological agent was identified 1950 by Stamp (Stamp *et al.*, 1950). *C. abortus* strains are endemic among ruminants and efficiently colonize the placenta (Rodolakis *et al.*, 1989; Rodolakis and Souriau, 1989). They have a distinctive serotype and nearly 100% conservation of ribosomal and *ompA* sequences. *C. abortus* is the reference strain for determining whether a new strain belongs to the *Chlamydiaceae* (16S or 23S rRNA should be > 90% identical to the *C. abortus* genes). An extrachromosomal plasmid has not been identified in any strain of *C. abortus*.

Infection with *C. abortus* has also been associated with abortion and severe respiratory disease in humans. Human infection can result from contact with infected goats (Pospischil *et al.*, 2002; Villemonteix *et al.*, 1990) and/or sheep (Jorgensen, 1997; Herring *et al.*, 1987). The incidence of this animal-acquired infection is not known, but goats and sheep infected with *C. abortus* strains represent an important potential risk to pregnant women to have spontaneous abortions following exposure to sheep infected with *Chlamydiae* (McKinlay *et al.*, 1985). Furthermore, inhalation of infected material from sheep might also result in human abortion or chlamydial respiratory disease in non-pregnant humans (Mare, 1994).

7.2.2.2 Chlamydophila psittaci

C. psittaci generally infects birds, often systemic. Infections can be acute, severe, asymptomatic or chronic with smooth transitions. Severe stages result in rapid health deterioration and death. Most organs become infected, as well as the conjunctiva, respiratory system and gastrointestinal tract. It can also be passed in the eggs. *C. psittaci* strains belong to eight known serovars. All seems to be readily transmissible to humans. *C. psittaci* serovar A is endemic among psittacine birds and has caused zoonotic disease in tortoises and mammals, including humans. Serovar B is endemic among pigeons. Serovars C and D are job-related hazards for slaughterhouse workers and for people in contact with birds. Serovar E isolates (known as Cal-10, MN or MP) have been obtained from a variety of avian hosts worldwide. The M56 and WC serovars were isolated from mammals. Several *C. psittaci* strains have an extrachromosomal plasmid.

7.2.2.3 Chlamydophila felis

C. felis (formerly *C. psittaci*) is endemic among house cats worldwide. It primarily causes inflammation of feline conjunctiva, rhinitis (Schachter, 1989; Gaillard *et al.*, 1984; Ostler *et al.*, 1969) and pneumonia. It can be recovered from the stomach and reproductive tract. *C. felis* was first isolated from cats affected by pneumonia by Baker in 1944 (Baker, 1944). Some strains have an extrachromosomal plasmid (FP Pring and FP Cello). An attenuated FP Baker strain is used as a live vaccine for cats. For a recent review see: Ramsey, 2000.

The disease caused by *C. felis* is probably transmitted via infected aerosols and secretions. If left untreated, infection will clear. Infection with *C. felis* has also been associated with atypical pneumonia and acute or chronic conjunctivitis in humans. Schachter *et al*. described a case of acute follicular conjunctivitis in the owner of several infected cats (Schachter *et al.*, 1969), Hartley *et al.* a case of chronic conjunctivitis where isolates of *C. felis* from the human and family cat were apparently identical (Hartley *et al.*, 2001). Other reports indicate that *C. felis* infections from cats can cause systemic infection in humans, including endocarditis and glomerulonephritis (Regan *et al.*, 1979). *C. felis* infection should be suspected in humans if acute follicular conjunctivitis or atypical pneumonia develops 1-3 weeks after exposition to an infected cat.

7.2.2.4 Chlamydophila caviae

C. caviae (formerly *C. psittaci*) strains are closely related and clearly specific for guinea pigs as the natural host. The basis for this host specificity is not known. Naturally occurring chlamydial agents were isolated from the conjunctiva of guinea pigs being the usual site of infection (Ahmad *et al.*, 1977; Kazdan *et al.*, 1967; Gordon *et al.*, 1966; Murray, 1964). *C. caviae* infects mainly the mucosal epithelium and is not invasive. There are five known *C. caviae* isolates. The *ompA* sequences of these isolates are almost identical. The strain GPIC contains an extrachromosomal plasmid, pCpGP1.

The guinea pig is an important experimental model of chlamydial genital tract infection in humans (Mount *et al.*, 1973). Guinea pigs with primary conjunctivitis develop immunity to reinfection of the eyes or the genital tract (Ahmad *et al.*, 1977; Mount *et al.*, 1973).

7.2.2.5 Chlamydophila pecorum

The species *Chlamydia pecorum* has been renamed *Chlamydophila pecorum* in 1999 (Everett *et al.*, 1999). In general, *C. pecorum* strains are non-invasive in a mouse model of virulence (Rodolakis *et al.*, 1989) and are serologically and pathogenically diverse (Kaltenboeck *et al.*, 1992). *C. pecorum* has been isolated only from mammals, including: cattle, sheep and goats (Fukushi and Hirai, 1992), koala (Girjes *et al.*, 1993a; Girjes *et al.*, 1993b) and swine (Anderson *et al.*, 1996; Kaltenboeck and Storz, 1992). Early reports described the recovery of chlamydial organisms from the faeces of clinically healthy cattle (Wilson, 1963), sheep (Storz, 1964) and goats (Omori *et al.*, 1957). In the koala, *C. pecorum* causes reproductive disease, infertility and urinary tract disease. In other animals, *C. pecorum* has been associated with abortion, conjunctivitis, encephalomyelitis, enteritis, pneumonia, polyarthritis, salpingitis and infertility in cattle. Biotyping (Spears and Storz, 1979) and immunotyping (Perez-Martinez and Storz, 1985) distinguished *C. pecorum* from other *Chlamydophila* strains:

Table 1: Bio- and Immunotypes of *C. pecorum* strains

Biotype	Immunotype	Disease	Host
2	2	polyarthritis, conjunctivitis, encephalomyelitis	cattle and sheep
3	3	intestinal infection	cattle
4	4	polyarthritis	pigs
4	6	pneumonia or abortion	pigs
-	9	intestinal infection	sheep

7.2.2.6 Chlamydophila pneumoniae

Chlamydophila pneumoniae (formerly *Chlamydia pneumoniae* (Everett *et al.*, 1999)) was once thought to be a specific human pathogen, but now similar *Chlamydia*-associated diseases and their sequelae were found in many animals, for example, trachoma-like blindness (Cockram and Jackson, 1981) or infertility (McColl *et al.*, 1984) in koalas and polyarthritis in sheep (Storz *et al.*, 1963).

C. pneumoniae was initially isolated in 1965 from a child's conjunctiva (Grayston *et al.*, 1965). This isolate was called TW-183. With respect to the respiratory tract, the organism was first isolated in 1983 from a student with pharyngitis. This isolate was labeled AR-39. Later TW-183 and AR-39 became known as TWAR isolates and was renamed 1989 *Chlamydia pneumoniae* (Grayston, 1989a; Grayston, 1989b). DNA and antigenic criteria are used to differentiate *C. pneumoniae* from other species in the *Chlamydiaceae*. Its entire genome was sequenced in 1998 (Kalman *et al.*, 1999). The genome has approximately 1.2 megabases.

Respiratory infection with *C. pneumoniae* occur in almost everyone during his lifetime (Patnode, 1990; Wang, 1990). *C. pneumoniae* is estimated to cause an average of 10% of the community-acquired pneumonia cases and 5% of the bronchitis and sinusitis cases (Kuo *et al.*, 1995). Less common presentations are pharyngitis, laryngitis and sinusitis. The degree of illness can range from asymptomatic infection to severe disease. *C. pneumoniae,* which can also disseminate from the site of the initial infection (Moazed *et al.*, 1998), is also associated with various chronic diseases such as asthma and atherosclerosis (Kuo *et al.*, 1993; Hahn *et al.*, 1991) and late-onset Alzheimer's disease (Balin *et al.*, 1998). This association supports the assumption that *C. pneumoniae* can persist for extended periods in its human host.

Infections show high rates of recurrence (Grayston, 2000; Blythe *et al.*, 1992), but currently available information usually does not allow unequivocal differentiation between recurrences due primarily to reinfection and those resulting from chronic, persistent infection. However, the large number of published case reports provide some evidence that *C. pneumoniae* can cause chronic respiratory infections that often do not respond to treatment with chlamydicidal antibiotics (Gieffers *et al.*, 2004; Worm *et al.*, 2004; Hammerschlag, 2003; Anand and Gupta, 2001; Gieffers *et al.*, 2001; Stamm, 2000; Hammerschlag *et al.*, 1992). Moreover, coronary artery disease and cerebro-vascular stroke are the most common causes of death worldwide and the increasingly strong association of *C. pneumoniae* with such chronic conditions as follicular conjunctivitis (Lietman *et al.*, 1998), adult-onset asthma (Hahn *et al.*, 1991), and atherosclerosis (Kuo *et al.*, 1993; Saikku *et al.*, 1988) provides substantial evidence that this organism indeed can persist in its human host. Any new approach to the prevention of these

conditions would be enormously attractive and highlight an urgent need to identify new potential drug targets and chlamydicidal drugs that are effective against persistent infection. In addition, markers of the persistent form of infection would provide valuable diagnostic tools.

7.3 LIFE CYCLE

The obligate intracellular bacterium *C. pneumoniae* has a unique biphasic productive cycle that involves functionally and morphologically distinct cell types adapted for extracellular survival and intracellular multiplication (see Figure 3 for schematic overview). An infectious, metabolically inert cell type called elementary body (EB) initiates the infection by attaching to and stimulating the uptake by the host-cell. EBs gain access into the host-cell via either parasite-specified phagocytosis or receptor-mediated endocytosis. Chlamydial elementary bodies are small, round or occasionally pear shaped structures approximately 0.2-0.3 µm in diameter. EB functions as a "spore-like" body to permit chlamydial survival in the non-supportive environment outside the host-cell. The EB seems to be metabolically inert until it attaches to, and is endocytosed by, a host-cell. It derives its outer envelope strength not due to large amounts of peptidoglycan, but from cross links [-S-S- bridges] formed between cysteine and methionine rich proteins in the outer envelope. The ultrastructure of chlamydial EBs has been extensively studied (Matsumoto, 1982; Louis *et al.*, 1980; Eb *et al.*, 1976; Matsumoto, 1973).

The internalized EB remains within a host-derived vacuole (inclusion) and differentiates to a larger form, termed the reticulate body (RB). The reticulate body is responsible for intracellular replication. Typically, reticulate bodies have a diameter of 1 µm and they are not infectious. RBs are metabolically active, so their cytoplasm is rich in ribosomes. They are surrounded by two sets of tri-laminar membranes, an inner cytoplasmic membrane and an external outer envelope, whose surface is covered with projections and rosettes. These projections can be seen extending from the chlamydial surface into the inclusion membrane.

The RB multiplies by binary fission and after 8 to 12 rounds of division the RB differentiates back to EB asynchronously (Fig. 2) (Moulder, 1991). At 30h to 72h p.i., depending on species and serovar (e.g. 36h for *C. trachomatis* serovar L2 and 72h for *C. pneumoniae*), EB progeny are released from the host-cell for subsequent rounds of infection (Wolf *et al.*, 2000; Moulder, 1991; Moulder, 1966).

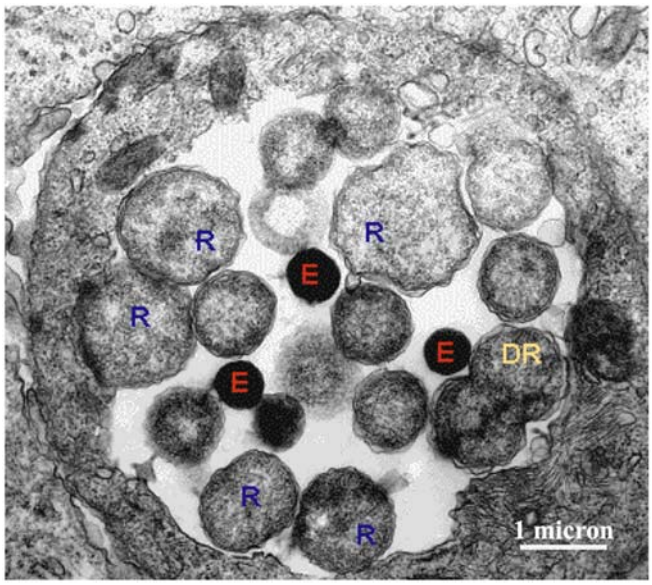

Figure 2: An immature inclusion of *C. trachomatis* LGV 404 consisting of a mixture of small, "red" elementary bodies (E), larger, "blue" reticulate bodies (R) and "yellow" dividing reticulate body (DR). (original figure from M. E. Ward. The chlamydial developmental cycle. In: Microbiology of *Chlamydia*, Barron, A. L. ed.; CRC Press, 1988).

The third, persistent form of *Chlamydiae* fails to complete development from RBs into infectious EBs, but retains (modified) metabolic activity (see chapter **Persistence**). These aberrant bodies show a viable but non-cultivatable growth stage resulting in a long-term relationship with the infected host-cell (Beatty *et al.*, 1994a).

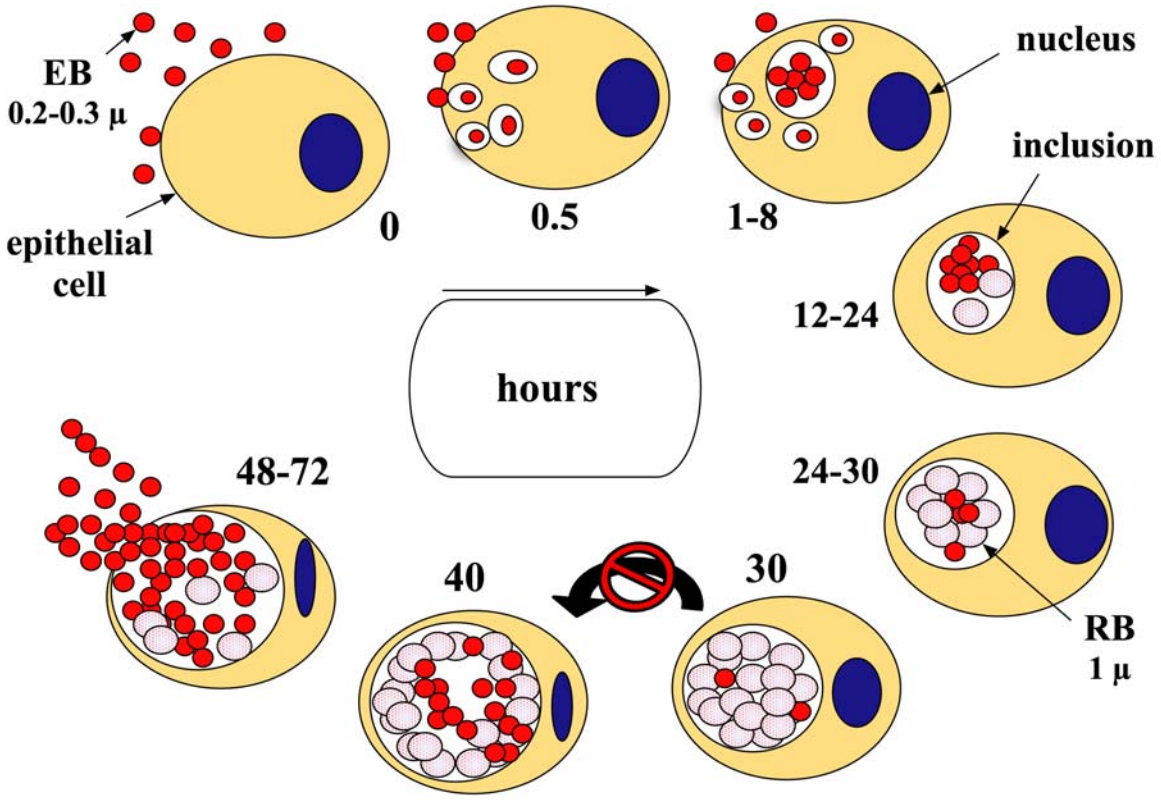

Figure 3: Chlamydial developmental cycle. The productive growth cycle of *Chlamydophila pneumoniae.* The red dots are infectious elementary bodies (EB). The larger red spotted dots are the intracellular replicating reticulate bodies (RB). At 72h p.i. *C. pneumoniae* EB progeny are released from the host-cell for subsequent rounds of infection. During persistent infection *Chlamydiae* fails to complete development from RBs into infectious EBs (black arrow).

7.4 STRUCTURE

A double membrane, a characteristic feature of gram-negative bacteria, surrounds chlamydial cells. However, unlike other gram-negative bacteria, *Chlamydiae* do not have a peptidoglycan layer in the space between the two membranes (Fox *et al.*, 1990; Barbour *et al.*, 1982). On the other hand, they contain penicillin-binding proteins and show peptide cross links analogous to those between peptidoglycan backbones (Barbour *et al.*, 1982). The genomic sequence of *C. trachomatis* revealed the presence of genes for peptidoglycan synthesis, membrane assembly, and recycling (Stephens *et al.*, 1998).

Lipopolysaccharide (LPS), which is a general endotoxin in gram-negative bacteria, is localized on the surface of EBs and RBs (Birkelund *et al.*, 1989). Chlamydial LPSs have both a cross-reactive epitope and a genus-specific epitope (Lukacova *et al.*, 1994; Brade *et al.*, 1987; Nurminen *et al.*, 1983). The structure of LPS is not identical in all chlamydial species (Ingalls and Golenbock, 1995; Brade *et al.*, 1987; Nurminen *et al.*, 1983).

The outer membrane contains proteins named outer membrane proteins (OMP) (Melgosa *et al.*, 1993). The most abundant of them is the major outer membrane protein (MOMP) of 38 to 42 kDa, comprising about 60% of OMPs (Caldwell *et al.*, 1981). MOMP contains serovar-, subspecies- and species-specific epitopes and is surface-localized on *C. trachomatis*, *C. psittaci* and on *C. pneumoniae* (Black *et al.*, 1992; Koehler *et al.*, 1992; Frost *et al.*, 1991; Sayada *et al.*, 1991; Pickett *et al.*, 1988).

Proteins named polymorphic outer membrane proteins (PMPs) have also been localized in the outer membrane (Knudsen *et al.*, 1999). The *C. pneumoniae* PMP gene family consists of a heterogeneous group of genes with low identity but with shared characteristics. Most of the genes encode proteins 90 to 100 kDa in size.

In the inclusion membrane, a group of proteins called inclusion membrane proteins (Inc) exists. Rockey *et al.* identified the first of them, named IncA, in 1995 (Rockey *et al.*, 1995). Since then, six other Incs, from IncB to IncG, have been characterized (Subtil *et al.*, 2005; Thomson *et al.*, 2005; Toh *et al.*, 2003; Rockey *et al.*, 2002; Bannantine *et al.*, 2000; Suchland *et al.*, 2000). The potential to export such a high number of Incs to the inclusion membrane suggests that the inclusion membrane may have several functions in vesicle trafficking, prevention of lysosomal fusion, inclusion development, and nutrient acquisition.

Chlamydiae also contain heat shock proteins. The genes encoding Hsp10, Hsp60 and Hsp70 are continuously expressed throughout the developmental cycle and therefore can be found in the outer membrane complexes of both EBs and RBs (Brunham and Peeling, 1994). The Hsps

have been sequenced and are highly conserved within chlamydial species (Kikuta *et al.*, 1991; Kornak *et al.*, 1991; Danilition *et al.*, 1990; Morrison *et al.*, 1989).

7.5 PERSISTENCE

Chlamydiaceae are associated with various chronic diseases such as asthma and atherosclerosis (Kuo *et al.*, 1993; Hahn *et al.*, 1991). This association supports the assumption that *Chlamydiaceae* can persist for extended periods in their human host. Long-term relationship with the infected host-cell have been established *in vitro*, usually through deviations from conventional cell culture conditions for productive chlamydial development by addition of gamma interferon (IFN-γ), penicillin G or deprivation of essential nutrients including iron (for an overview see Hogan *et al.*, 2004). The different *in vitro* persistence systems often share altered chlamydial growth characteristics, for example enlarged and morphologically aberrant RBs, a loss of infectivity and the development of relatively small inclusions containing fewer *Chlamydiae* (Pantoja *et al.*, 2001; Beatty *et al.*, 1993).

7.5.1 Nutrient deficiency-induced persistence

Depletion of cysteine interrupts chlamydial RB-to-EB differentiation in *C. trachomatis*. This effect is reversible, with resumed differentiation to infectious forms, upon the addition of cysteine. Deficiency of other amino acids has little or no effect on chlamydial development. These observations suggest that this amino acid is primarily important for alteration in growth and differentiation (RB-to-EB) as a requirement for the biosynthesis of three cysteine-rich proteins (MOMP, 12 and 60 kDa). In a medium lacking thirteen amino acids intracellular development of *C. trachomatis* serovars E and L2 was reversible altered showing reduced infectious yield and enlarged abnormal chlamydial forms. In conclusion, under conditions in which nutrients become limited, *Chlamydiae* may fail to successfully compete for macromolecular precursors and may enter an arrested growth stage.

7.5.2 Antimicrobial agents and persistence

Treatment with penicillin has no effect on initial differentiation of the infecting EB to RB, but it does prevent the process of binary fission. Penicillin induces the development of enlarged, morphologically abnormal chlamydial forms with a life cycle arrest before conversion of RBs to EBs. Because *Chlamydiae* are deficient in peptidoglycan, the mechanism of chlamydial

growth inhibition by penicillin is unknown. Ampicilin, Chloranfenicol, and chlortetracycline have also been shown to interrupt the intracellular development of *Chlamydiae*. Addition of these inhibitors early in infection prevents primary differentiation of EB to RB, whereas exposure later in infection interrupts RB division and secondary differentiation. Erythromycin inhibits the RB-to-EB differentiation but also induces smaller inclusions containing RBs.
5-fluorouracil, Hydroxyurea and Sulfonamides, as trimethoprim and sulfomethazole, can also induce chlamydial persistence. For an overview see Hogan *et al.*, 2004.

7.5.3 Immunologically induced persistence

In early studies, interferon gamma (IFN-γ) was identified as the active component in supernatant fluids from stimulated T-cells that inhibited replication of *C. psittaci* 6BC in fibroblast (Byrne and Krueger, 1983) and macrophage (Rothermel *et al.*, 1983) cultures that had been preexposed to the supernatant. Preexposure of epithelial cells for 24 h to high concentrations of IFN-γ inhibited inclusion formation by *C. trachomatis* serovar L2 (Shemer and Sarov, 1985), *C. psittaci* 6BC (Byrne *et al.*, 1986) and *C. pneumoniae* BAL-37 (Summersgill *et al.*, 1995). However, lower IFN-γ levels only partially restricted chlamydial development (Summersgill *et al.*, 1995; Byrne *et al.*, 1986; Shemer and Sarov, 1985). In this way, persistence was established for *C. trachomatis* serovar A in HeLa-cells at IFN-γ levels as low as 0.2 ng (2.4 U)/ml (Beatty *et al.*, 1993) and for *C. pneumoniae* A-03 in HEp-2 cells at a level of 25 U/ml (Pantoja *et al.*, 2001). Persistence of *C. trachomatis* serovar A was maintained for several weeks (Beatty *et al.*, 1995).
Exposure of *in vitro* chlamydial infections to IFN-γ provides a well defined system of deficiency-induced persistence that could plausibly reflect *in vivo* events (Pantoja *et al.*, 2001). The most important mechanism underlying the effects of IFN-γ (in particular in cell culture) is tryptophan depletion through activation of the host tryptophan-degrading enzyme indoleamine 2,3-dioxygenase (IDO) (Pantoja *et al.*, 2000). IDO induction was confirmed to be the major mechanism of IFN-γ-mediated persistence for *C. trachomatis* serovar A in HeLa-cells (Beatty *et al.*, 1994b) and *C. pneumoniae* A-03 in aortic smooth muscle cells (Pantoja *et al.*, 2000). However, other mechanisms such as the inducible nitric oxide synthase effector pathway and iron deprivation could also be attributable to IFN-γ, representing different *in vivo* situations (Igietseme *et al.*, 1998). In the IFN-γ model, after removal of the cytokine and addition of tryptophan, persistent *Chlamydia* can be reactivated into the productive cycle to a

high percentage exhibiting a further proof of survival during their non-cultivatable persistent state (Peters *et al.*, 2005).

Ultrastructurally, the IFN-γ-induced persistent *Chlamydiae* were enlarged and aberrant (Pantoja *et al.*, 2001; Beatty *et al.*, 1993). In *C. trachomatis* serovar A, there was also evidence of budding and endopolygeny, the production of multiple progeny from a single enlarged form, during resumption of productive infection after removal of IFN-γ from the cultures (Beatty *et al.*, 1995). These morphological observations were consistent with those from other persistence induction systems (Coles *et al.*, 1993; Matsumoto and Manire, 1970). However, a direct comparison of IFN-γ- and amino acid depletion-induced persistent *C. trachomatis* serovars E and L2 in HeLa-cells revealed different growth characteristics between the two systems, since only IFN-γ-exposed cultures showed decreases in inclusion size and the number of infected cells (Jones *et al.*, 2001).

Recently, tryptophan depletion provided an important link between IFN-γ and differential tissue tropisms among *C. trachomatis* serovars. Caldwell and colleagues (Caldwell *et al.*, 2003) showed that, in agreement with the previous study of direct tryptophan depletion (Fehlner-Gardiner *et al.*, 2002), *C. trachomatis* serovar D, I or L2 but not serovar A in HeLa-cells displayed the indole-rescuable phenotype after exposure to 5 ng (60 U) of IFN-γ/ml. Interplay between the IFN-γ concentration and other factors such as the availability of exogenous indole, the ability of the infecting strain to use it (Caldwell *et al.*, 2003; Fehlner-Gardiner *et al.*, 2002) and the IDO expression level of the host-cell type (Sakash *et al.*, 2002) may affect the outcome of a chlamydial infection *in vivo*.

7.6 HOST-CELL INTERACTION

In productive *C. pneumoniae* infection, host-cell gene expression is drastically altered in epithelial HeLa-cells, as recently shown by microarray and real-time RT-PCR (Hess *et al.*, 2003). These induced host-cell responses are strictly dependent on the viability of the *Chlamydia* - UV- or heat-inactivated *Chlamydia* do not activate HeLa-cells; most likely, an active bacterial mechanism such as chlamydial effector proteins, which are transported by the type III secretion system into the host-cell cytosol, is the basis of this biological effect. In contrast to HeLa-cells and several other cells, monocytes also respond to UV- or heat-inactivated *Chlamydia* (Peters *et al.*, 2005). In these leukocytes, additional signaling cascades are triggered via Toll-like receptors.

It is still not clarified how host-cells are modified in persistence. Several responses of HeLa-cells, known to be strongly up-regulated in productive infection, have recently been investigated in three models of long-term *C. pneumoniae* persistence: IL-6, IL-8, IL-11, LIF, Connective tissue growth factor and the transcription factors EGR-1 and ETV-4. Intriguingly, direct comparison of IFN-γ, penicillin G, and iron-depletion-induced persistence recently revealed two modes of host-cell reaction depending on the model used (Peters *et al.*, 2005).

In the IFN-γ (and the Penicillin G) model regulation of all investigated host-cell genes turns back to basal expression levels, as determined on day 4 and 7, after an initial increase in the expression of all investigated host-cell genes 24h p.i.. The responses at 24h might simply indicate remaining productivity before conditions causing persistence (depletion) are finally reached. Additionally, the *Chlamydia*-independent signal-transduction of the persistently infected HeLa-cells is altered in this model (Peters *et al.*, 2005). This suggests a silencing of the infected host-cells, which may suppress inflammation and prevent recognition of persistently infected cells by the immune system.

However, only a few genes have been analyzed so far. Hence, these former investigations did not prove that *C. pneumoniae* induced host-cells responses are generally shut down in persistence. Alternatively, other reactions of the host-cells to *C. pneumoniae* may take place in persistence, and may influence the survival of the intracellular *Chlamydia* and the pathogenesis of *C. pneumoniae* induced diseases. It has been shown that chlamydial infection alters the gene expression pattern of their host-cells (Peters *et al.*, 2005; Hess *et al.*, 2003; Hogan *et al.*, 2003; Yang *et al.*, 2003; Molestina *et al.*, 2002; Molestina *et al.*, 2000). An intervention in the *Chlamydia*-host-cell interaction in persistence or the immune response could be the means for preventing or controlling chlamydial infections, but would require an

understanding of these mechanisms in the various stages of *C. pneumoniae* infection. Additionally, markers of the persistent form of infection would provide valuable diagnostic tools.

7.7 RNA AMPLIFICATION

High throughput DNA microarray technology has proved to be a powerful approach for *C. pneumoniae* gene expression profiling (Fischer *et al.*, 2004; Shi and Tokunaga, 2004; Virok *et al.*, 2003; Coombes and Mahony, 2001) and has begun to play a role in the understanding of chlamydial persistence mechanisms *in vitro* (Belland *et al.*, 2003). To generate a meaningful gene expression pattern *in vivo*, it is essential to isolate either a infected (persistent or productive) or a normal cell using techniques such as cell sorting or laser capture microdissection (Trogan and Fisher, 2005; Craven and Banks, 2001; Burgess and Hazelton, 2000; Simone *et al.*, 1998; Bonner *et al.*, 1997). However, such techniques yield low amounts of RNA. The amount of mRNA within a single cell is estimated to be between 0.1 and 1 pg, usually insufficient to perform DNA microarray experiments and therefore hamper the change from *in vitro* to *in vivo* models.

In such cases, it is necessary to employ RNA amplification methods to generate the microgram quantities of RNA required to perform microarray experiments. The technique of amplified antisense RNA (aRNA) facilitates the linear amplification of large mRNAs. The RNA made using this technique is antisense to the poly$(A)^+$ RNA and can either be used as a probe or be cloned (Lin, 2003; Van Gelder *et al.*, 1990). Using RNA amplification methods one must be able to distinguish between the real effects of the biological system being analyzed and changes introduced due to a difference in the methods used to generate the data. In the past, a linear, isothermal amplification strategy based on *in vitro* transcription (IVT) with T7 RNA polymerase was used (Eberwine *et al.*, 1992; Van Gelder *et al.*, 1990). In this procedure, mRNA was converted into double stranded cDNA (dsDNA), using a T7-promotor/oligo(dT) primer for first strand cDNA synthesis and limited RNase H digestion for self-priming during second strand synthesis. For amplification, these dsDNA molecules were used as templates for IVT. Resulting in linear amplification maintaining the expression patterns of the original mRNAs (Puskas *et al.*, 2002; Poirier *et al.*, 1997). With this approach a number of problems were observed, because amplified RNA is 3'-biased since transcription and cDNA synthesis with the T7-promotor/oligo(dT) primer start at the poly(A)-tail of the original mRNA and a second amplification is based on random priming, causing reduction of

fragment length, which is even more pronounced, when only small amounts of input RNA are available. A third problem occurs due to production of large amounts of non-template high molecular weight artifacts by T7-promotor/oligo(dT) primer in the first cDNA synthesis, which will become dominant if less template is used (Baugh *et al.*, 2001).

New technologies solve these problems. In the experimental work of this thesis, an amplification Kit (ExpressArt® mRNA Amplification Kit, AmpTec® GmbH, Germany) was used where the original mRNA is converted to cDNA with an anchored oligo(dT) primer, but without T7-promotor. To further minimize 3'-bias in the next step, double stranded cDNA is generated with a special Box-random-trinucleotide primer, which results in preferential priming near the 3'-ends of all nucleic acid molecules. After denaturation, the second cDNA strand is primed in reverse orientation, using a T7-promotor/oligo(dT) primer. This leads to double stranded cDNA with a functional T7-promotor at one end and the Box sequence tag at the other end. This dsDNA product is used as template for IVT, generating amplified, antisense oriented RNA with defined sequences at both ends (see Figure 4 for schematic overview). This is a major advantage for second and third round amplifications, where size reductions of amplified RNAs are avoided. This is crucial and enables the comparison of samples that contain divergent amounts of input RNA.

In this thesis, a comparative analysis was performed of gene expression data generated using two different total RNA starting amounts (2.5 µg versus 10 ng) and two different methods for preparation, namely, a standard protocol for microgram starting amounts (involving *in vitro* transcription, IVT) and a two round amplification protocol (involving double *in vitro* transcription, dIVT) for nanogram RNA samples.

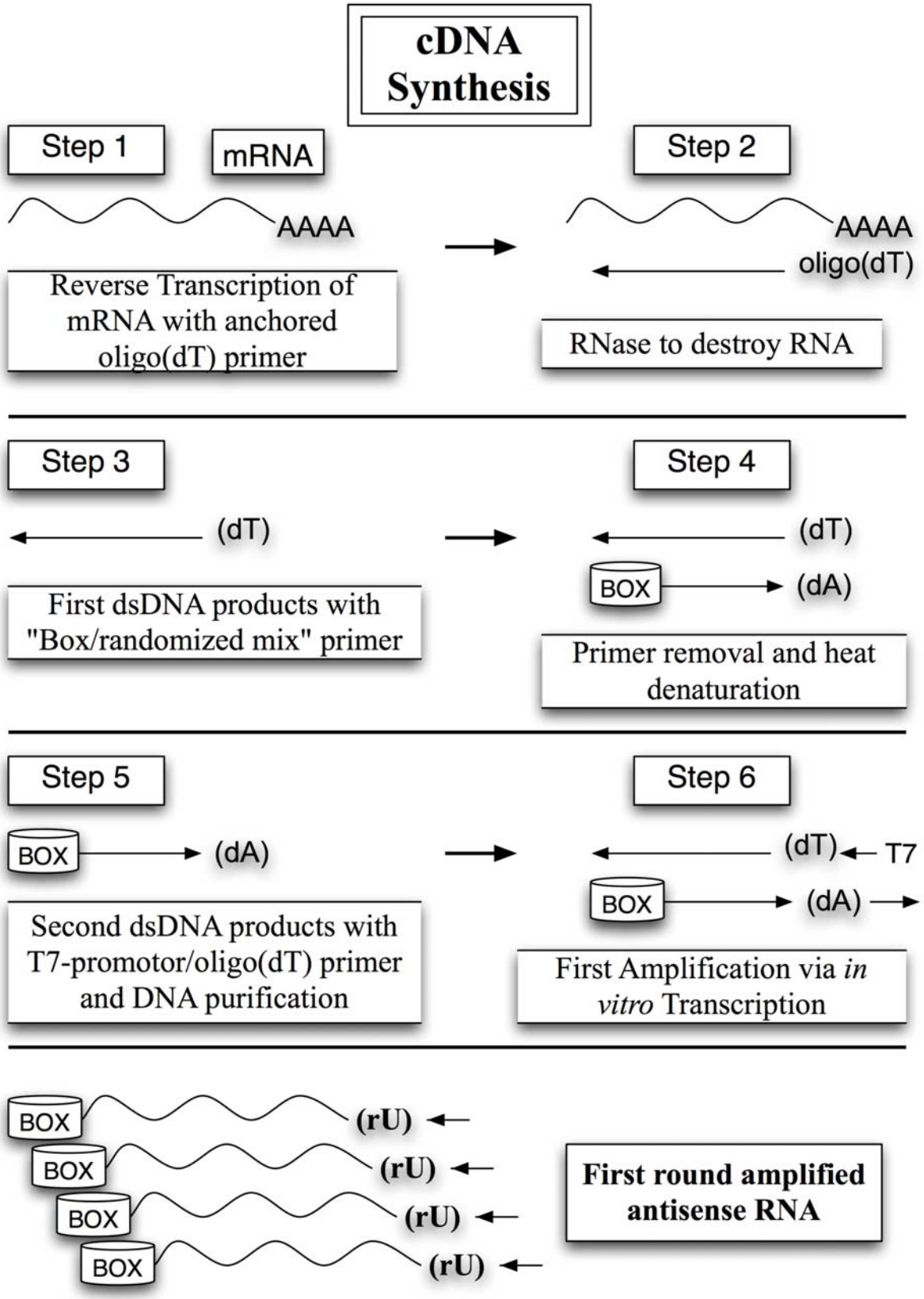

Figure 4: Schematic overview of first round amplified antisense RNA amplification using the ExpressArt® mRNA Amplification Kit (AmpTec® GmbH). dsDNA can be used either with an RNA labeling kit to generate labeled antisense RNA for hybridization or as template for generation of unmodified, amplified antisense RNA. This unmodified RNA can be utilized for further amplification or to generate labeled sense DNA by reverse transcriptionwith labeled dNTPs.

8. Aims of this Thesis

Chlamydiaceae are obligate intracellular bacteria seemingly associated with chronic diseases. An improved understanding of the persistence mechanism underlying chlamydial chronic diseases will be critical for the development of targeted therapeutic strategies. Currently, gene expression studies are carried out with cell cultures in which persistence is induced by agents like gamma interferon (IFN-γ). *In vivo* models have a great potential for advancing our knowledge of persistence processes but are often impeded by small amounts of sample material. Improved diagnostic tools will be necessary to sensitively detect *Chlamydiaceae* during all stages of their developmental cycle thereby, allowing the monitoring of chlamydiacial drug therapy.

The aims of the thesis are:

1.) To analyze the gene expression pattern of HeLa-cells *in vitro* after acute and persistent infection with *C. pneumoniae* to gain a better understanding of the host-pathogen interaction.
2.) To establish a new technique for the linear amplification of small amounts of RNA as a basis for the investigation of *C. pneumoniae* host-cell interaction using *in vivo* models in the future.
3.) To devise highly sensitive and specific diagnostic tools for routine diagnostic and therapy monitoring.

The human pathogens *C. pneumoniae* and *C. trachomatis,* representing the two genera of the family *Chlamydiaceae,* were chosen to investigate their interrelationship with the host. The chlamydial host-cell interaction should be analyzed by evaluating the gene expression pattern using microarray screening. HeLa-cells should be productively and IFN-γ-induced persistently infected with *C. pneumoniae*. Gene expression should be determined at early and late time points of infection to discover regulated genes as potential key elements of induced or inhibited pathways. A detailed analysis of chosen genes by real-time PCR should follow and thereby verify the obtained microarray results.

A procedure of linear amplification should be established by comparing two different amounts of RNA (2.5 µg versus 10 ng) and two different methods of preparation (IVT and dIVT).

For *C. trachomatis* qualitative and quantitative *in vitro* diagnostics should be developed. The qualitative assay should be capable to detect all *C. trachomatis* strains including those that do not express the cryptic plasmid.

9. Materials and Methods

9.1 INSTRUMENTS

Name	Company	City	Country
ABI PRISM™ 7000 SDS	Applied Biosystems	Foster City	U.S.A.
ABI PRISM™ 7700 SDS	Applied Biosystems	Foster City	U.S.A.
ABI PRISM™ 7900HT SDS	Applied Biosystems	Foster City	U.S.A.
Agilent Bioanalyzer 2100	Agilent Technologies	Palo Alto	U.S.A.
BrightStar®-Plus positively charged nylon membrane	Ambion	Huntingdon	U.K.
Biofuge pico	Heraeus Sepatech	Osterode	Germany
Centrifuge 5415D	Eppendorf	Hamburg	Germany
Centrifuge J2-21	Beckman Coulter	Unterschleißheim	Germany
Centrifuge Rotanta 96 RSC	Hettich	Tutlingen	Germany
Electrophoresis Documentation and Analysis System: Model 120	Kodak digital science	Rochester	U.S.A.
Electrophoresis Power-Supply: Life Technologies, Model 250 EX	GIBCO BRL	Gaithersburg	U.S.A.
Exposure Cassette	Molecular Dynamics	Sunnyvale	U.S.A.
Foilsealer: Model FS 500, Vacufix electronic	Petra electric	Burgau	Germany
Gel Casting System: Life Technologies, Model 11.14	GIBCO BRL	Gaithersburg	U.S.A.
Horizontal Gel Electrophoresis Apparatus: Horizon 11.14	GIBCO BRL	Gaithersburg	U.S.A.
Image Eraser: Model 810-UNV	Molecular Dynamics	Sunnyvale	U.S.A.
Incubator: Model B 5090 E, Model function line	Heraeus	Osterode	Germany
LightCycler® 1.2 and 2.0	Roche Diagnostics	Mannheim	Germany
MagNA Pure® LC instrument	Roche Diagnostics	Mannheim	Germany
Mastercycler®: Model 5333	Eppendorf	Hamburg	Germany
Microwave: AEG Micromat 16	AEG-Electrolux	Stockholm	Sweden
Minishaker: Model MS1, Speed: 200-2500 rpm	IKA® Works	Willmington	U.S.A.
Phosphoimager: Typhoon 9210, variable Mode Imager	Molecular Dynamics	Sunnyvale	U.S.A.
Rotor-Gene™ 2000 and 3000	Corbett Life Science	Sydney	Australia
Scale: Model PB3002-S DeltaRange®, Max: 3100 g, Min: 0,5 g	Mettler Toledo	Giessen	Germany
Scintillation counter: Model LB 122	Berthold Technologies	Bad Wildbad	Germany

Shake ‘n Stack	Hybaid	Heidelberg	Germany
Storage Phosphor Screen	Molecular Dynamics	Sunnyvale	U.S.A.
Thermomixer: Model comfort, 2 ml and 1.5 ml	Eppendorf	Hamburg	Germany
Turboblotter, Rapid Downward Transfer Systems	Schleicher & Schuell	Dassel	Germany
UV photometer: BioPhotometer, 8.5 mm cuvette	Eppendorf	Hamburg	Germany
UV spectrophotometer: Spectron™ Helios™ β	Thermo Electron GmbH	Dreieich	Germany
UV Transilluminator: Life Technologies, Model TFX-35M	GIBCO BRL	Gaithersburg	U.S.A.
UV-Crosslinker: UV-Stratalinker™	Stratagene	La Jolla	U.S.A.

9.2 SOFTWARE

Name	Company	City	Country
ABI 7900HT SDS 2.1	Applied Biosystems	Foster City	U.S.A.
ABI PRISM™ 7000 SDS Software Vers. 1.1	Applied Biosystems	Foster City	U.S.A.
ABI PRISM™ 7700 SDS Software	Applied Biosystems	Foster City	U.S.A.
Agilent 2100 Bioanalyzer Bio Sizing Software Vers. A.02.11	Agilent Technologies	Palo Alto	U.S.A.
artus 3000 Vers. 5.0 and 6.0, Rotor-Gene® Software	Corbett Life Science	Sydney	Australia
Chromas Vers. 1.45	Griffith University	Queensland	Australia
DNASTAR: MegAlign and EditSeq Vers.5.06	DNASTAR	Madison	U.S.A.
EndNote Vers. 9.0.0 for Mac OS X	Thomson Scientific	London	U.K.
GraphikConverter V4.3	Lemke Software	Peine	Germany
ImageQuant Vers. 5.2	Molecular Dynamics	Sunnyvale	U.S.A.
Kodak ds 1D Vers. 2.0.3	Kodak digital science	Rochester	U.S.A.
LightCycler® Software Vers. 3 and 4	Roche Diagnostics	Mannheim	Germany
Macromedia® FreeHand® MX Vers. 10.3.9	Adobe Systems	München	Germany
Microsoft® Excel 2004 for Mac® Vers. 11.2	Microsoft GmbH	Unterschleißheim	Germany
Microsoft® Word 2004 for Mac® Vers. 11.2	Microsoft GmbH	Unterschleißheim	Germany
OmniGraffle Pro Vers. 3.2.4 (v74.18) for Mac OS X	The Omni Group	Seattle	U.S.A.
Primer Express Vers. 2.0.0	Applied Biosystems	Foster City	U.S.A.
PriProbit® Vers. 1.63	Kyoto University	Kyoto	Japan
SPSS 11 for Mac OS X	SPSS Inc.	Chicago	U.S.A.

9.3 REAGENTS

9.3.1 Commercial Kits

Name	Company	City	Country
BioArray High Yield RNA Transcript Labeling Kit (T7)	Enzo Life Sciences	Farmingdale	U.S.A.
ExpressArt™ mRNA Amplification Kit, Micro and Nano Vers.	AmpTec	Hamburg	Germany
MagNA Pure LC DNA Isolation Kit III (Bacteria, Fungi)	Roche Diagnostics	Mannheim	Germany
NorthernMax-Gly Kit	Ambion	Huntingdon	U.K.
QIAamp DNA Mini Kit	QIAGEN	Hilden	Germany
QIAamp Viral RNA Mini Kit	QIAGEN	Hilden	Germany
QIAquick Spin Kit	QIAGEN	Hilden	Germany
RevertAid H^- First Strand cDNA Synthesis	Fermentas GmbH	St. Leon-Rot	Germany
RNeasy Mini Kit	QIAGEN	Hilden	Germany

9.3.2 Biochemicals, growth media, solutions

Name	Company	City	Country
Agarose (ultra-pure grade)	Invitrogen	Karlsruhe	Germany
Agarose (LE, Analytical Grade)	Promega Corporation	Madison	U.S.A.
Cycloheximide	CALBIOCHEM® (brand of EMD Biosciences)	Darmstadt	Germany
100 bp DNA ladder (TriDye, 50 µg/ml)	New England BioLabs	Ipswich	U.S.A.
1 kb DNA ladder (0.5 mg/ml, GeneRuler).	MBI Fermentas	St. Leon-Rot	Germany
Earle's minimal essential medium	Biochrom	Berlin	Germany
Ethidium bromide	Merck	Darmstadt	Germany
Fetal Calf Serum	Biochrom	Berlin	Germany
FirstChoice™ Human Cell Line Total Cervical Adenocarcinoma RNA	Ambion Europe Ltd.	Huntingdon	U.K.
L-glutamine	Biochrom	Berlin	Germany
Gentamicin	Biochrom	Berlin	Germany
IFN-γ	R&D Systems	Wiesbaden	Germany

6x Loading dye	MBI Fermentas	St. Leon-Rot	Germany
Non-essential amino acids	Biochrom	Berlin	Germany
Panserin 401 medium	Cytogen	Berlin	Germany
1x PBS	Sigma-Aldrich Chemie	München	Germany
Proteinase K	Novagen® (brand of EMD Biosciences)	Darmstadt	Germany
RPMI 1640 medium	Sigma-Aldrich Chemie	München	Germany
Sodium pyruvate	Biochrom	Berlin	Germany
SybrGreen-Mix	Sigma-Aldrich Chemie	München	Germany
Tris buffer	Sigma-Aldrich Chemie	München	Germany

All the other biochemicals and chemicals not listed in the table were purchased from Merck (Darmstadt, Germany) or Sigma-Aldrich Chemie (München, Germany).

9.4 CELL AND CHLAMYDIAL CULTURE

Human cervical epithelial HeLa-cells (kindly provided by R. Heilbronn, Berlin, Germany) were cultured in Earle's minimal essential medium supplemented with 10% fetal calf serum, 2 mM L-glutamine, 0.1 M nonessential amino acids and 1 mM sodium pyruvate. HeLa-cells were grown as monolayers at 37°C and 5% CO_2.

Chlamydia pneumoniae CWL-029 (ATCC) were propagated in HeLa-cells (Peters et al., 2005). For stock production, HeLa-cell monolayers were infected with elementary bodies (EBs) by 55 min. centrifugation at 35°C and 2,000xg in Panserin 401 medium and 1 µg/ml cycloheximide. *Chlamydia* or the host-cells were checked for mycoplasma contamination by PCR. EBs were harvested 3 days p. i. by opening the infected cells mechanically. Cell debris was removed by centrifugation (500xg for 15 min.) and the EBs in the supernatant were collected by centrifugation at 22,000xg for 1 h. The EBs were washed in transport medium (1x PBS including 6.86% saccharose, 40 g ml^{-1} Gentamicin, 0.002% Phenol red, 2% FCS), and again collected by centrifugation. To obtain buffer samples for an optimal mock control, the complete purification procedure for EBs was performed in the absence of *C. pneumoniae*, in parallel.

9.5 IFN-γ MODEL OF PERSISTENCE IN HELA-CELLS

Infection with *C. pneumoniae* (MOI 30 or MOI 3) was performed in RPMI 1640 medium (10% FCS, 0.1 M nonessential amino acids and 10 mM Hepes) by centrifugation (55 min., 35°C, 2,000xg). To obtain a defined starting point for kinetic studies (time 0), the infected cells were washed with 1x PBS and incubated with fresh medium. After 30 min. p.i. the medium was replaced with medium containing 100 U ml^{-1} of IFN-γ in order to induce persistence. The minimal concentration of the persistence-inducing IFN-γ was selected as evaluated by Peters et al. (Peters *et al.*, 2005) where less than 1% infectious EBs was recoverable after 4 days, as compared to productive infection. Daily exchange of the medium with IFN-γ assured constant concentrations of growth factors and persistence inducer. A multiplicity of infection of 30 and in preliminary experiments of 3 was used in all HeLa-cell experiments. With a MOI 30 an infection efficiency of more than 95% was achieved as determined by immunofluorescence. With a MOI of 3 an infection efficiency of more than 90% was achieved. If IFN-γ was replaced by tryptophan on day 4 p.i., *C. pneumoniae* could be reactivated within 3 days to approximately 50% as compared to productive infection

(Peters et al., 2005). Infections were performed in 12-well cell-culture dishes with 8,6E+5-infected cells (MOI 30) in 1.5 ml medium per well. For productive infection, when compared to persistence RPMI 1640 including 10% fetal calf serum, 0.1 M non-essential amino acids and 10 mM Hepes were used. Infected cells were always grown at 35°C and 5% CO_2.

9.6 NUCLEIC ACID EXTRACTION

DNA used for bacterial load analysis was isolated using the RNeasy Mini kit according to the manufacturers instructions. Cells were harvested by removal of the supernatant and adding of 350 µl RLT buffer per well. After first round of extraction 10 µl eluat was stored at -20°C to measure the bacterial load. Rest of the eluat (90 µl) was reextracted with additional on column DNase I digestion according to the RNeasy Mini kit user manual. RNA was eluated in 50 µl RNase-free water.

Manual DNA isolation for the evaluation of the new developed *C. trachomatis* real-time PCR assays was carried out by using the QIAamp Viral RNA Mini for urine specimens and the QIAamp DNA Mini Kit for swab and semen specimens. For all kinds of validated specimens the manufacturers' nucleic acid extraction protocols were optimized as described below.

9.6.1 Purification of urine specimens

Buffer AVL, described in the QIAamp Viral RNA Mini Kit, inactivates the numerous unidentified PCR inhibitors found in urine. Therefore, for isolation of cellular, bacterial, or viral DNA from urine the QIAamp Viral RNA Mini Spin Protocol was used. The samples were first equilibrated to room temperature (19 - 23°C). Urine often contains very low numbers of bacteria, therefore the samples (5 - 30 ml) were centrifuged at a maximum of 10,000 xg for 15 - 20 minutes. The supernatant was carefully discarded and the pellet was resuspended in 1,200 µl 1x PBS by vortexing thoroughly to redissolve and disperse the sample. This step was performed by pulse vortexing for 15 - 30 seconds. 140 µl from the prepared samples were used for the DNA extraction following the QIAamp Viral RNA Mini Kit Handbook, 01/99 from step 1 on. The recommended optional centrifugation step 9a (13,000 rpm, 5 minutes) in the protocol was always performed to remove any residual ethanol. An elution volume of 60 µl buffer AE was used.

9.6.2 Purification of swab and semen specimens

The samples were first equilibrated to room temperature (19 - 23°C). Swab specimens that are stored in a transport media were mixed by vortexing thoroughly. The swab was pressed against the side of the tube in order to squeeze out the liquid. Any excess mucus in the specimen was removed at this time by collecting it on the swab. Any residual liquid from the mucus and the swab was then be recovered by pressing the swab against the side of the tube. Finally the swab and the mucus was removed and discarded. 200 µl of the transport medium was pipetted to 180 µl buffer ATL into a 1.5 ml microcentrifuge tube and vortexed thoroughly.

Dry swabs were directly put into a 1.5 ml microcentrifuge tube and vortexed with 180 µl buffer ATL for 15 - 30 seconds. Alternatively, 200 µl buffer ATL was pipetted into the transport tube and the swab was vortexed for 15 - 30 seconds in the tube. Subsequently, 180 µl were pipetted into a 1.5 ml microcentrifuge tube, the swabs were removed and discarded.

For the DNA extraction of seminal specimens 60 µl of the sample material were diluted with 140 µl 1x PBS in a 1.5 ml microcentrifuge tube and mixed by vortexing. 100 µl of the dilution were pipetted to 180 µl buffer ATL and mixed by pulse-vortexing for 15 - 30 seconds.

20 µl Proteinase K were added, mixed by pulse-vortexing and incubated at 56°C for 15 minutes (swabs) or 1 - 12 hours (seminal specimens) in a thermomixer. 200 µl buffer AL were pipetted to the sample, mixed by pulse-vortexing for 15 seconds and incubated at 70°C for 10 minutes. Afterwards 200 µl ethanol (96 - 100 %) were added to the sample, mixed by pulse-vortexing for 15 seconds and then 500 µl of the mixture (inclusive precipitate) were carefully applied to the QIAamp Column (in a 2-ml collection tube) without wetting the rim. After centrifugation at 6,000 xg (8,000 rpm) for 1 minute the filtrate was discarded. This step was repeated by applying all of the remaining mixture to the column.

After washing with 500 µl buffer AW1 and 500 µl buffer AW2 an additional centrifugation step at maximum speed (e.g. 13,000 rpm) was performed for 5 minutes. The QIAamp Column was placed in a clean 1.5 ml collection tube as a collect vessel and 50 µl buffer AE were applied on the column. After incubation for 1 minute at room temperature the column were centrifuged at 6,000 xg (8,000 rpm) for 1 minute and the eluate was collected.

9.6.3 Purification of lyophilized or freeze-dried specimens

The samples were first equilibrated to room temperature (19 - 23°C). Lyophilized or freeze-dried samples were reconstituted in 500 µl 1x PBS by careful shaking by hand. Subsequently, the samples were incubated for at least 30 minutes at room temperature in a thermomixer.

200 µl of the reconstituted sample were pipetted to 360 µl buffer ATL into a 1.5 ml microcentrifuge tube, vortexed and 20 µl Proteinase K were added. After pulse-vortexing the mixture was incubated at 56°C for 1 - 12 hours in a thermomixer. After addition of 400 µl buffer AL, pulse-vortexing and incubation at 70°C for 10 minutes, 400 µl ethanol (96 - 100 %) were pipetted to the sample and 700 µl of the mixture were applied to the QIAamp Column. The columns were centrifuged at 6,000 xg (8,000 rpm) for 1 minute and the filtrate discarded. The last step was repeated by applying all of the remaining mixture to the column. Afterwards the manufacturers' Tissue Protocol (QIAamp DNA Mini Kit and QIAamp DNA Blood Mini Kit Handbook, 02/2003, page 35) was followed from step 6. Thereby the optional centrifugation step 7a (13,000 rpm, 5 minutes) in the protocol was performed to remove any residual ethanol. For elution 50 µl buffer AE was used.

Automated sample preparation for urine, swab and semen specimens were carried out with the MagNA Pure LC DNA Isolation Kit III on the MagNa Pure LC instrument according to the manufacturer's instructions (Roche Diagnostics, Mannheim, Germany).

9.7 RNA QUALITY ASSURANCE AND QUANTITATION

Integrity of RNA samples is essential in the context of gene expression analysis via microarray technology. RNA quality and quantity was analyzed on the Agilent 2100 Bioanalyzer using the RNA 6000 Nano chip. Using Agilent's Lab-on-a-Chip technology sample RNA was added to the RNA 6000 Nano LabChip and the chip run was started on the Agilent 2100 Bioanalyzer.

Watching real-time data display the Agilent system automatically calculates the ratio of ribosomal bands in total RNA samples and shows the percentage of ribosomal impurities in mRNA samples. A lower marker allows for sample alignment and permits comparison of samples to distinguish different types of mRNA based on the electrophoretic traces.

In addition, RNA was quantitated by OD measurement and checked for degradation by agarose gel electrophoresis. For agarose gel electrophoresis 2% agarose and a 1 kb DNA

ladder were used. 2 µl sample were mixed with 1 µl SybrGreen-Mix (Sybr II 1/100 in DMSO) and 3 µl 6x loading dye.

The RNA concentration was calculated via OD measurement based on 1 A_{260} Unit of ssRNA = 40 µg/ml H_2O. OD value should lie between 0.1 and 1.0 to ensure an optimal measurement. The value 40 µg/ml is based on the extinction coefficient of RNA in H_2O. Pure RNA should have a A_{260}/A_{280} ratio ≥ 2.0. Buffered solutions provide more accurate values than water since the A_{260}/A_{280} ratio is influenced by pH. Therefore the measurement was performed in a low salt buffer. Pure RNA has a ratio of 1.9-2.1 in a 10 mM Tris buffer. A ratio smaller than 2.0 means that the preparation is contaminated with proteins and aromatic compounds.

9.8 cDNA SYNTHESIS

5 µl RNA eluate from nucleic acid extraction used for transcript analysis by real-time PCR was reverse transcribed with RevertAid H^- First Strand cDNA Synthesis kit according to the manufacturer's instructions. As reference 2 µg total cervical adenocarcinoma RNA was used. For microarray analysis cDNA was synthesized using the ExpressArt™ mRNA Amplification Micro and Nano Kit according to manufacturer's instructions. cDNA was quantitated by OD and Agilent 2100 Bioanalyzer measurement. For all experiments no RT controls were run in parallel.

9.9 AGAROSE GEL ELECTROPHORESIS

Agarose gel electrophoresis is a way to separate DNA fragments by their sizes and visualize them by running DNA through an ethidium bromide-treated gel and exposing it to UV light. The technique of electrophoresis is based on the fact that DNA is negatively charged at neutral pH due to its phosphate backbone. For this reason, when an electrical potential is placed on the DNA it move toward the positive pole. Making the DNA move through an agarose gel slows the rate at which the DNA will move toward the positive pole. The agarose forms a porous lattice in the buffer solution and the DNA must slip through the holes in the lattice in order to move toward the positive pole. This slows the molecule down. Larger molecules will be slowed down more than smaller molecules, since the smaller molecules can fit through the holes easier. The conformation of DNA is also a factor and is demonstrated by the topoisomeres of a plasmid: supercoiled, nicked, linear and single-stranded. Each conformation runs at a different rate, with supercoiled running the fastest and open circle

running the slowest. As a result, a mixture of large and small fragments of DNA that has been run through an agarose gel will be separated by size.

For gene expression studies agarose gel electrophoresis using 2% agarose and a 1 kb DNA ladder were performed. 2 µl sample were mixed with 1 µl SybrGreen-Mix (Sybr II 1/100 in DMSO) and 3 µl 6x loading dye.

For the development of new *C. trachomatis* real-time PCR assays ethidium bromide-treated agarose gel electrophoresis was used to control for unspecific amplifications. Therefore 2% agarose and a 100 bp DNA ladder were used. 2 µl sample material were loaded into the gel wells by addition of 10 µl 6x loading dye.

9.10 MICROARRAY ANALYSIS

RNA transcription labeling was performed using the BioArray™ HighYield™ RNA Transcript Labeling kit (T7). cRNA from two independent preparations was hybridized onto Affymetrix® human genome U133A chips (duplicates). Images were scanned and analyzed by Affymetrix® Microarray Suite software (version 5.0). The Affymetrix® standard normalization technique was used (global scaling, normalization factor 1,000). Microarray data analysis was performed using Spotfire Software. Results were filtered using following values: change call = I or D, I and SLR > 1.32 or D and SLR < -1.32; $\alpha 1 = 0.05$; $\alpha 2 = 0.065$; $\tau = 0.015$; TGT = 1000. The detection algorithm used probe pair intensities to assign a present, marginal or absent call. A score was calculated for each probe pair and compared to a predefined threshold Tau ($\tau = 0.015$). Probe pairs with scores higher than Tau vote for the presence of the transcript. Probe pairs with scores lower than Tau vote for the absence of the transcript. In a comparison analysis, two samples, hybridized to two microarrays of the same type, were compared against each other in order to detect and quantify changes in gene expression. One array was designated as the baseline and the other as an experiment (treatment versus mock at the corresponding time-point). Expression changes between two arrays are designated as “Fold Change” and defined as ratio between normalized intensities of the two arrays. Comparison analysis was done with Microsoft Excel X for Mac.

9.11 STATISTICAL ANALYSIS

Statistical analysis was performed using SPSS 11 and Microsoft Excel X for Mac. A probit analysis to determine the limit of detection for the *artus™ C. pneumoniae TM PCR Kit*, the *artus™ C. trachomatis Plus LC/RG PCR Kit* and the *artus™ C. trachomatis LC/RG/TM PCR Kit* was performed using PriProbit version 1.63 (designed by Dr. M. Sakuma http://bru.gmprc.ksu.edu/proj/priprobit/index.asp).

For quantitation normalized to endogenous controls, standard curves were prepared for both the target and the endogenous controls (in a total of three independent controls: 18S rRNA, TBP and GUS). For each experimental sample the amount of target and endogenous control was determined from the appropriate standard curve. Then, the mean of the in replicates measured concentrations of the three endogenous controls for each sample were calculated in a total of three independent experiment regarding MOI 30-infected cells and two independent experiments for MOI 3-infected cells, respectively. For example:

*Calculated Normalized Concentration of Sample „*24h mock-infected“ *from Experiment A*

	18S rRNA	**TBP**	**GUS**	**Mean (replicate)**	**Mean (total)**
Replicate 1	1.15	0.201	0.521	0.625	**0.659**
Replicate 2	1.18	0.215	0.597	0.666	
Replicate 3	1.16	0.211	-	0.687	

To obtain a normalized target value the target amount was divided by the total mean of the endogenous controls amount. As three independent experiments were performed three different normalized target values were obtained. In addition the standard deviation was calculated for each normalized sample value. Then the mean and the standard deviation of the normalized sample values of the independent experiments were calculated. Moreover, each of the normalized target values and their standard deviation were divided by the normalized mock-infected control sample value 24 h after infection. Finally the regulation factors were calculated by dividing the productive- or persistently-infected sample values over the corresponding mock-infected sample values.

Statistical evaluation for gene regulation, by using a 2-fold regulation cut-off, was performed by General Linear Model (GLM) analysis ($p \leq 0.05$). The GLM Univariate procedure provides regression analysis and analysis of variance for one dependent variable by one or more factors and/or variables. Using the General Linear Model procedure, an overall F test using Type III sums of squares was performed to show significance of differences of gene regulations between different sample types. In addition, post hoc tests were used to evaluate differences among specific means.

9.12 DNA SEQUENCING

For sequence analysis of real-time PCR products DNA fragments from PCR were first purified from primers, nucleotides, polymerases and salts using the QIAquick PCR Purification Kit. 30 µl of purified DNA (10-50 ng/µl) and primers (10 pmol/µl) were sent to GATC Biotech AG (Konstanz, Germany) for sequencing analysis. At GATC a Run24 Supreme Single sequencing reaction was performed.

9.13 REAL-TIME PCRS

After the invention of the polymerase chain reaction (PCR) method by Kary Mullis the development of novel chemistries and instrumentation platforms enables the detection of PCR products on a real-time basis. Traditional PCR is measured at end-point (plateau), while real-time PCR collects data in the exponential growth phase as an indicator of amplicon production during each PCR cycle. An increase in reporter fluorescent signal is directly proportional to the number of amplicons generated. A small amplicon size results in increased amplification efficiency. The real-time progress of the reaction can be viewed in some systems (e.g. Rotor-Gene). Real-time PCR quantitation eliminates post PCR processing of PCR products. This helps to increase throughput and reduce the chances of carryover contamination. In comparison to conventional PCR, real-time PCR also offers a much wider dynamic range. Dynamic range of any assay determines how much target concentration can vary and still be quantified. Available for real-time PCR are five main different chemistries, LightCycler® HybProbe (Roche Diagnostics, Mannheim, Germany), TaqMan® (Applied Biosystems, Foster City, CA, U.S.A.), Molecular Beacons, Scorpions® and SYBR® Green (Molecular Probes). All of these chemistries allow detection of PCR products via the generation of a fluorescent signal. SYBR Green is a fluorogenic dye that emits a strong fluorescent signal upon binding to double-stranded DNA. LightCycler® HybProbes, TaqMan probes, Molecular Beacons and Scorpions depend on Förster Resonance Energy Transfer (FRET) to generate the fluorescence signal via the coupling of a fluorogenic dye molecule and a quencher moiety to the same or different oligonucleotide substrates.

9.13.1 SYBR Green

SYBR Green is the most economical choice for real-time PCR. Since the dye binds to double-stranded DNA and upon excitation emits light, there is no need to design a probe for any particular target being analyzed. Thus, as a PCR product accumulates, fluorescence increases. However, since the dye cannot distinguish between specific and non-specific product accumulated during PCR, an overestimation of the target concentration or a false positive detection may result.

9.13.2 LightCycler® HybProbe

The LightCycler® HybProbe format is based on fluorescence resonance energy transfer (FRET). Two sequence-specific oligonucleotide probes are labeled with different dyes (donor and acceptor). During the annealing phase, HybProbe probes hybridize to the target sequences on the amplified DNA fragment in a head-to-tail arrangement, thereby bringing the two dyes close to each other. The energy emitted by the instrument excited donor dye excites the acceptor dye on the second HybProbe probe, which then emits fluorescent light at a different wavelength. This fluorescence is directly proportional to the amount of target DNA generated during PCR. HybProbe probes are displaced during the elongation and denaturation steps.

9.13.3 TaqMan Probes

TaqMan probes depend on the 5'- nuclease activity of the DNA polymerase used for PCR. TaqMan probes are oligonucleotides that have a fluorescent reporter dye (FAM, TAMRA, TET, ROX) attached to the 5' end and a quencher moiety (e.g. Dabcyl) coupled to the 3' end. These probes are designed to hybridize to an internal region of a PCR product. In the unhybridized state, the closeness of the reporter and the quench molecules prevents the detection of fluorescent signal from the probe. During PCR, when the polymerase replicates a template on which a TaqMan probe is bound, the 5'- nuclease activity of the polymerase cleaves the probe. This decouples the fluorescent and quenching dyes and FRET no longer occurs. Thus, fluorescence increases in each cycle, proportional to the amount of probe cleavage.

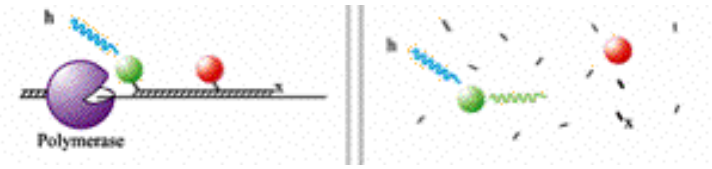

Figure 5: TaqMan Probes show an increase in fluorescence with each cycle. The signal depends on hydrolysis after hybridization.

9.13.4 Molecular Beacons

Molecular Beacons use FRET to detect and quantitate the synthesized PCR product via a reporter coupled to the 5' end and a quencher attached to the 3' end of an oligonucleotide. Molecular Beacons are designed to remain intact during the amplification reaction. They must rebind to the target in every cycle for signal measurement. Molecular Beacons form a stem-loop structure in unbound state. Thus, the close proximity of the reporter and quencher molecules prevents the probe from fluorescing. When a Molecular Beacon hybridizes to a target, the fluorescent dye and quencher are separated, FRET does not occur and the fluorescent dye emits light upon irradiation.

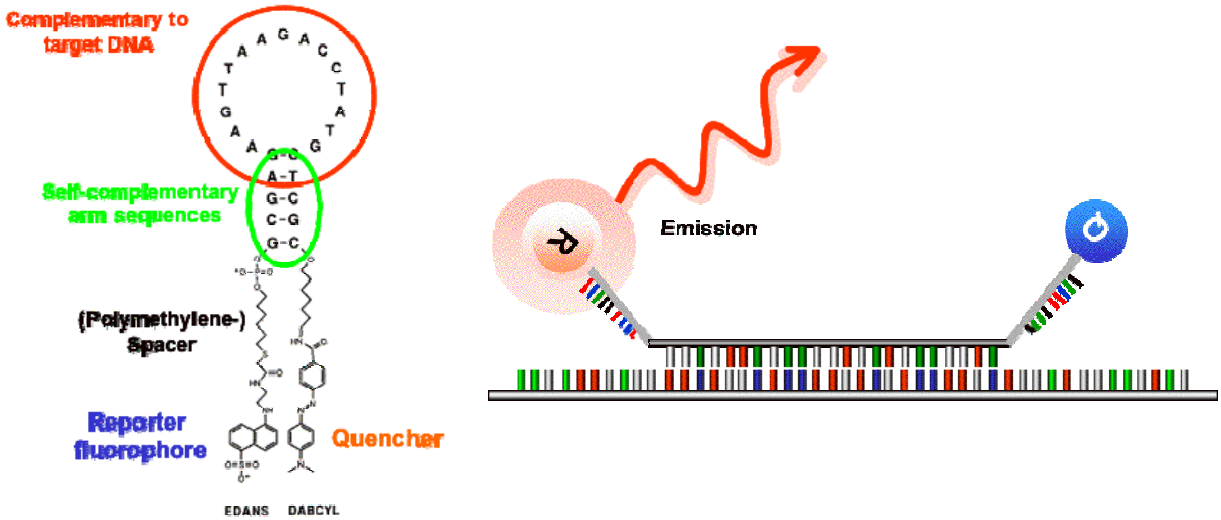

Figure 6: Molecular Beacons are sequence specific probes with self-complementary hairpin configuration. Their ends allow vicinity of reporter and quencher molecule.

9.13.5 Scorpions

With Scorpion probes, sequence-specific priming and PCR product detection is achieved using a single oligonucleotide. The Scorpion probe maintains a stem-loop configuration in the unhybridized state. The fluorophore is attached to the 5' end and is quenched by a moiety coupled to the 3' end. The 3' portion of the stem also contains a sequence that is complementary to the extension product of the primer. This sequence is linked to the 5' end of a specific primer via a non-amplifiable monomer. After extension of the Scorpion primer, the

specific probe sequence is able to bind to its complement within the extended amplicon thus opening up the hairpin loop. This prevents the fluorescence from being quenched and a signal is observed.

9.13.6 Multiplex PCR

TaqMan probes, Molecular Beacons and Scorpions allow multiple DNA species to be measured in the same reaction (multiplex PCR), since fluorescent dyes with different emission spectra may be attached to the different probes. Multiplex PCR allows for example internal controls to be co-amplified.

9.13.7 Quantitation by standard curves

A standard curve is constructed from RNA, DNA, plasmid dsDNA, *in vitro* generated ssDNA or any cDNA of known concentration. This curve is then used as a reference standard for extrapolating quantitative information for RNA or DNA targets of unknown concentrations. The important parameter for quantitation is the cycle threshold (CT). The higher the initial amount of genomic DNA, the sooner accumulated product is detected in the PCR process, and the lower the CT value. Besides being used for quantitation, the CT value can be used for qualitative analysis. The threshold should be placed above any baseline activity and within the exponential increase phase. Some software allows determination of the CT by a mathematical analysis of the growth curve. This provides better run-to-run reproducibility. The calculated CT value is the cycle at which the system begins to detect the increase in the signal associated with an exponential growth of PCR product during the log-linear phase. This phase provides the most useful information about the reaction (certainly more important than the end-point in traditional PCR).

The slope of the log-linear phase is a reflection of the amplification efficiency. The efficiency (E) of the reaction can be calculated by the formula: $E = 10(-1/slope) - 1$

The efficiency of the PCR should be 90 - 100% ($-3.6 > slope > -3.1$). A number of variables can affect the efficiency of the PCR including length of the amplicon, secondary structure and primer quality.

9.13.8 Instrumentation

Real-time PCR requires an instrument that consists of a thermal cycler, a computer, optics for fluorescence excitation and emission collection, data acquisition and analysis software. These instruments differ in sample capacity, method of excitation, reaction vessels, data processes and run time. Real-time PCR platforms from three different manufacturers were used:

9.13.8.1 LightCycler® instrument

The LightCycler® System is offered as two different instruments: the LightCycler® 1.5 Instrument for single dye or duplex assays and the LightCycler® 2.0 Instrument for a wider range of multiplexing (Figure 7).

Figure 7: The LightCycler® 2.0 (left side) and the LightCycler® 1.5 (right side).

9.13.8.2 Rotor-Gene™ instrument

The Corbett Research Rotor-Gene™ uses a centrifugal design. After the displacement of the Rotor-Gene™ 2000, the Rotor-Gene™ 3000 is available in two different configurations: the Four Channel model 3000 (also available as artus™ 3000) and the Two Channel model 3000A (Figure 8).

Figure 8: The Rotor-Gene™ 3000 (left side) and the Rotor-Gene™ 2000 (right side).

9.13.8.3 ABI PRISM ™ instrument

The ABI PRISM™ 7000, 7700 and 7900HT Sequence Detection System were used with main focus on the ABI PRISM™ 7000 SDS (Figure 9). All of the ABI PRISM instruments are Peltier-based thermal cycling systems.

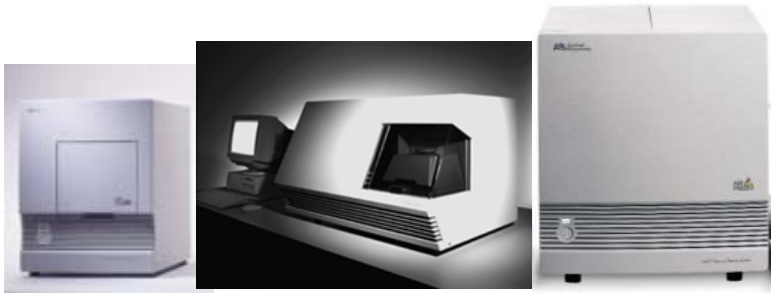

Figure 9: The ABI PRISM™ 7000, 7700 and 7900HT SDS (left to right).

9.14 ASSAY DEVELOPMENT

For improved *in vitro* diagnostic of *C. trachomatis* new real-time PCR assays were developed for the LightCycler®, Rotor-Gene™ and the ABI PRISM™ instruments. Primers and probes were designed using the Primer Express® software (version 1.0; Applied Biosystems). Sequences were selected after patent analysis. For the *artus™ C. trachomatis Plus* assay patent is pending. After primer and probe design the real-time PCRs were optimized regarding: thermal cycler conditions, Taq DNA polymerase choice and concentration, primer and probes concentration, probe labeling, magnesium concentration, internal control implementation and titration, assay volume and ROX concentration (in the case of the ABI PRISM assays).

All of the new developed assays should be used for *in vitro* diagnostics. Therefore they were CE-marked according to European directive for *in vitro* diagnostic medical devices 98/79/EC. Based on quality management guidelines validations of all assays were performed. The validation includes: pre-analytics (specimen collection, storage and transport), DNA isolation, analytical sensitivity, specificity, precision, robustness, reproducibility and diagnostic evaluation.

The analytical detection limit as well as the analytical detection limit in consideration of the purification (sensitivity limits) was assessed. The analytical detection limit in consideration of the purification is determined using *C. trachomatis*-positive clinical specimens in combination with a particular extraction method. In contrast, the analytical detection limit is determined without clinical specimens and independent from the selected extraction method, using

serovars of known concentration. Testing is carried out on three different days on eight replicates per dilution and day. The results were determined by a probit analysis (p = 0.05).

The specificity of the assays is first and foremost ensured by the selection of the primers and probes, as well as the selection of stringent reaction conditions. The primers and probes were checked for possible homologies to all in gene banks published sequences by sequence comparison analysis. The detectability of all relevant serovars has thus been ensured. Moreover, the specificity was validated with 100 different *C. trachomatis* negative swabs, 30 urine and 30 semen samples. In addition the control group listed in the following table (Table 2) has been tested for cross-reactivity.

Table 2: Testing the specificity of the kit with potentially cross-reactive pathogens.

Control group	Control group
Escherichia coli	*Proteus mirabilis*
Candida glabrata	*Proteus vulgaris*
Candida albicans	*Enterococus faecalis*
Chlamydia psittaci	*Enterobacter coloacea*
Chlamydia pneumoniae	*Klebsiella pneumoniae*
Neisseria gonorrhoeae	*Haemophilus partainfluenzae*
Salmonella enteritides	*Bordetella pertussis*
Salmonella typhimurium	*Acinetobacter spp.*
Staphylococcus aureus	*Gardnerella vaginalis*
Streptococcus pyogenes	Herpes-simplex-Virus 1 und 2
Streptococcus pneumoniae	

The precision data allow the determination of the total variance of the assay. The total variance consists of the intra-assay variability (variability of multiple results of samples of the same concentration within one experiment), the inter-assay variability (variability of multiple results of the assay generated on different instruments of the same type by different operators within one laboratory) and the inter-batch variability (variability of multiple results of the assay using various batches). The data obtained were used to determine the standard deviation, the variance and the coefficient of variation for the pathogen specific and the *Internal Control* PCR.

The verification of the robustness allows the determination of the total failure rate of the assays. 100 *C. trachomatis* negative samples of swabs, 30 of urine and 30 of semen were spiked with *C. trachomatis* control DNA (approximately threefold concentration of the analytical sensitivity limit). After extraction these samples were analyzed. In addition, the

robustness of the *Internal Control* was assessed by purification and analysis of 100 *C. trachomatis* negative swabs, 30 urine and 30 semen samples.

Reproducibility data permit a regular performance assessment of the assays as well as an efficiency comparison with other products. These data are obtained by the participation in established proficiency programs.

In addition to the *C. trachomatis* assay, a qualitative *C. pneumoniae* assay on the ABI PRISM™ 7000 SDS was developed for bacterial load measurement.

9.14.1 Measurement of bacterial load

The bacterial load was measured in each sample as well for *C. pneumoniae* DNA as for cDNA. DNA and cDNA of three independent preparations were analyzed quantitatively according to the manufacturers instructions using the *artus™ C. pneumoniae TM PCR Kit*, with each sample run in triplicate. All real-time PCRs were run on the ABI PRISM™ 7000 SDS. The sensitivity of the *artus™ C. pneumoniae TM PCR Kit* was determined by probit analysis with a dilution series from 10 to nominal 0.0125 copies/µl. All dilutions were run at least eight fold on each of three different days (24 values/dilution). On each day a different ABI PRISM™ 7000 SDS instrument was used to consider the instrument variations.

9.14.2 Real-time PCR

Primers and probes were designed using the Primer Express® software. TaqMan probes were labeled at the 5’ end with the reporter dye molecule FAM (emission wavelength, 518 nm) and at the 3’ end with the black hole quencher dye BHQ1. All real-time PCRs were run on the ABI PRISM™ 7000 SDS. Each real-time PCR sample was run in quadruplicate, on each of three independent MOI 30 experiments and two independent MOI 3 experiments, respectively.

All real-time PCR data were normalized to levels of three parallel used endogenous controls, beta-glucuronidase (GUS), TATA-Box binding protein (TBP), and 18S rRNA, which ran in triplicate on each experiment. Relative quantitation was performed using the standard curve method. As sample of known concentration to construct a standard curve total cervical adenocarcinoma RNA was used. For quantitation normalized to endogenous controls, standard curves were prepared for both the target and the endogenous control. For each experimental sample the amount of target and endogenous control was determined from the appropriate standard curve. For each analyzed gene, negative controls and RNA samples

undergoing cDNA synthesis without addition of reverse transcriptase (no RT controls) were run to control for genomic DNA contaminations.

9.14.3 PCR efficiency measurements

Efficiency values were measured using the CT slope method. This method involves generating a dilution series of the target template and determining the CT value for each dilution. A plot of CT versus log cDNA concentration was constructed. Linear regression gave a linear equation (y = ax+b). The expected slope (a) for a 10-fold dilution series of template is -3.32, when $E_x = 1.0$. Amplification efficiency was calculated from the slope of the linear regression equation using: $E_X = 10^{(-1/slope)} -1$. For example, if the slope is -3.33, then the amplification efficiency is: $E_X = 10^{(-1/-3.33)} -1 = 1.995-1 = 0.995$ or 99.5%.

9.15 NORTHERN BLOT ANALYSIS

Northern blot analysis was performed on RNA from mock- and *C. pneumoniae*-infected HeLa-cells (MOI 30) of one out of three independent preparations in the IFN-γ persistence model. RNA was blotted on BrightStar-Plus positively charged nylon membranes using the TurboBlotter™ System according to the manufacturers instructions. ^{32}P-labeled specific probes (UN2910 radioactive material, 10,000 MBq, 0.2703 mCi, purity ≥ 90%, KRT17 11.14 kIPS, CYR61 22.6 kIPS, TBP 10.3 kIPS and HSPA1 9.8 kIPS, labeled with α-^{32}P dATP, specific activity 110 TBq/mmol, Hartmann Analytic GmbH, Braunschweig, Germany) were hybridized to the membranes according to the BD Atlas™ cDNA Expression Arrays user manual (BD Biosciences Clontech, protocol #PT3140-1, version #PR26790), wrapped in plastic foil and exposed 14 days to a storage phosphor screen. The imaging screen was scanned and analyzed using the Typhoon™ 9210 scanner in combination with the ImageQuant® software version 5.2. *File Info:* Header Size = 8; File Size = 7533432; Width = 2140; Height = 1760; Bits/Pix = 16; Samples/Pix 1; Min Value = 0.00; Max Value = 99999.89; Background = White. *Scan Info:* Pixel Size = 200; Scan Resolution = 50 dots/cm; Image Type = Single Channel; Storage Phosphor Mode; 750 V; Normal Sensitivity; Scanned A1 to R22; 390BP/Red (633nm). All analyzed genes were normalized on RNA levels in each sample, measured with the Agilent Bioanalyzer Total RNA Nano chip before Northern blotting, or on the endogenous control TBP, measured in each sample during Northern blot analysis. The regulation factors for Northern blot analysis were obtained from normalized signal volumes and compared to the corresponding mock-infected sample.

10. Results

10.1 *CHLAMYDIA PNEUMONIAE* PERSISTENCE IN THE IFN-γ MODEL - HOST-CELL RESPONSES

10.1.1 Screening of host-cell gene regulation by microarrays

During chlamydial persistence different gene expression patterns occur in the infected host-cell depending on the persistence model (Peters *et al.*, 2005; Hess *et al.*, 2003). In two of the three analyzed models a shut down of *Chlamydia*-induced host-cell responses was observed for several genes at later time points of persistent infection. This led to the hypothesis that other pathways might be stimulated or down-regulated by *C. pneumoniae*, especially at later time points of persistence, which influence the fate of the bacteria and the clinical course of *Chlamydia*-related diseases.

To verify the first part of this hypothesis, the transcriptional responses of HeLa-cells to *C. pneumoniae* and mock infection with and without IFN-γ-induced persistence were examined 24h and 96h post infection. Affymetrix® U133A human genome chips consisting of 22,284 human gene probe sets were used as the first step of this analysis in two independent experiments. To achieve high sensitivity in the screening and to permit direct comparison with the data obtained in former investigation (Peters *et al.*, 2005), a multiplicity of infection (MOI) 30 was used (and later compared to the effect of a MOI of 3 in more specific assays). The two experiments correlated with a mean Pearson coefficient of 0.99 (standard deviation: 0.0028) by comparing equivalent samples (subset of data shown in Figure 10).

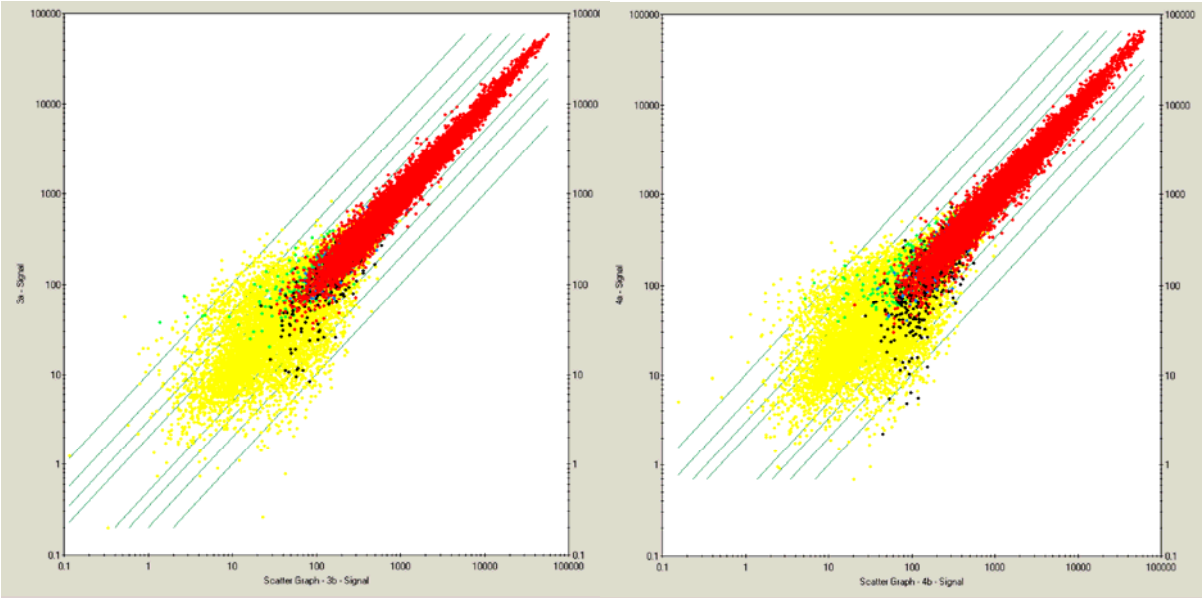

Figure 10: Scatter plot analysis for two independent microarray experiments of 24h mock-IFN-γ-infected (left) and *C. pneumoniae*-IFN-γ-infected (right) HeLa-cells. The lines displayed in the graph represent 2-, 3-, 5- and 10-fold changes. Red colored signals are present in baseline and in experiment (P-P call), black colored signals are present in baseline but absent in experiment (P-A call), green colored signals are absent in baseline but present in experiment, yellow dots represent absent or marginal signals and blue colored signals are marginal or present in baseline or experiment. Pearson's correlation coefficient for mock-IFN-γ comparison analysis is 0.991 and for *C. pneumoniae*-IFN-γ comparison analysis is 0.986.

Analysis of HeLa-cell gene expression data showed that in comparison to mock-infected HeLa-cells, the mRNA expression of 66 genes was in both experiments up- or down-regulated by at least 2.5-fold in *C. pneumoniae* productive-infected cells or during IFN-γ-induced persistence (data shown in supplementary Table S1). All selected genes with altered gene expression had signal log ratios higher 1.32 or lower -1.32 ($\alpha 1 = 0.05$; $\alpha 2 = 0.065$; $\tau = 0.015$) and represent calls in both samples (treatment versus mock at the corresponding time-point). Approximately half of these genes showed a decrease in at least one sample type (24h p.i., 24h and 96h p.i. with IFN-γ persistence induction). The other half of which were up-regulated.

10.1.2 Determination of *C. pneumoniae* ompA cDNA by real-time PCR as an additional indicator of persistence

To confirm our DNA microarray findings, we performed semiquantitative real-time PCRs for 19 HeLa-cell genes that were regulated during infection with *C. pneumoniae* using total RNA obtained in three sets (A, B, C) of biologically independent experiments (Table 3 or supplementary Table S2 for detailed information - including complete gene name, abbreviation, probe set and accession number). Prior to relative quantitation of these genes the total RNA was reverse transcribed and analyzed quantitatively by the *artus™ C. pneumoniae TM PCR Kit* for the expression of ompA from *C. pneumoniae*. This gene coding for a cell-wall component is down-regulated in persistent chlamydial infection (Beatty *et al.*, 1994b). As expected, the level of ompA-cDNA decreased 96 h post-infection (~15-20%), further confirming that this was the optimal time-point to study persistence (upper panel of Figure 11). In the mock-infected control samples, no *C. pneumoniae* ompA mRNA was detected, thus no contamination had taken place during RNA preparation and processing.

10.1.3 Determination of bacterial load by real-time PCR of chlamydial DNA

To confirm similar rates of infection in the corresponding samples, ompA-DNA levels were determined by the *artus™ C. pneumoniae TM PCR Kit* on the ABI PRISM™ 7000 SDS.

HeLa-cells of three independent preparations were infected with *C. pneumoniae* and mock-infected with or without IFN-γ-induced persistence. RNA and DNA was harvested from cell culture 24h and 96h post infection.

The testing of 48 control groups, such as *B. pertussis*, *C. trachomatis*, *C. psittaci*, *Haemophilus* and *Mycobacteria*, confirmed the specificity of the *artus™ C. pneumoniae TM PCR Kit* (see Table 23 for details). No cross-reactivity was seen, while both *C. pneumoniae* types were detected with a detection limit of 0.9 copies/µl (Figure 36).

The bacterial load differed no more than ~3-fold between the samples of one biological replicate, and it was also very similar when comparing the three independent sets (lower panel of Figure 11).

Table 3: List of genes selected for real-time PCR confirmation

Gene Name	Gene symbol
BCL2 adenovirus E1B 19kD-interacting protein 3	BNIP3
carbonic anhydrase IX	CA9
cystathionase	CTH
cysteine-rich, angiogenic inducer 61	CYR61
Dapper homolog 1	DACT1 or LOC51339
Adlican	DKFZP564I1922
dickkopf (Xenopus laevis) homolog 1	DKK1
hairy/enhancer-of-split related with YRPW motif 1	HEY1
heat shock 70kD protein 1A	HSPA1A
heat shock 70kD protein 1B	HSPA1B
insulin induced gene 1	INSIG1
keratin 17	KRT17
lysyl oxidase	LOX
IFN-induced, microtubular aggregate protein (44kD)	MTAP44 or IFI44
N-myc downstream regulated	NDRG1
2'-5'oligoadenylate synthetase-like	OASL
prostaglandin E receptor 4 (subtype EP4)	PTGER4
retinoic acid induced 3	RAI3
serum-inducible kinase or polo-like kinase 2	SNK or PLK2

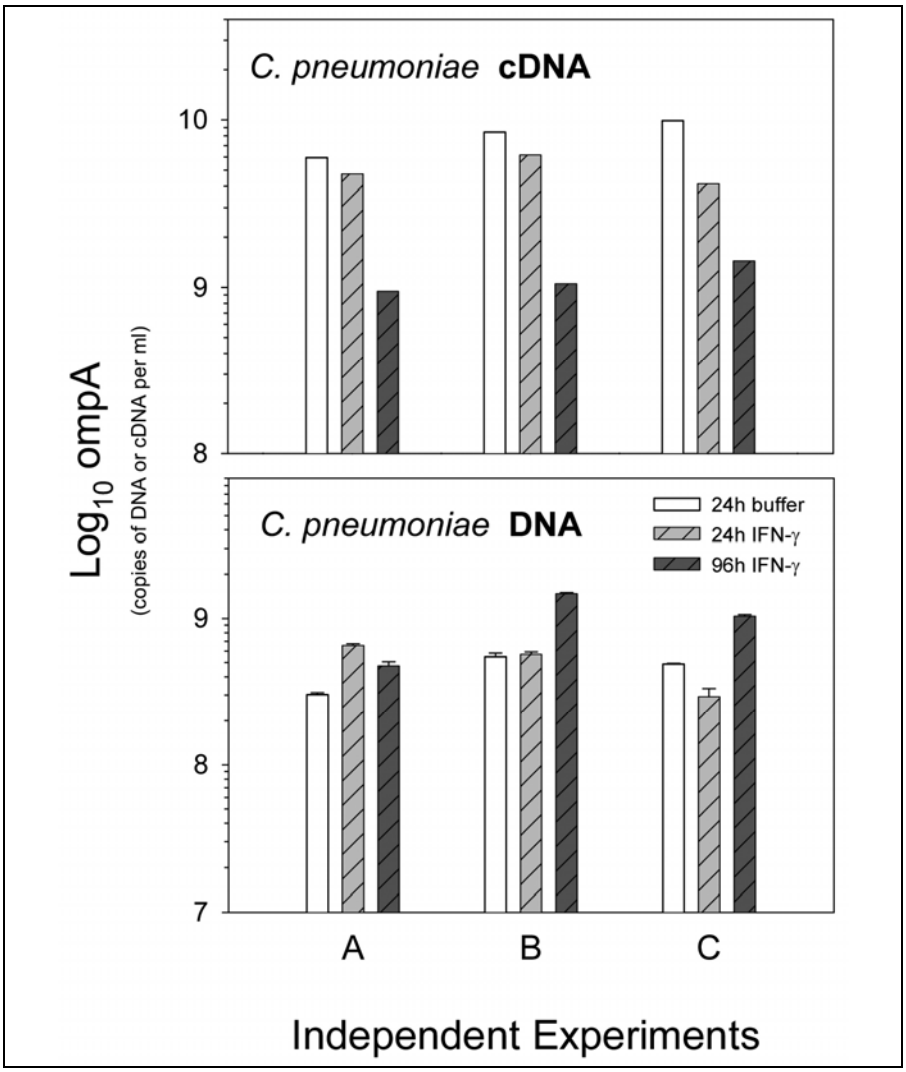

Figure 11: Determination of cDNA and DNA for ompA of *C. pneumoniae*, demonstrating changes in the expression of this chlamydial gene in IFN-γ-induced persistence as well as similar bacterial loads in the three biologically independent infection experiments (A, B, C) which were analyzed by real-time PCR. The amount of ompA-DNA was determined in triplicate for each of the three infection experiments. Depicted are mean ± SD. The quantification of ompA-RNA (cDNA) was performed on a single sample of each of the three infection experiments due to the limited amount of this material.

10.1.4 Endogenous controls for the analysis of *C. pneumoniae*-induced host-cell responses

Gene expression analysis by real-time PCR is a sensitive and accurate method consisting of several steps, including cell processing, RNA extraction, RNA storage and cDNA synthesis prior to PCR. To compensate for potential variability the expression of endogenous controls is commonly assessed in parallel with the gene of interest. Ideally the endogenous control is not influenced by the experimental conditions and so constantly regulated. Therefore, its exact quantification permits the normalization of the individual samples.

Seven genes were examined to find suitable controls for normalizing the gene expression in *C. pneumoniae*-infected HeLa-cells with and without persistent induction using real-time PCR: Glyceraldehyde-3-phosphate dehydrogenase (GAPDH), beta-glucuronidase (GUS), glucose 6-phosphate dehydrogenase (G6PDH), RNA polymerase 2 (RNAPII), TATA-Box binding protein (TBP), alpha-tubulin (TUB) and 18S rRNA. The expression data of these genes were measured in the different sample types (not infected 24h, productively infected 24h, not infected with addition of IFN-γ 24h and 96h, infected and persistently induced 24h and 96h). Afterwards, the single genes became combined as a couple together (ΔC_T) and their relative quantity was set into ratio to each other. Under the assumption that constantly regulated genes do not change their relation to one another in the different sample types ($\Delta C_T = 1$), those genes were selected, that showed the lowest variation (subset of data shown in Figure 12 and Table 4).

Table 4: Pairwise variations of selected endogenous controls. To have more comparable results the expression levels for all three genes were correlated to one control sample (24h mock-infected + IFN-γ = 1.00).

Sample Type	ΔC_T 18S/GUS	ΔC_T 18S/TBP	ΔC_T GUS/TBP
24h *C. pneumoniae*-infected	1.00	1.00	1.00
24h *C. pneumoniae*-infected + IFN-γ	0.99	0.98	0.99
24h mock-infected	1.01	1.01	1.00
24h mock-infected + IFN-γ	1.00	1.00	1.00
96h *C. pneumoniae*-infected + IFN-γ	0.98	1.00	1.01
96h mock-infected + IFN-γ	1.00	1.01	1.01

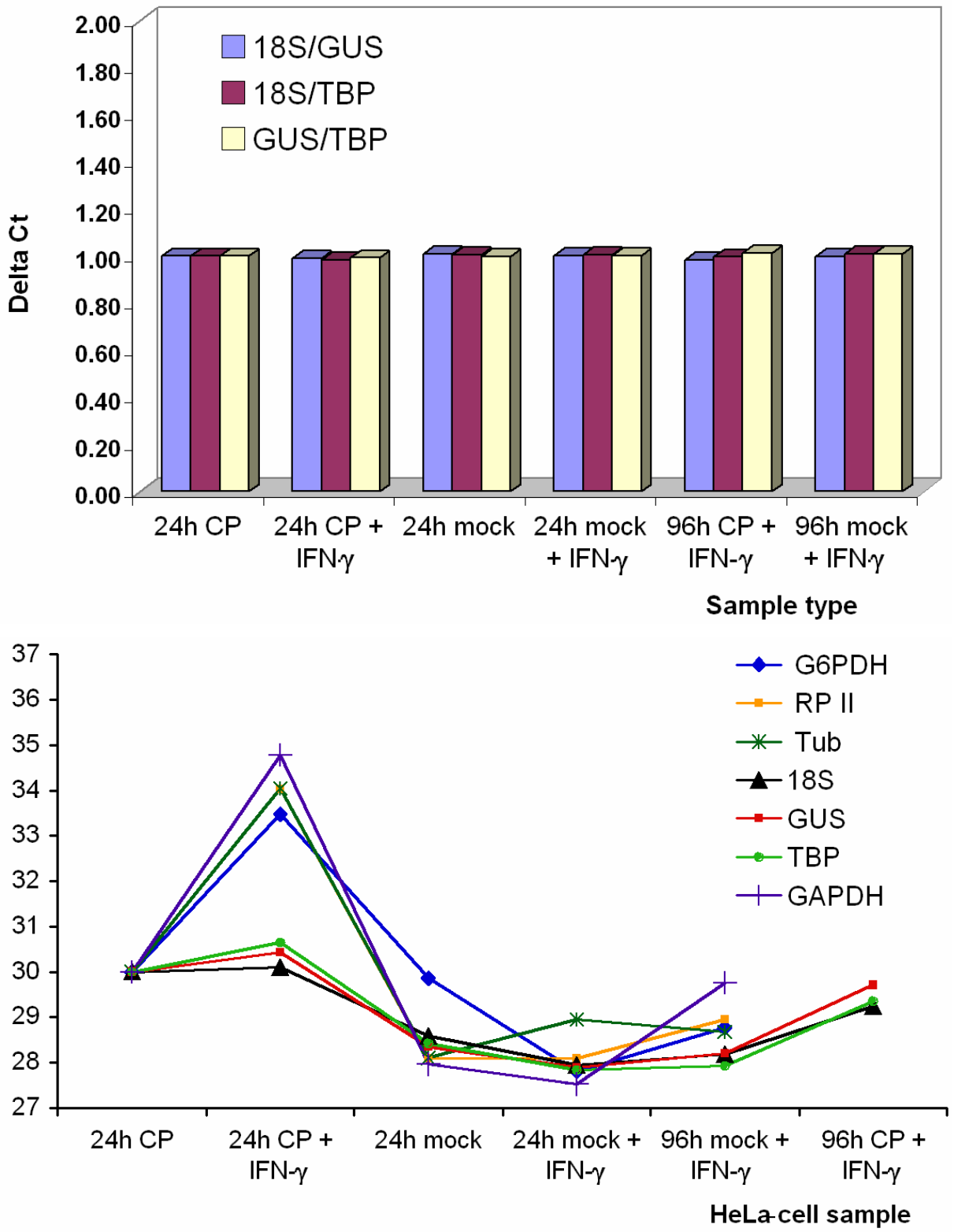

Figure 12: Evaluation of endogenous controls. Gene expression of seven HeLa-cell genes in different sample types was analyzed by real-time PCR. Striking are the similar expression levels of the genes 18S rRNA, GUS and TBP showing delta CT values around 1.0 (upper diagram). In comparison, G6PDH, RP II, Tub, and GAPDH strongly vary in their expression (lower diagram).

Using real-time PCR, significant differences in the expression of some control genes were detected between the different HeLa-cell samples; gene G6PDH showed the largest deviation. The genes 18S rRNA, GUS, and TBP were identified as endogenous controls with a 0.02 variation in expression ratios. The similar expression levels of the three selected genes was verified in an experimental setting using dilution series of different HeLa-cell samples (Figure 13). To compensate for the small variations observed, all three genes (18S rRNA, GUS and TBP) were chosen for normalization in parallel by taking the geometric average, instead of using only one endogenous control. The selected genes, which are members of distinct gene families, underlie different transcription mechanisms and show different transcription levels. Therefore, by using these multiple endogenous controls, the control genes are not co-regulated and accurate normalization is achieved.

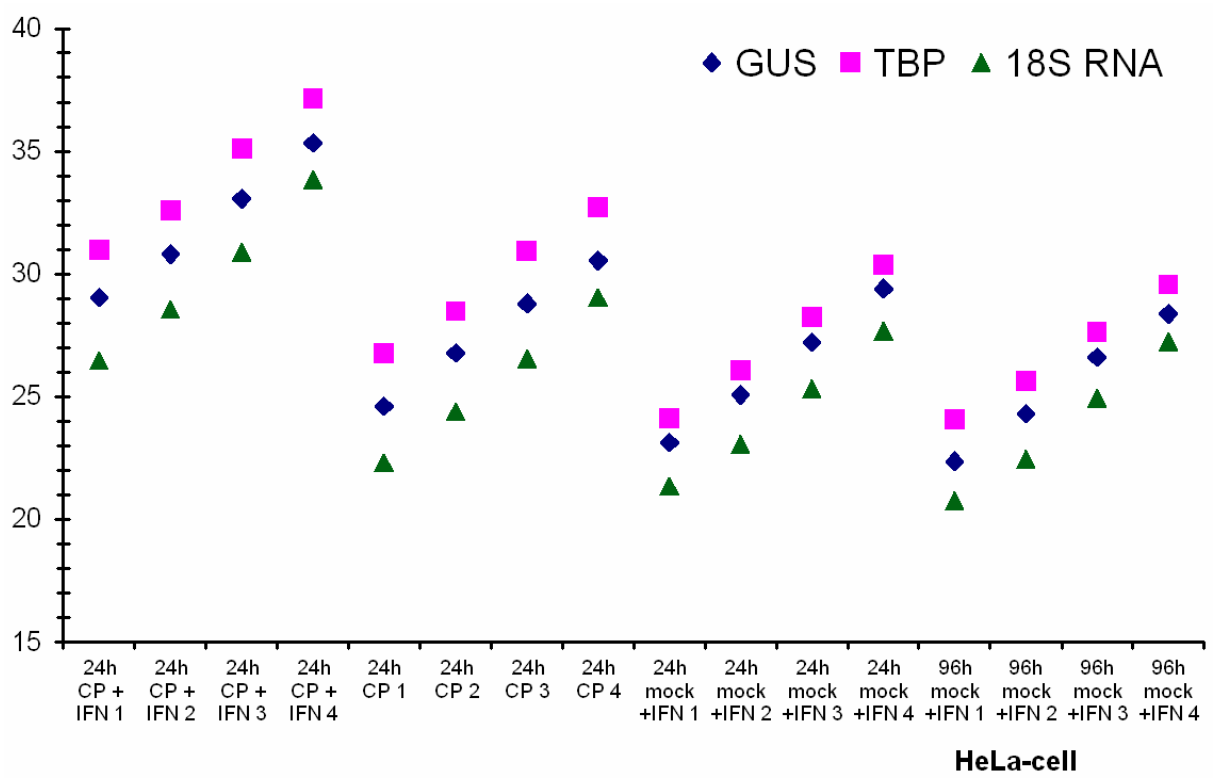

Figure 13: Expression levels of 18S rRNA, GUS and TBP in different dilutions (stock, 1:2, 1:4 and 1:16) of particular HeLa-cell samples.

10.1.5 Host-cell gene expression profiling during active and persistent *C. pneumoniae* infection by real-time PCR

After choosing the endogenous controls for determining *C. pneumoniae*-induced host-cell responses, real-time PCRs (two-step RT-PCRs) were set up for eight genes from the microarray screening and the three endogenous controls (for primer und probe sequences see supplementary Table S3). For the remaining eleven genes, TaqMan pre-developed assay reagents (Applied Biosystems, see supplementary Table S4) were used. The PCR efficiency of all assays was determined using the CT slope method on the ABI PRISM™ 7000 SDS. All real-time PCR assays had PCR efficiencies greater than 90% and the calculated R-squared value for each standard curve was at least 0.99. All of the analyzed samples (target genes of different sample types) were within the linear range of the standard curves to ensure accurate quantitation (see Figure 14 for example of ABI PRISM™ 7000 SDS run to access relative gene expression data by real-time PCR). For generation of a standard curve Ambion HeLa-S3 RNA was used (1 µg/µl). Real-time PCR ensured linearity of cDNA synthesis by comparison of dilution series of RNA and cDNA (0.17; 0.017 and 0.0017 µg/µl). Therefore, standard dilutions were prepared after cDNA synthesis.

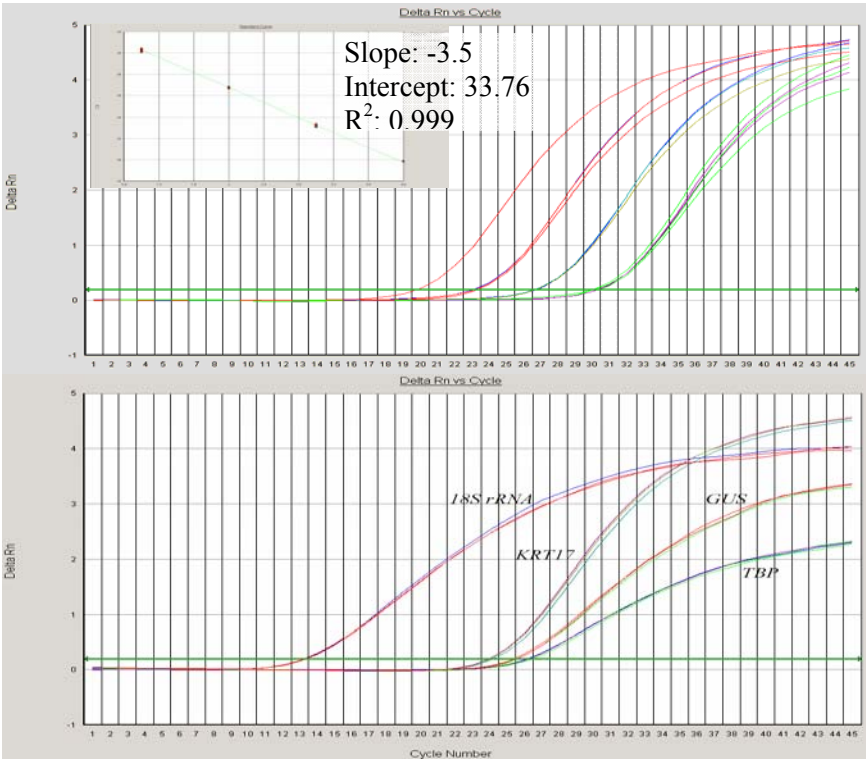

Figure 14: Example of relative quantitation of KRT17 cDNA on the ABI PRISM™ 7000 SDS. On the upper panel, a dilution series of cDNA (prepared from HeLa-cell S3 RNA) is depicted, which was used to generate a standard curve (small embedded picture). In the same run, mock- and *C. pneumoniae*-infected samples were analyzed, detecting KRT17 and the endogenous controls 18S rRNA, GUS and TBP cDNA (quadruplicates on sample 96h mock+IFN-γ, lower panel).

Real-time PCR results identified two sets of differentially regulated genes: permanently up- or down-regulated. In the first group, seven genes are permanently up-regulated: DKK1, CYR61, RAI3, OASL, IFI44, PLK2 and PTGER4 whereby DKK1, CYR61 and RAI3 showed a decrease in up-regulation during the persistent infection (Figure 15).

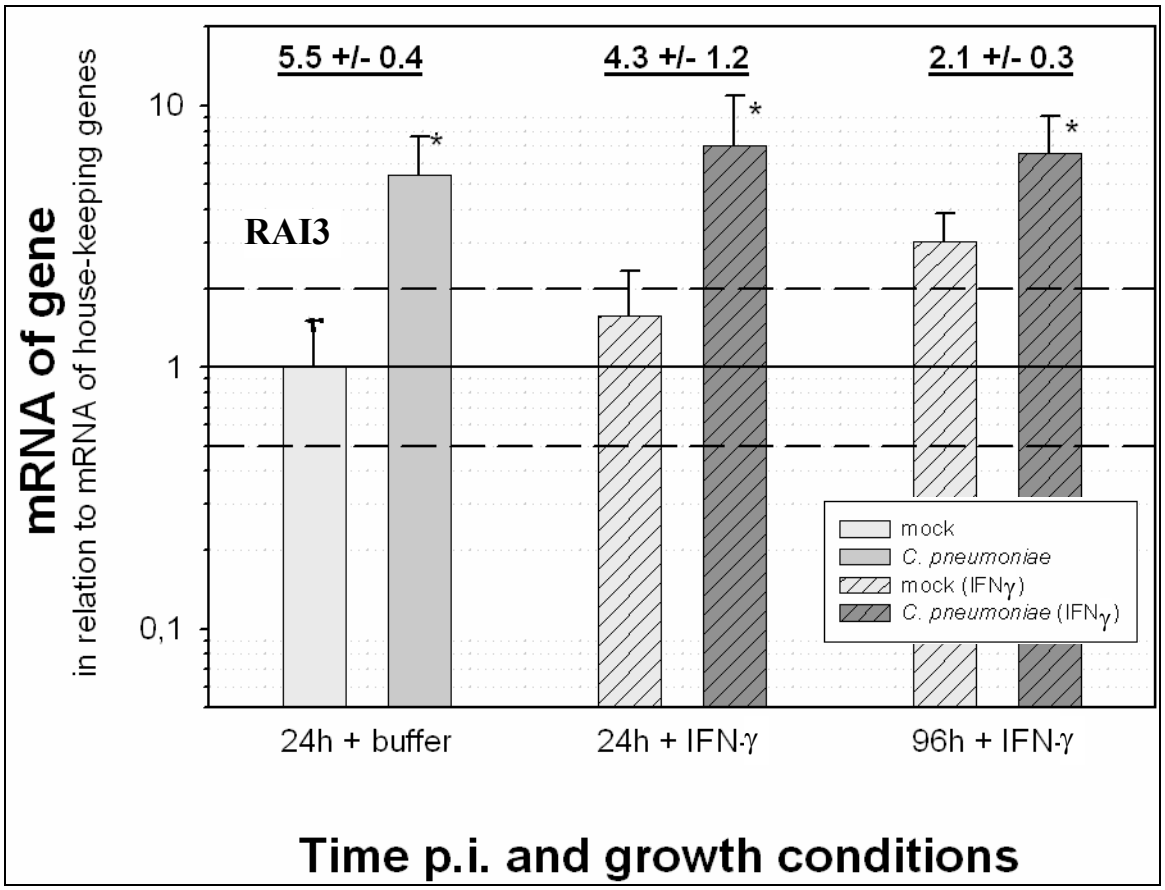

Figure 15 (Part 1): Changes in the expression of RAI3 detected by real-time PCR. A permanent increase in RAI3 was observed after productive chlamydial infection and IFN-γ-induced persistent infection. Depicted are the normalized mRNA values and means ±SD obtained in three independent experiments, with quadruplicate data sets for each experiment (*$p < 0.05$, significant mRNA difference).

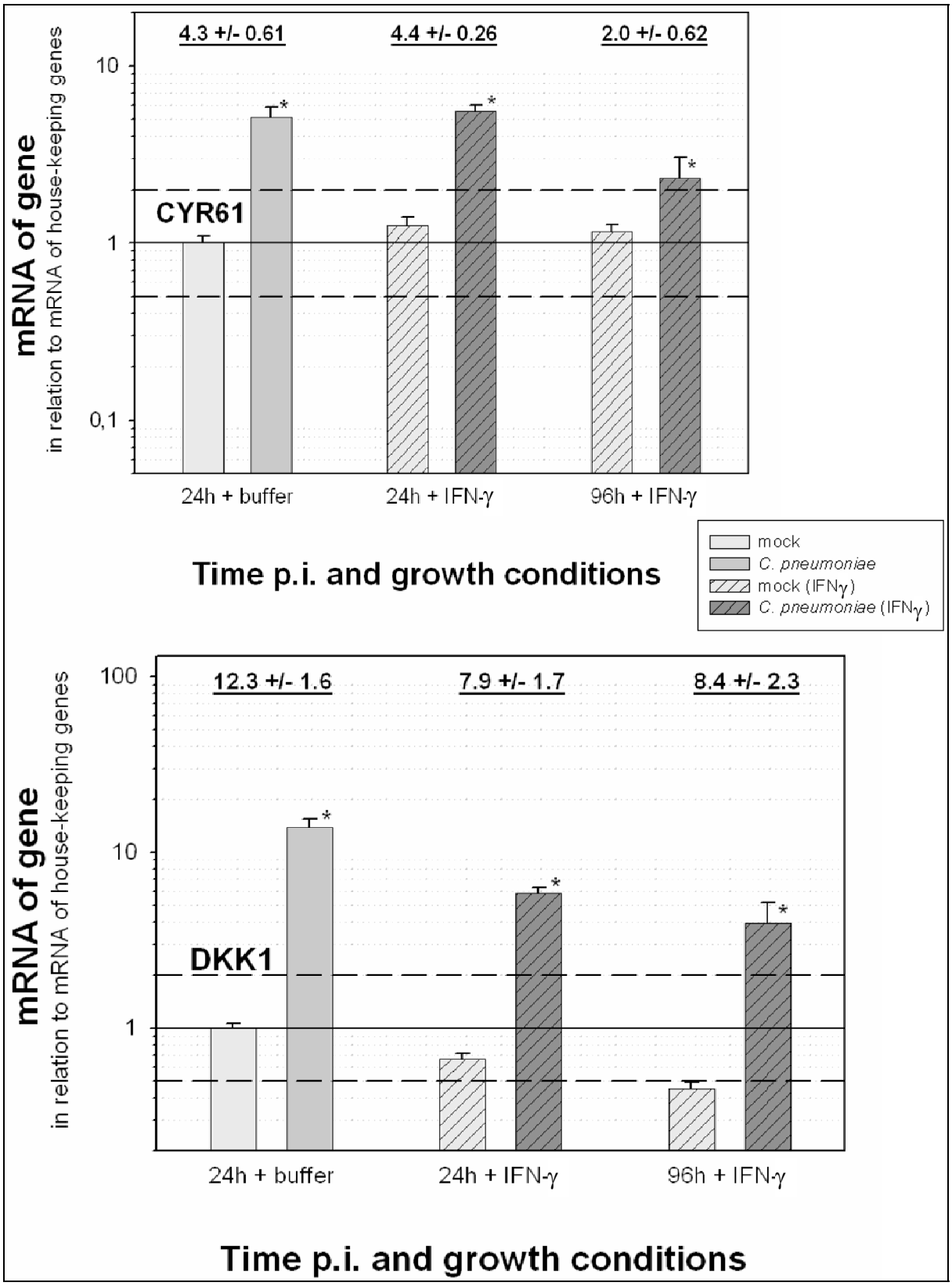

Figure 15 (Part 2): Changes in the expression of DKK1, CYR61 and RAI3 detected by real-time PCR. A permanent increase in the three genes was observed after productive chlamydial infection and IFN-γ-induced persistent infection. Depicted are the normalized mRNA values and means ±SD obtained in three independent experiments, with quadruplicate data sets for each experiment (*$p < 0.05$, significant mRNA difference).

OASL, IFI44, PLK2 and PTGER4 showed a slightly higher up-regulation after 96h of chlamydial persistence compared to 24h and productive infection (Figure 16). A 2-fold change in gene regulation was termed significant and chosen as a suitable cut-off point.

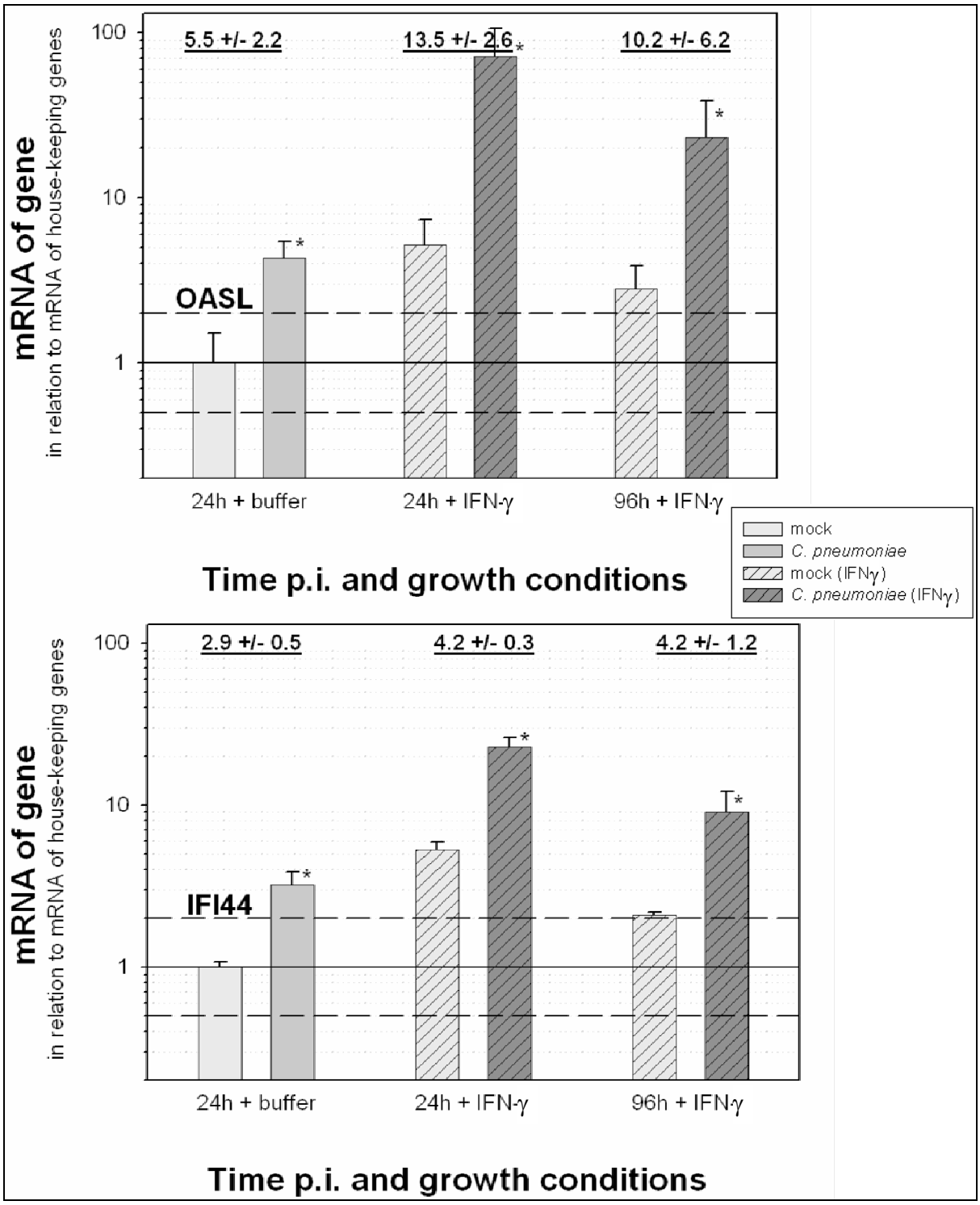

Figure 16 (Part 1): Changes in the expression of OASL and IFI44 detected by real-time PCR. A permanent increase in the two genes was observed after productive chlamydial infection and IFN-γ-induced persistent infection. Depicted are the normalized mRNA values and means ±SD obtained in three independent experiments, with quadruplicate data sets for each experiment (*$p < 0.05$, significant mRNA difference).

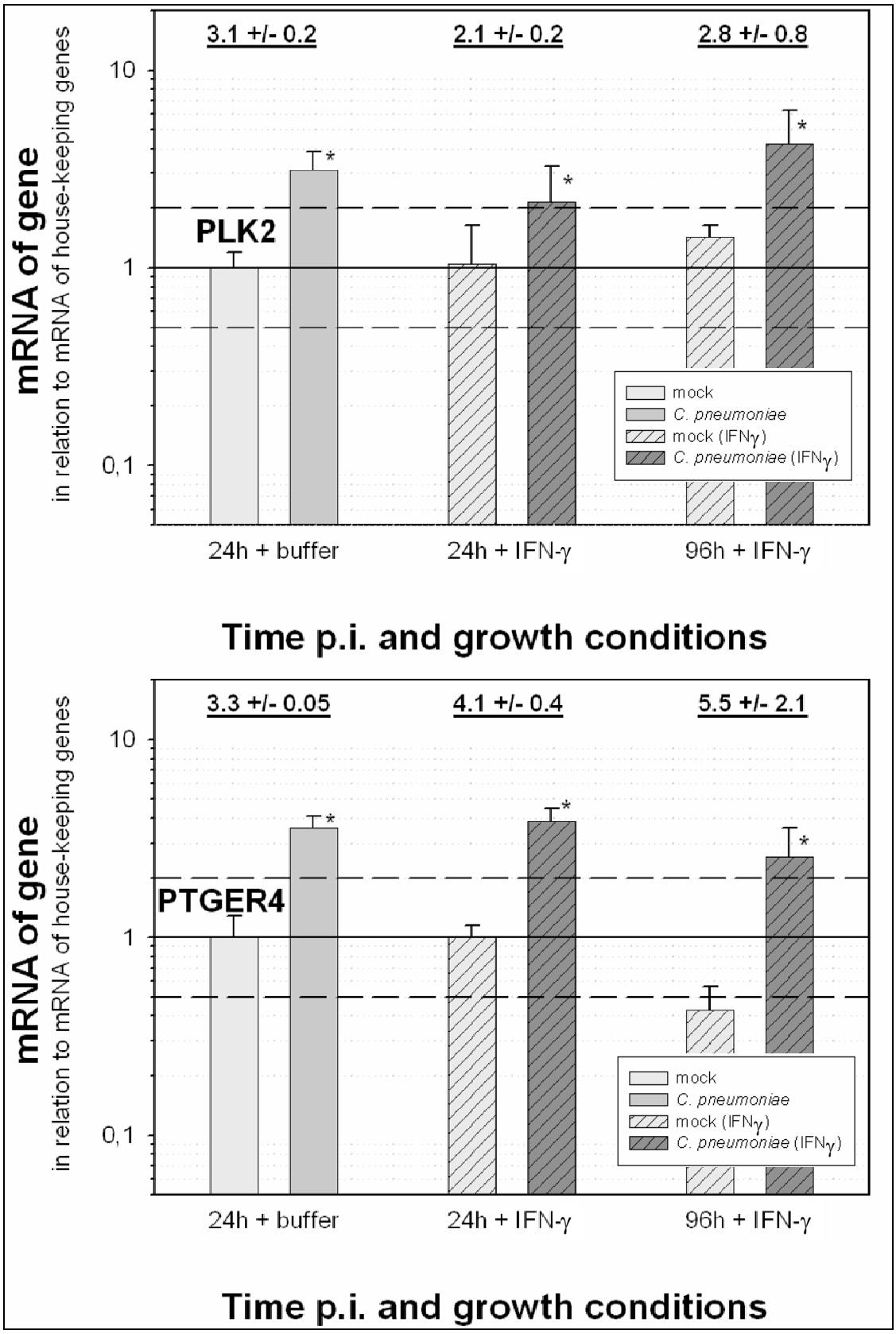

Figure 16 (Part 2): Changes in the expression of PLK2 and PTGER4 detected by real-time PCR. A permanent increase in the two genes was observed after productive chlamydial infection and IFN-γ-induced persistent infection. Depicted are the normalized mRNA values and means ±SD obtained in three independent experiments, with quadruplicate data sets for each experiment (*$p < 0.05$, significant mRNA difference).

The second group contains nine permanently down-regulated genes: Adlican, BNIP3, CA9, CTH, Insig1, LOC51337, LOX, NDRG1 and HEY1. The majority of these genes showed an increased down-regulation at 96h of persistence (Figure 17). Hence, Adlican, BNIP3, CA9, LOC51337, LOX and NDRG1 passed the 2-fold gene regulation cut-off point only 96h after induction of persistence representing a significant change.

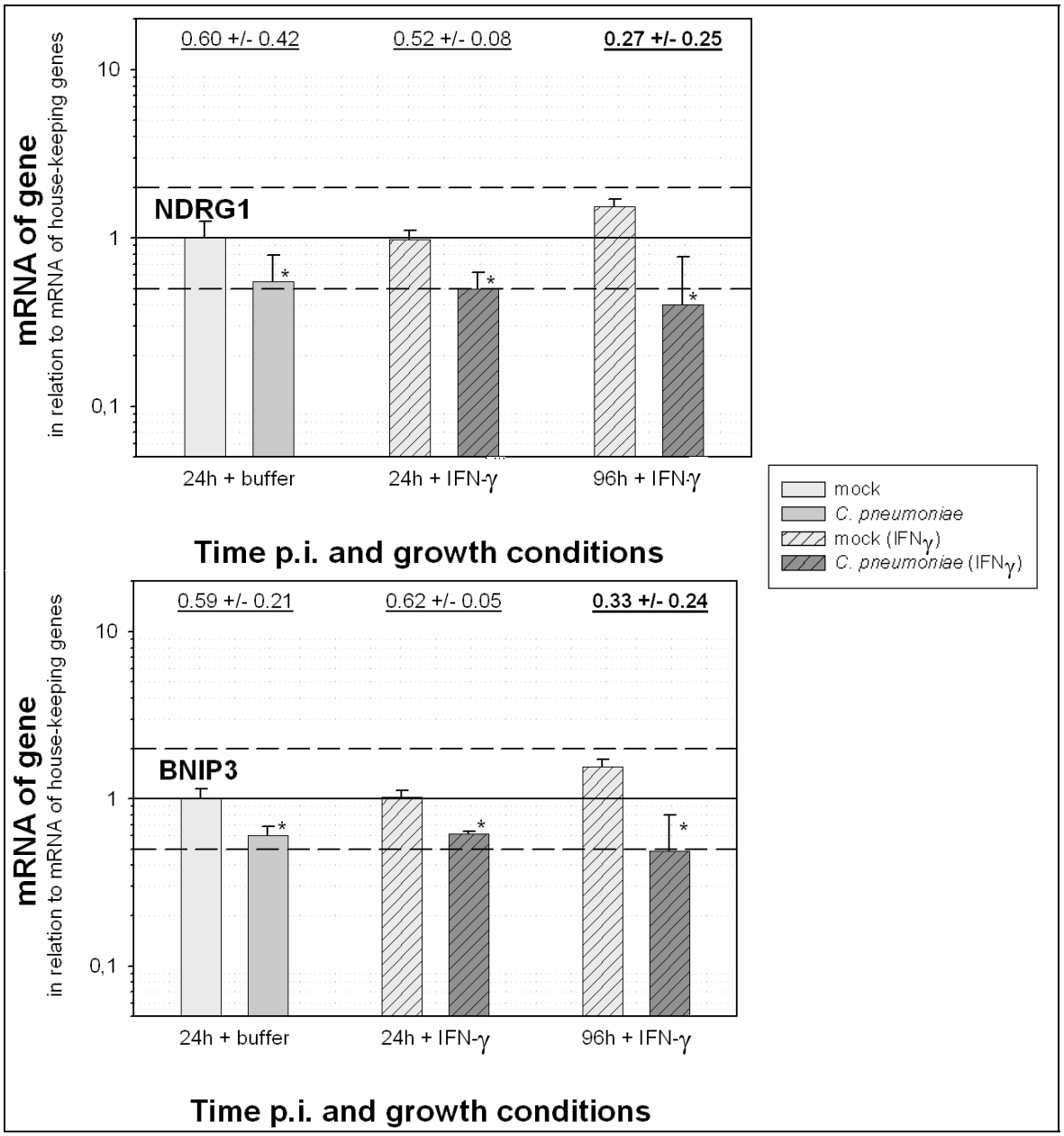

Figure 17 (Part 1): Changes in the expression of NDRG1 and BNIP3 detected by real-time PCR. A permanent decrease in the two genes was observed at 96h after IFN-γ-induced persistence. Depicted are the normalized mRNA values and means ±SD obtained in three independent experiments, with quadruplicate data sets for each experiment (*$p < 0.05$, significant mRNA difference).

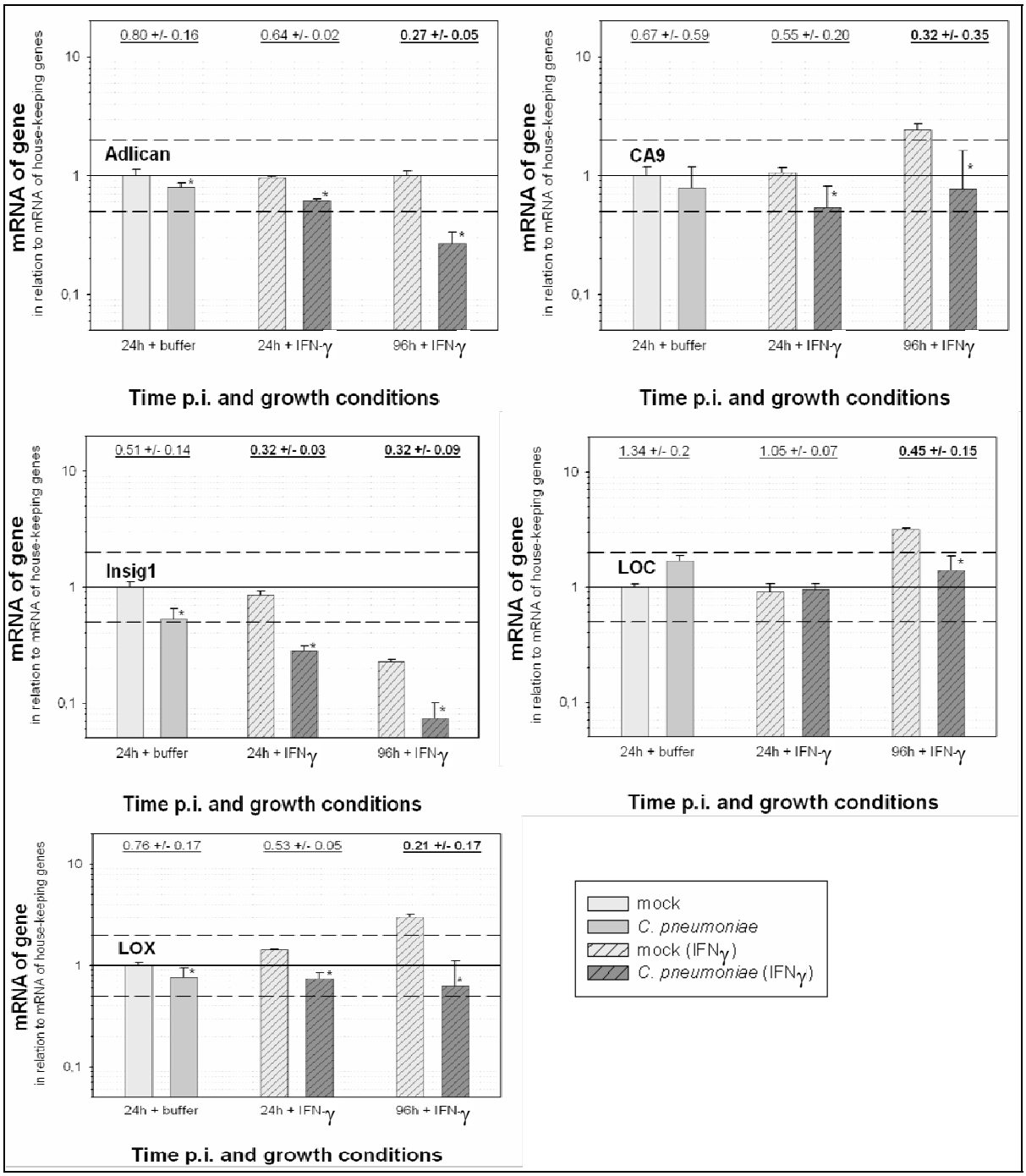

Figure 17 (Part 2): Changes in the expression of Adlican, CA9, Insig1, LOC51337, and LOX detected by real-time PCR. A permanent decrease in the five genes was observed at 96h after IFN-γ-induced persistence. Depicted are the normalized mRNA values and means ±SD obtained in three independent experiments, with quadruplicate data sets for each experiment (*$p < 0.05$, significant mRNA difference).

The genes, CTH and HEY1, were only significantly down-regulated 24h after induction of persistence passing the 2-fold cut-off point (Figure 18).

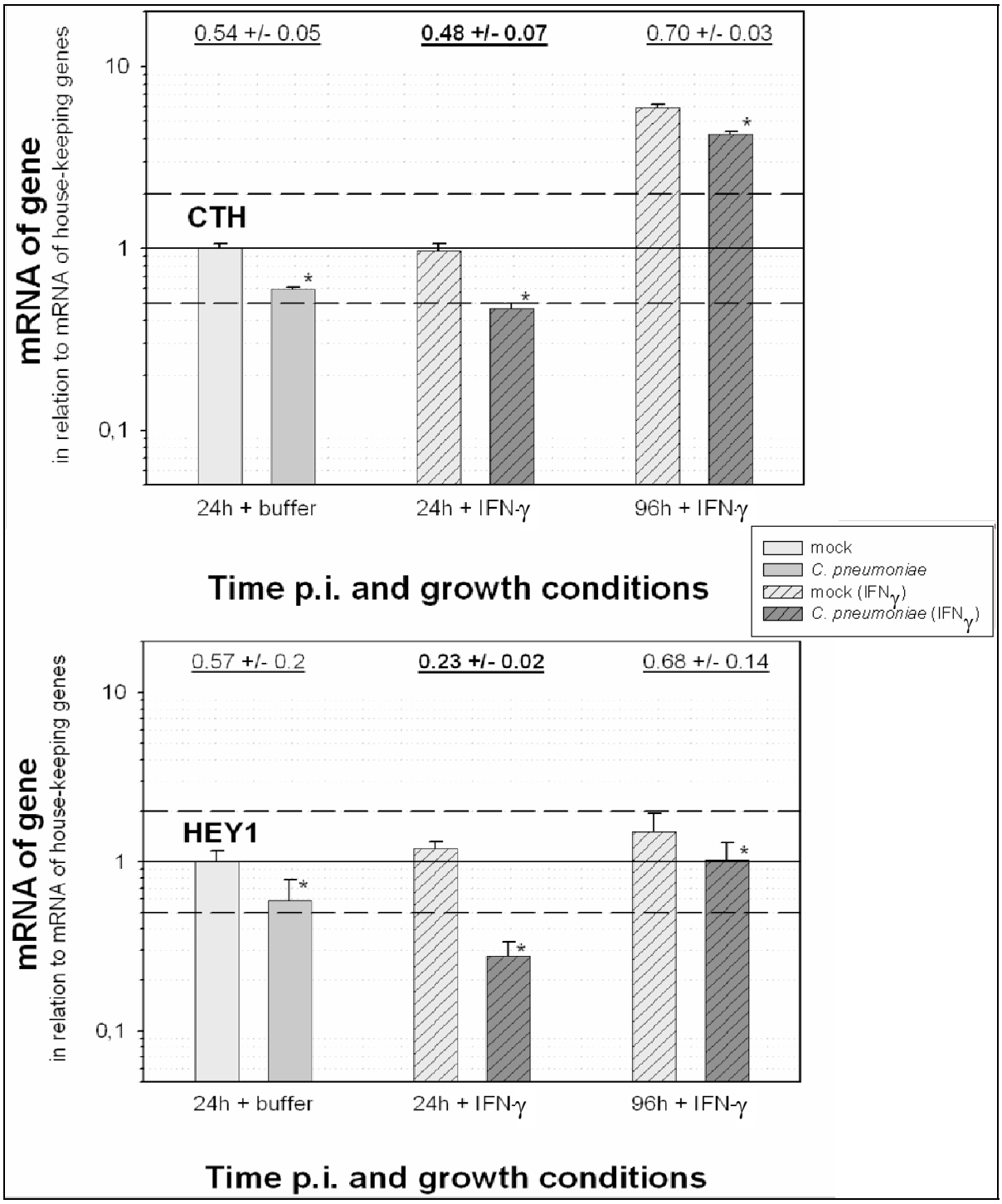

Figure 18: Changes in the expression of CTH and HEY1 detected by real-time PCR. A permanent decrease in the two genes was observed at 24h after IFN-γ-induced persistence. Depicted are the normalized mRNA values and means ±SD obtained in three independent experiments, with quadruplicate data sets for each experiment (*$p < 0.05$, significant mRNA difference).

The gene, KRT17, could be placed into both groups of gene regulation because it showed an increase in expression 24h after chlamydial productive infection and 24h after IFN-γ-induced persistent infection as well as a decrease in expression 96h after persistence (Figure 19).

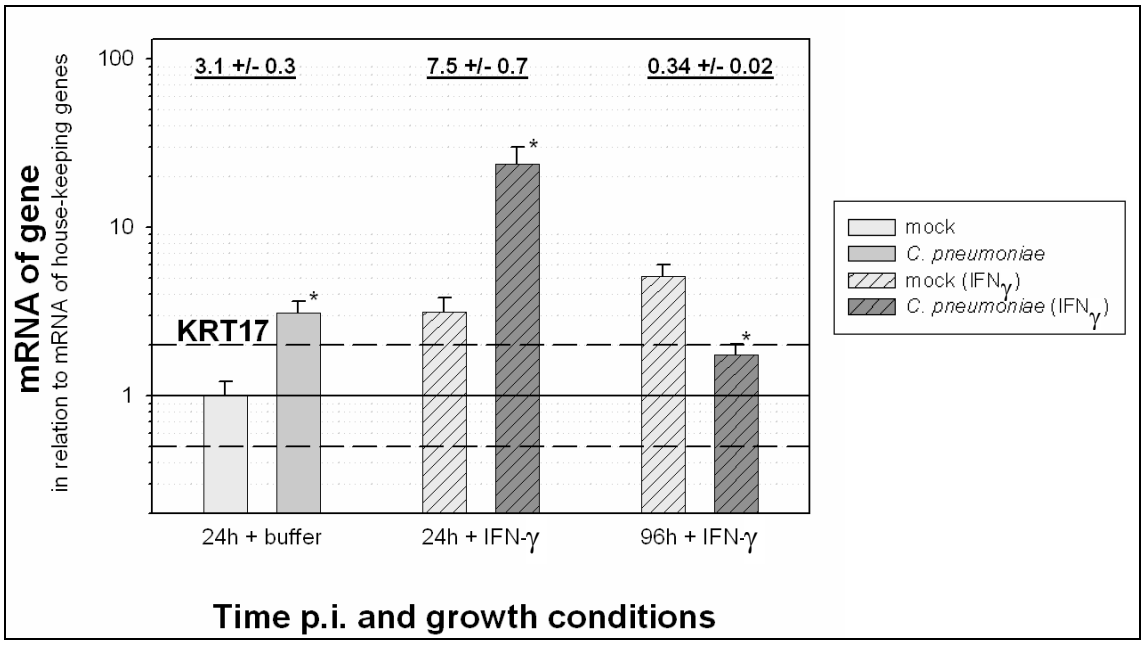

Figure 19: Changes in the expression of KRT17 detected by real-time PCR. The gene expression of KRT17 was up-regulated 24h after productive infection and IFN-γ-induced persistence but down-regulated 96h after induction of persistence. Depicted are the normalized mRNA values and means ±SD obtained in three independent experiments, with quadruplicate data sets for each experiment (*$p < 0.05$, significant mRNA difference).

The regulation of two (HASPA1-A and HSPA1-B) out of the 19 genes identified by genome chips and by real-time PCR could not be confirmed. To confirm that our negative results are not due to unspecificity by co-amplifying and detecting related (non-regulated) genes, three different PCRs were developed based on different target regions of those two genes. The third PCR target region was the same as used by Affymetrix® for microarray analysis (Annotation Transcript Cluster [# of Matching Probes]: ENST00000244526 [11], ENST00000211738 [11], GENSCAN00000035132 [11], GENSCAN00000035133 [11], NM_005345 [11], BC063507 [11], AK097113 [11]). However, none of the HSPA1-PCRs showed an altered gene expression in chlamydial infection. In comparison, by using microarray analysis, these two genes were up-regulated about 11-fold 24h post IFN-γ-induced persistence (Figure 20).

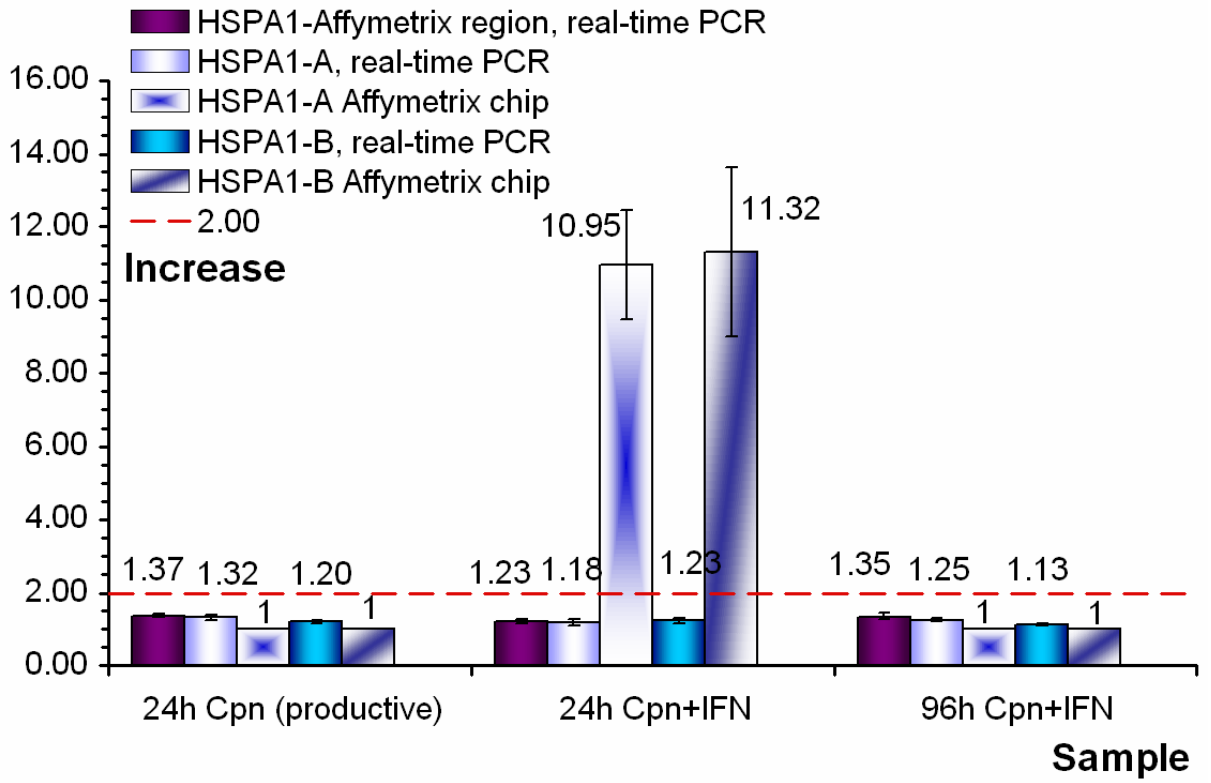

Figure 20: Comparison of gene expression data from Affymetrix® U133A human genome chips with real-time PCR results for HSPA1-A and HSPA1-B during productive and persistent infection (24h and 96h) of HeLa-cells. Affymetrix® chips were run in duplicates whereas three-independent real-time PCR experiments were carried out. Depicted are the mean changes in regulation compared to mock-infected HeLa-cells with or without IFN-γ addition, respectively. All depicted mean changes in regulation were significant ($p \leq 0.05$) since they passed the ≥ 2-fold cut-off point.

The PCR product for the Affymetrix® region-based-PCR was analyzed by sequencing to ensure specificity (supplementary data shown in Supplement Table S1).

Real-time PCR analysis for some of the genes (BNIP3, CA9, DKK1, KRT17, LOX and OASL) was repeated after infection with *C. pneumoniae* at a MOI of 3, which is a more physiological condition than a MOI of 30. At lower multiplicity, essentially the same types of functional responses were observed. However, as expected, the extent of regulation was less (smaller factor). Three down-regulated (BNIP3, CA9 and LOX) and two up-regulated genes (DKK1 and OASL) are compared in Figure 21.

KRT17 gene expression was analyzed by Northern blotting (Figure 23).

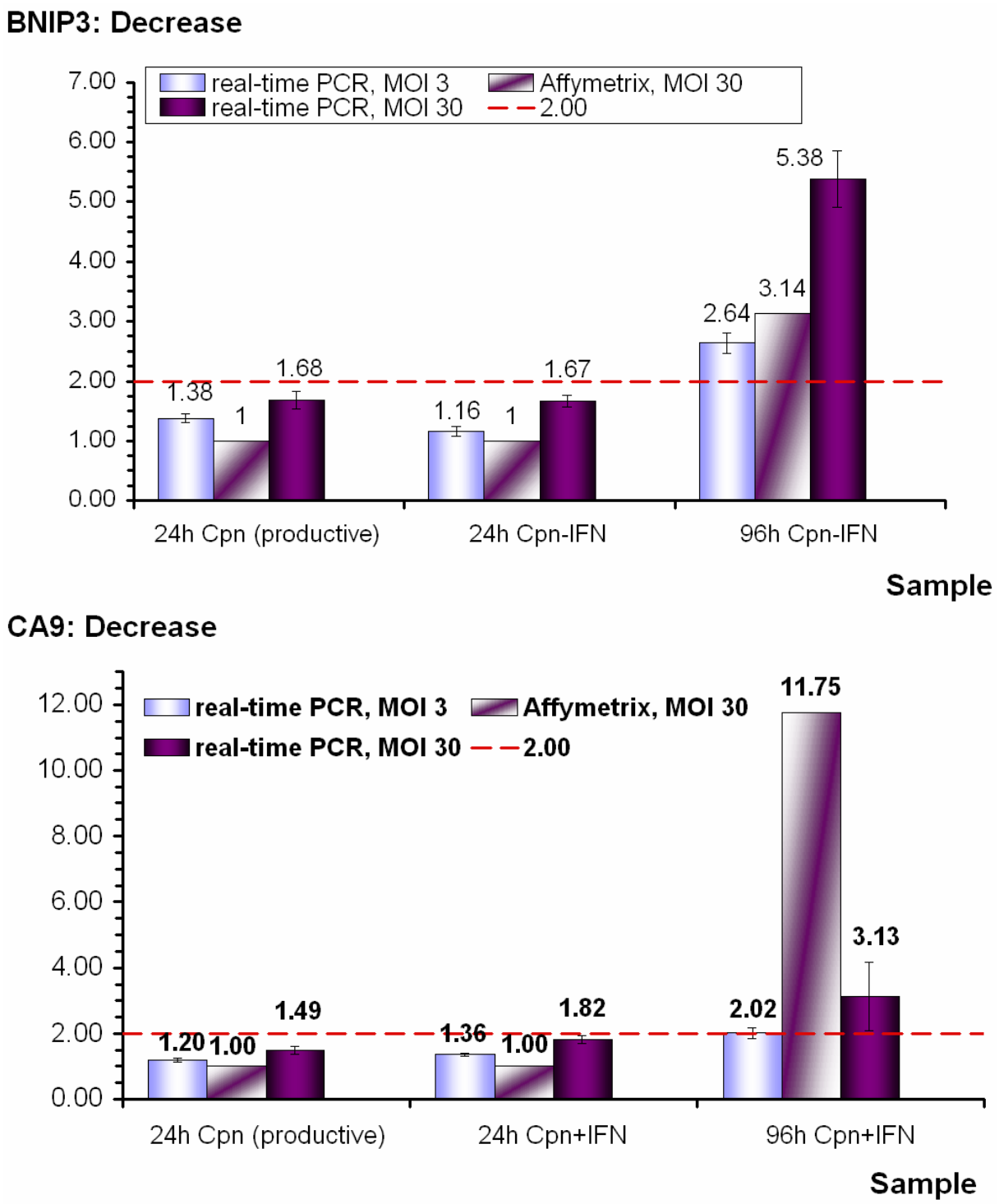

Figure 21 (Part 1): Comparison of changes in the expression of BNIP3 and CA9 due to *C. pneumoniae* infection of HeLa-cells with different multiplicities of infection (MOI 3 vs. MOI 30). Altered gene expression was analyzed with Affymetrix® U133A human genome chips in duplicate and real-time PCR in quadruplicate, in three independent MOI 30 experiments and two independent MOI 3 experiments. Depicted are the means ±SD compared to mock-infected HeLa-cells with or without IFN-γ addition, respectively.

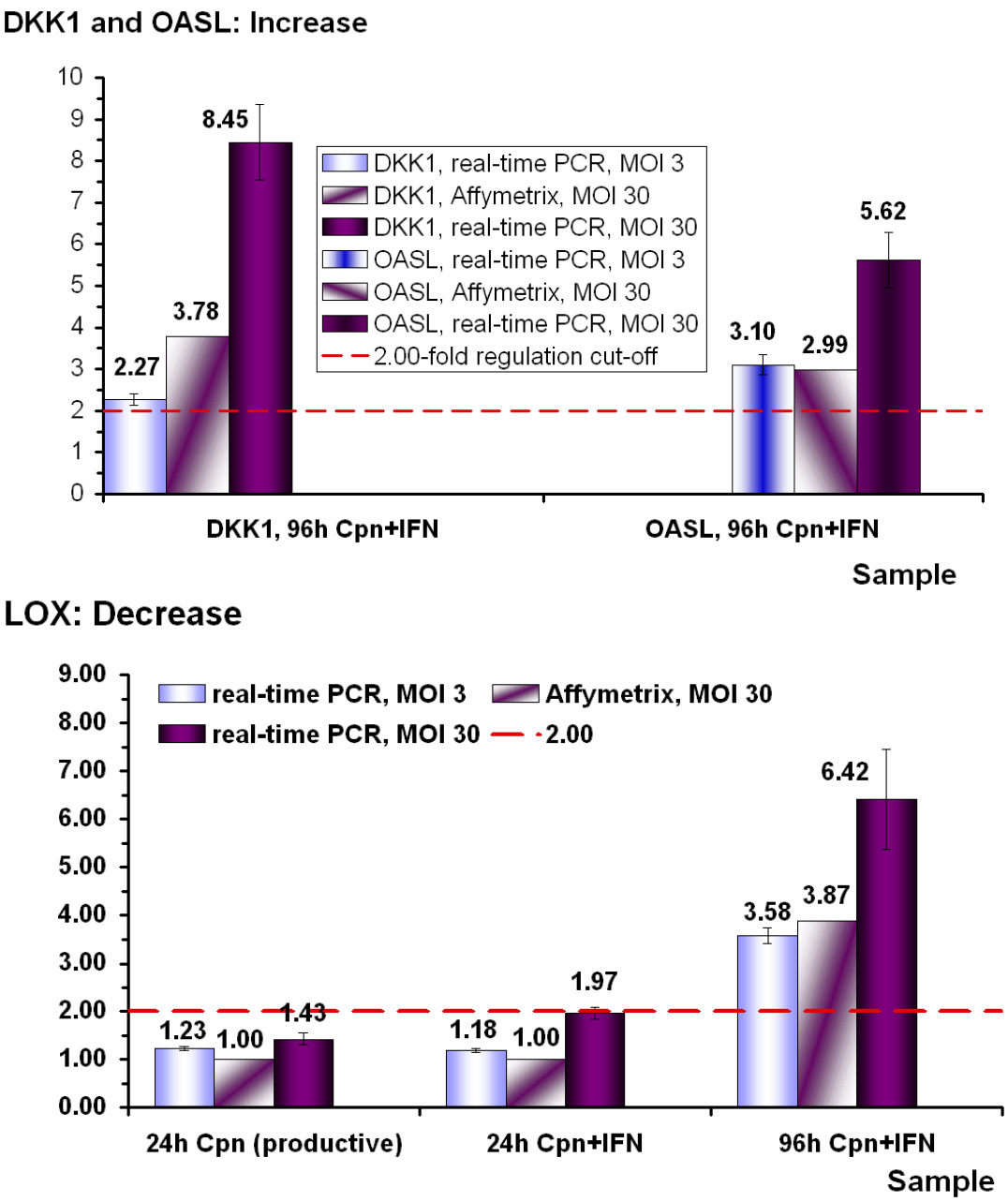

Figure 21 (Part 2): Comparison of changes in the expression of DKK1, OASL and LOX due to *C. pneumoniae* infection of HeLa-cells with different multiplicities of infection (MOI 3 vs. MOI 30). Altered gene expression was analyzed with Affymetrix® U133A human genome chips in duplicate and real-time PCR in quadruplicate, in three independent MOI 30 experiments and two independent MOI 3 experiments. Depicted are the means ±SD compared to mock-infected HeLa-cells with or without IFN-γ addition, respectively.

10.1.6 Northern blot analysis for host-cell genes

To evaluate (partially) divergent results in gene expression analysis by Affymetrix® U133A chip and real-time PCR, a Northern blot analysis was performed on HSPA1-A/B, CYR61 and KRT17 in mock- and *C. pneumoniae*-infected HeLa-cells (MOI 30) in the IFN-γ persistence model. RNA from HeLa-cells of one out of the three independent experiments prepared for real-time PCR analysis was blotted on positively charged nylon membranes.

^{32}P-labeled specific probes for TBP, HSPA1-A/B, CYR61 and KRT17 were hybridized to the membranes, wrapped in plastic foil, and exposed 14 days to a phosphor imaging screen (Figure 22 for blot result). As indicated in Table 5, signal intensities of the genes were normalized to RNA levels in each sample, measured with the Agilent 2100 Bioanalyzer Total RNA Nano chip before Northern blotting, or on the endogenous control TBP, measured in each sample during Northern blot analysis. Both normalization methods almost gave the same regulation factors.

Table 5: Gene expression analysis of HSPA1-A/B, CYR61 and KRT17 by Northern blotting. Depicted are the signal volumes of each sample and the corresponding percentages based on one sample pair (infected sample and mock control). The regulation factors were obtained from normalized signal volumes (infected sample vs. mock control sample). Normalization was done on RNA levels, measured with the Agilent 2100 Bioanalyzer before Northern blotting, or on the endogenous control TBP, measured in each sample during Northern blot analysis.

Sample Name	Volume	Percent (%)	Regulation#		Regulation*	
			Increase	Decrease	Increase	Decrease
HSPA1-A/B						
24h mock	1.97E+06	72.43				
24h CP (prod.)	7.50E+05	27.57		1.28		1.25
24h mock+IFN-γ	4.25E+06	76.12				
24h CP+IFN-γ	1.33E+06	23.88		1.45		1.40
96h mock+IFN-γ	3.80E+05	76.16				
96h CP+IFN-γ	1.19E+05	23.84		1.55		1.47
CYR61						
24h mock	2.91E+05	30.02				
24h CP (prod.)	6.79E+05	69.98	4.80		4.91	
24h mock+IFN-γ	9.39E+05	66.49				
24h CP+IFN-γ	4.73E+05	33.51	1.11			1.18
96h mock+IFN-γ	4.93E+05	53.65				
96h CP+IFN-γ	4.25E+05	46.35	1.78		1.88	
KRT17						
24h mock	4.45E+05	46.57				
24h CP (prod.)	5.10E+05	53.43	2.36		2.42	
24h mock+IFN-γ	4.00E+06	35.38				
24h CP+IFN-γ	7.30E+06	64.62	4.02		3.96	
96h mock+IFN-γ	5.86E+06	91.28				
96h CP+IFN-γ	5.60E+05	8.72		5.08		4.81

#normalized on TBP; *normalized on Agilent RNA measuring

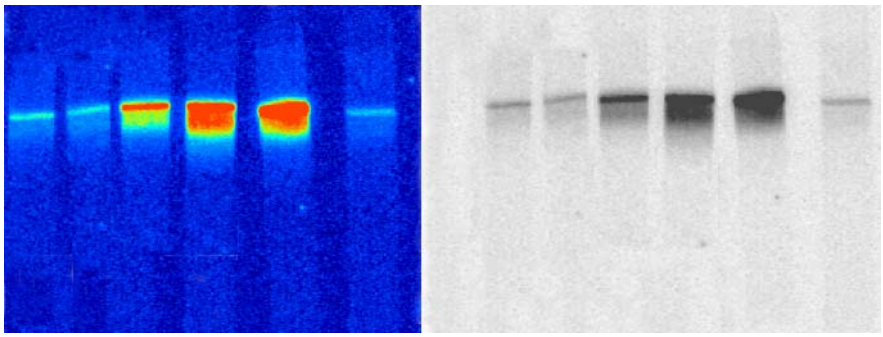

Figure 22: Analysis of KRT17 Northern blotting result using ImageQuant® software. An intensity picture (left) and a black/white picture (right) as part of the scanned phosphorimage screen (Typhoon 9210, 50 dots/cm, 390BP/Red 633nm) show KRT17 HeLa-cell mRNA after mock, productive or persistent infection (24h mock and Cpn, 24h mock and Cpn + IFN-γ, 96h mock and Cpn + IFN-γ, from left to right).

Expression of the HSPA1-A/B gene did not change, thus confirming the real-time PCR result. Expression of CYR61 increased 5-fold 24h post productive infection as determined by all three methods (microarray, real-time PCR and Northern blotting). In the IFN-γ model, no changes in gene expression of CYR61 were seen 24h and 96h p.i. by microarray and Northern blotting. Using real-time PCR, a 4.4-fold and 2.0-fold increase in CYR61 expression was observed 24h and 96h p.i., respectively. The altered gene expression of KRT17 obtained from real-time PCR (MOI 30 experiment) was confirmed by Northern blotting (Figure 23). By Affymetrix® U133A chip analysis, only the decrease 96h post persistent infection was observed, which was confirmed by real-time PCR MOI 3/30 and Northern blotting.

In summary, the gene expression patterns obtained by real-time PCR were confirmed using Northern blotting except for CYR61.

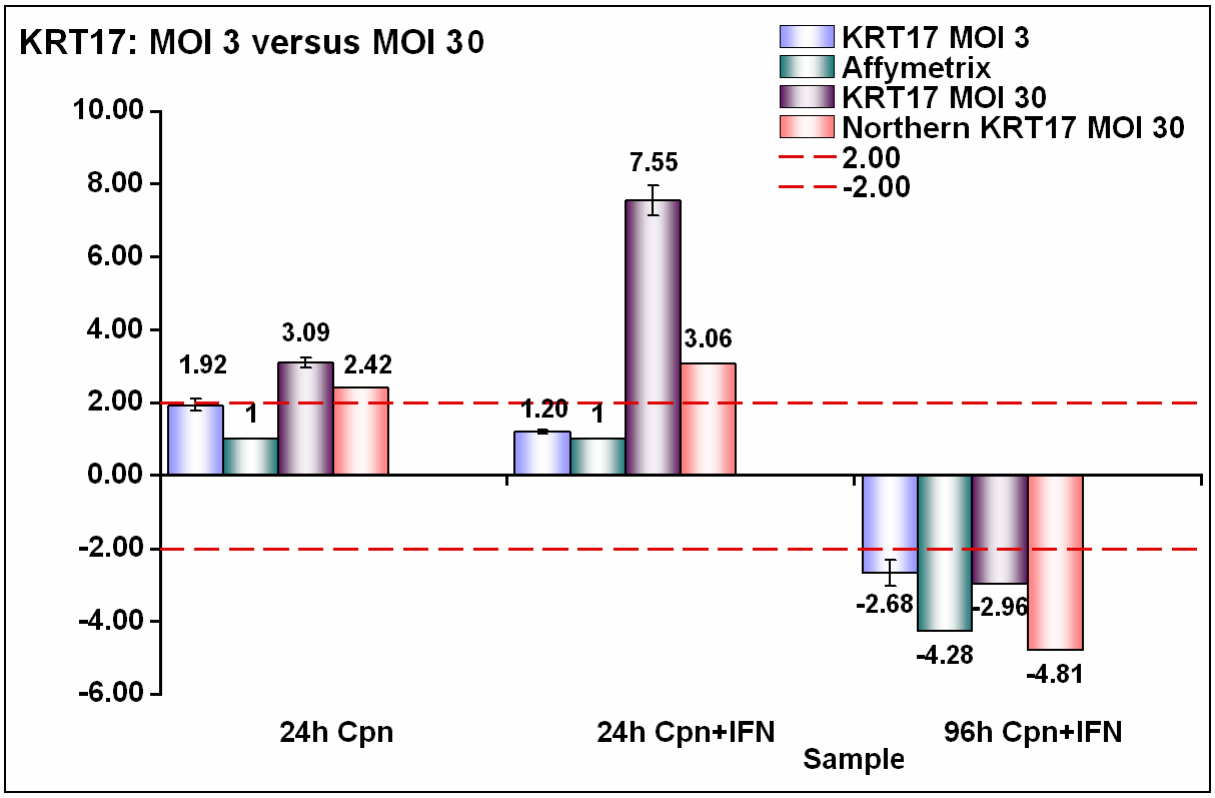

Figure 23: Comparison of gene expression results for KRT17 obtained from Affymetrix® U133A chip analysis, Northern blotting and real-time PCR with MOI 3- or MOI 30- infected HeLa-cells in the IFN-γ persistence model. For Affymetrix® chip and real-time PCR the mean regulations are depicted compared to mock-infected HeLa-cells with and without IFN-γ addition respectively. The error bars represent the standard error of the mean (SEM). Statistical evaluation for gene regulation analyzed by real-time PCR was performed by one way ANOVA analysis ($p = 0.05$) using a 2-fold regulation cut-off (dashed line). Real-time PCR data shown were normalized to levels of three parallel used endogenous controls, which run in triplicate on each experiment.

10.2 aRNA AMPLIFICATION

In recent years, high throughput DNA microarray technology has proven to be a powerful approach for *C. pneumoniae in vitro* gene expression profiling (Fischer *et al.*, 2004; Shi and Tokunaga, 2004; Virok *et al.*, 2003; Coombes and Mahony, 2001). To generate a meaningful gene expression pattern, *in vivo* RNA amplification methods are necessary because of low RNA starting amounts. In these cases, it is necessary to distinguish between the real effects of the biological system being analyzed and changes introduced due to a difference in the methods used to generate the data. In this experimental part, two different target preparation techniques for hybridization to high-density oligonucleotide microarrays (HG-U133A, Affymetrix®) are compared: an *in vitro* transcription (IVT) protocol that requires 2.5 µg of total RNA and a double *in vitro* transcription amplification protocol (dIVT) using 10 ng starting material. RNA prepared from HeLa-cells 96h post infection by *C. pneumoniae* and

IFN-γ-persistence-induction and HeLa-cells 96h mock-infected with addition of IFN-γ were analyzed. To compare the different protocols, one *C. pneumoniae*-infected 2.5 µg sample (experiment A) was compared with two 10 ng samples (experiments A and B). To analyze the changes in gene expression, mock-infected 2.5 µg samples (experiments A and B) were utilized as controls. In a total five samples were used to investigate both cell types (normal and persistence-induced) and the protocol-based effects (IVT and dIVT) on the final results.

10.2.1 Quality Control

RNA Extracted RNA was quantified by UV and by the Agilent 2100 Bioanalyzer (Table 6 and Figure 24) thereby the quality of the RNeasy Mini Kit in combination with DNase I on column digestionwas controlled. Mock-infected samples were diluted to a final RNA concentration of 2.5 µg with RNase-free water. The *C. pneumoniae*-infected samples where diluted either to 2.5 µg (96h experiment A) or to 10 ng (96h experiments A and B).

Table 6: RNA quantitation using UV photometer and Agilent 2100 Bioanalyzer.

Sample	Experiment	UV measurement (µg total)	Bioanalyzer measurement (µg total)
96h mock-infected	A	12.90	13.41
96h mock-infected	B	9.86	12.50
96h *C. pneumoniae*-infected	A	4.21	4.24
96h *C. pneumoniae*-infected	B	3.26	3.62

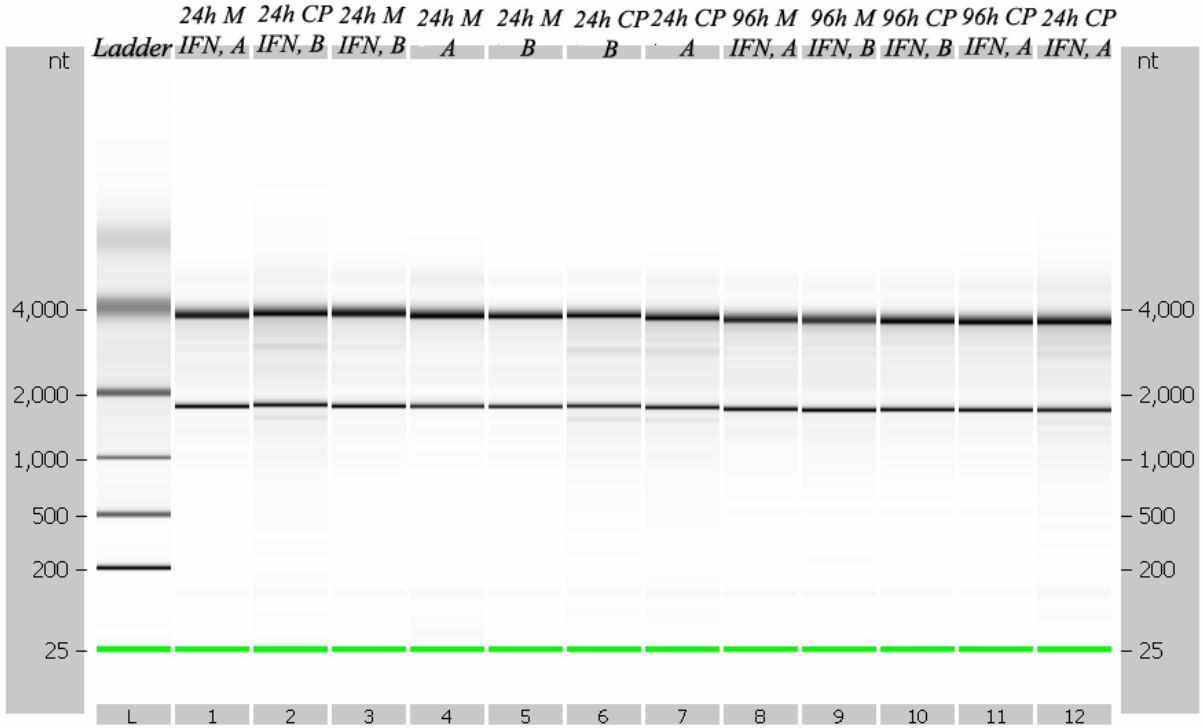

Figure 24: RNA quality check and quantitation using the Total RNA Nano Chip on the Agilent 2100 Bioanalyzer. First lane shows Agilent's RNA ladder (150 ng/µl). In lane 1 to 12 different HeLa-cell samples of two independent experiments (A and B) are depicted showing 18S and 28S rRNA bands. Samples analyzed in lane 8 to 11 were used for aRNA amplification experiment. (M: mock-infected; CP: *C. pneumoniae*-infected)

After *in vitro* transcription and double *in vitro* transcription (for the 10 ng samples), the quality and quantity of the RNA was controlled on a 2% agarose gel (Figure 25). No degradation or contamination was found despite high yields of RNA. After biotin labeling RNA of 96h mock- and IFN-γ-infected HeLa-cells was quantitated to control whether the concentration is sufficient for microarray hybridization (15 µg needed, see Table 7 and Figure 26).

Table 7: RNA quantitation using UV photometer.

Sample	RNA	Experiment	UV measurement (µg total)
96h mock-infected	2.5 µg	A	26.49
96h mock-infected	2.5 µg	B	42.32
96h *C. pneumoniae*-infected	2.5 µg	A	32.44
96h *C. pneumoniae*-infected	10 ng	A	70.54
96h *C. pneumoniae*-infected	10 ng	B	40.10

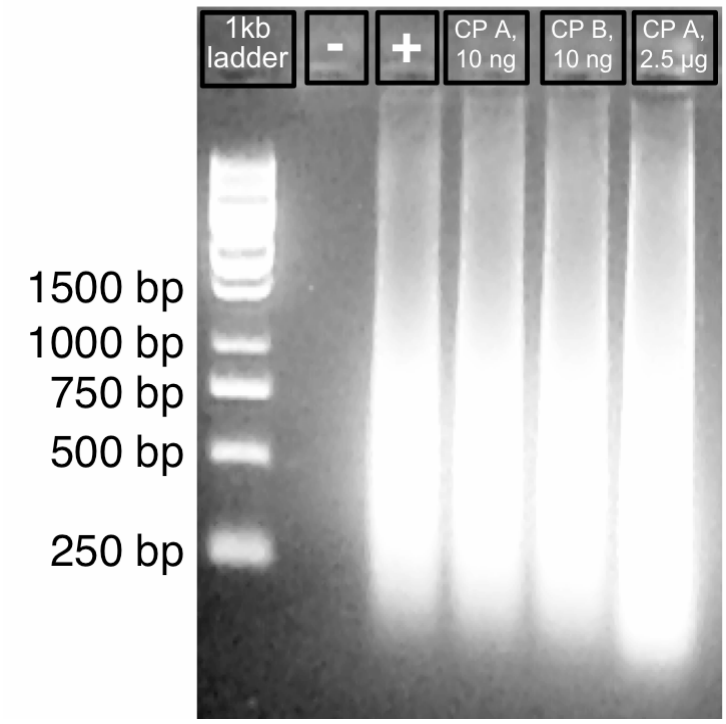

Figure 25: After *in vitro* transcription and before biotin labeling RNA was controlled for quantity and quality on a 2% agarose gel (80 V, 132 mA, 60 min.). Depicted are from left to right a 1 kb DNA ladder, a control without template and positive control after two rounds of amplification and three 96h *C. pneumoniae*-infected samples (10 ng starting material after two rounds of amplification from experiment A and B, 2.5 µg starting material after *in vitro* transcription).

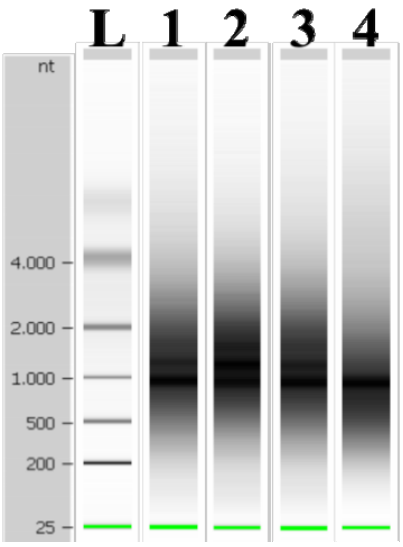

Figure 26: Quality control of RNA on the Agilent 2100 Bioanalyzer using the Total RNA Nano Chip. The first lane shows Agilent's RNA ladder (150 ng/µl). In lane 1 to 4 RNA from mock-infected (experiments A and B, 2.5 µg starting material) and *C. pneumoniae*-infected HeLa-cell samples (experiments A, 2.5 µg and 10 ng starting material) in the IFN-γ model is depicted after *in vitro* transcription and biotin labeling for microarray analysis.

Affymetrix® U133A human genome chips consisting of 22,284 human gene probe sets were used to compare the gene expression profiles generated by different RNA starting amounts (2.5 µg versus 10 ng) and different methods of preparation (IVT versus dIVT). To check for variations introduced by differences in target preparation, labeling, hybridization, and handling of individual samples, the data sets were compared for all the arrays as generated by MAS 5.0. The background levels and the range of percentage of probe sets called present (49-53%) were within acceptable levels as described previously (Affymetrix, 2001). All exogenously added eukaryotic hybridization controls showed signal intensities significantly above the threshold limits (Affymetrix, 2001). Similar results were obtained for housekeeping genes such as GAPDH and β-actin, underscoring the efficiency and accuracy of target preparation and hybridization.

After visual examination of the arrays to detect any spatial artifacts, as a final quality control the percentage of probe sets on each array were analyzed with detection *p*-values less than 0.01 or 0.05 (Table 8). Detection *p*-values are a probability measure of how likely a transcript is expressed at a level designated present on the chips. Arrays with less than 15% of probe sets detected with $p < 0.01$ were excluded from further analysis as derived from extensive experimentation. All GeneChips in this experimental part of the thesis passed the quality control checks.

Table 8: Quality control for Affymetrix HG-U133A GeneChips using MAS 5.0 (percentage of probe sets with significant detection *p*-values)

No	Samples in the IFN-γ model of persistence	RNA	Experiment	Detection P < 0.01%	Detection P < 0.05%
1	96h mock-infected	2.5 µg	A	39.39	49.35
2	96h mock-infected	2.5 µg	B	42.01	51.98
3	96h *C. pneumoniae*-infected	2.5 µg	A	43.16	52.92
4	96h *C. pneumoniae*-infected	10 ng	A	38.81	49.14
5	96h *C. pneumoniae*-infected	10 ng	B	38.89	49.03

10.2.2 Comparison of gene expression profiles using IVT and dIVT protocols

The corresponding sample number will be used instead of the sample name as shown in Table 8 to facilitate comparison.

The comparison analysis of HG-U133A Affymetrix® chip data from sample 3 versus sample number 5 led to a correlation coefficient of 0.96 comparing IVT protocol of experiment A with dIVT protocol of a second independent experiment B and 0.94 compared with dIVT protocol of the same experiment (sample number 4). Comparing two independent experiments using an IVT protocol led to a correlation coefficient of 0.99 (sample 1 versus 2), which was slightly higher than for dIVT protocols with 0.97 (sample 4 versus 5).

Gene comparison of *C. pneumoniae*-infected versus mock-infected HeLa-cells revealed Pearson coefficients of 0.99, 0.96 and 0.93 using sample 3 versus 1, sample 5 versus 2 and sample 4 versus 1 (scatter plots are shown in Figure 27). These coefficients correlate with the number of differentially expressed genes found by the three comparison analyses. Using the dIVT protocol, 8 times more differentially expressed genes in experiment B and 17 times more in experiment A were detected.

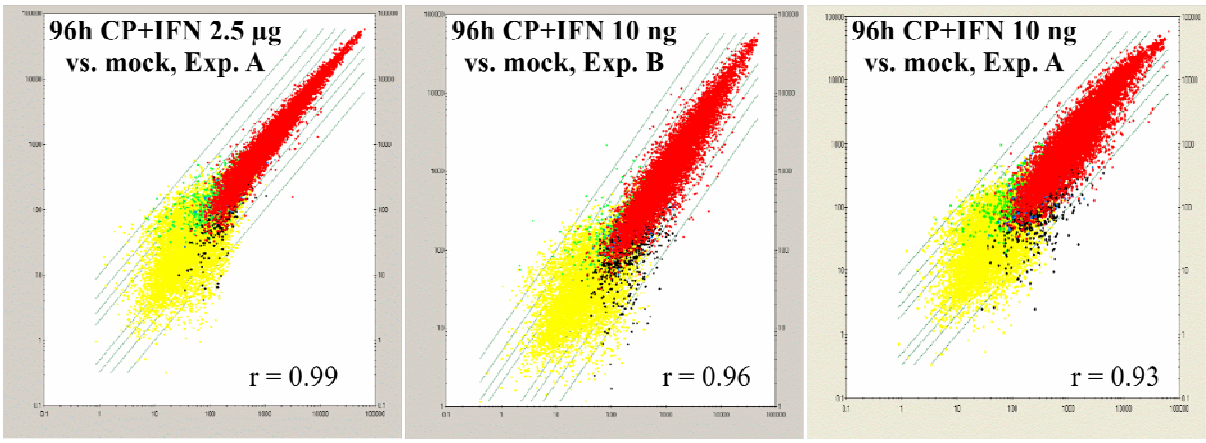

Figure 27: Scatter plot analysis for two independent microarray experiments A and B. The graphs show the comparison of 96h *C. pneumoniae*-IFN-γ-infected HeLa-cells with mock-infected cells using 2.5 µg starting material (left graph, exp. A) or 10 ng starting material after two rounds of amplification (middle graph, exp. B; right graph, exp. A). The lines displayed in the graph represents 2-, 3-, 5- and 10-fold changes. Red colored signals are present in baseline and in experiment (P-P call), black colored signals are present in baseline but absent in experiment (P-A call), green colored signals are absent in baseline but present in experiment, yellow dots represent absent or marginal signals and blue colored signals are marginal or present in baseline or experiment. Pearson's correlation coefficient for this comparison analysis is 0.99, 0.96 and 0.93 from left to the right.

All selected genes with altered gene expression had signal log ratios higher than 1.32 or lower than -1.32 ($\alpha 1 = 0.05$; $\alpha 2 = 0.065$; $\tau = 0.015$) and represent calls in both samples (treatment versus mock at the corresponding time-point). At this cut-off, the mRNA expression of 37 genes (2.5 µg RNA, exp. A), 295 genes (10 ng RNA, exp. B) and 615 genes (10 ng RNA, exp. A) were up- or down-regulated in 96h *C. pneumoniae*-infected and IFN-γ-induced persistent HeLa-cells. The filtered dataset consisting of 3,871 genes was used for comparing differentially expressed genes detected by IVT and dIVT protocols. Comparison of the altered genes revealed that approximately 27% of the genes detected using IVT were also identified by dIVT (10 out of the 37). At the same cut-off, 54% of genes detected using IVT were not recognized with dIVT (20 genes) and 18.92% (7 genes) were only confirmed by one out of the two dIVT experiments (Figure 28 left panel). Use of less stringent filter options by accepting changes of < 2.5-fold, enabled detection of almost all altered genes with the IVT protocol as well as the dIVT protocol (26 genes ≡ 70.27%), except for one gene, which showed a decrease of 2.79. Using these criteria, 54 genes out of 797 were found to be differentially expressed in both protocols, 128 found in dIVT experiment A alone and 26 in dIVT experiment B alone. 80.55% (588 genes) were detected by at least two of the experimental setups (Figure 28 right panel). Therefore, although fewer differentially expressed genes were discovered in the IVT protocol, most were detectable for differential expression at a lower threshold by both protocols.

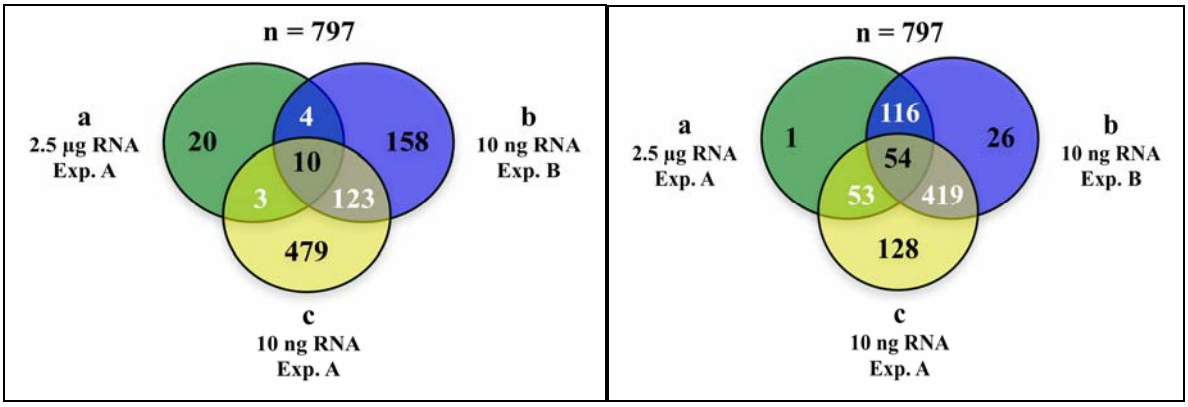

Figure 28: The Venn diagrams shows 797 genes overlapping from data sets generated by the IVT and dIVT protocols. Three 96h *C. pneumoniae*-infected samples from two independent experiments were analyzed with Affymetrix® U133A human genome chips. (Experiments A and B; **a:** 2.5 µg starting material, exp. A; **b:** 10 ng starting material after two rounds of amplification, exp. B; **c:** 10 ng starting material after two rounds of amplification, exp. A). All selected genes of the left panel had signal log ratios greater than 1.32 or lower than -1.32 ($\alpha 1 = 0.05$; $\alpha 2 = 0.065$; $\tau = 0.015$) and represent calls in both samples (treatment versus mock at the corresponding time-point). The right panel depicts the same selected genes compared at lower stringent filter options ($\alpha 1 = 0.05$; $\alpha 2 = 0.065$; $\tau = 0.015$).

10.2.3 Confirmation by real-time PCR

Among the genes that were identified as differentially expressed by at least one protocol exceeding a factor of 2.5, fifteen genes were selected for analysis using real-time PCR on the ABI PRISM™ 7000 SDS. Differences in expression of these genes between the *C. pneumoniae*-infected and mock-infected HeLa-cells were estimated using the standard curve method (ABI, 1997), normalizing the values with respect to three endogenous controls, 18S rRNA, GUS and TBP. Each gene was tested in quadruplicate, on each of three independent experiments. Statistical evaluation for gene regulation, by using a 2-fold regulation cut-off, was performed by one-way ANOVA analysis ($p \leq 0.05$).

Four gene sets were selected that:

i. perfectly match the 2.5-fold change criterion in both protocols and experiments (NDRG1, BNIP3, LOX, DKK1, PTGER4, KRT17 and DACT1),
ii. match only in the dIVT protocols (IFI44, OASL probe set 1, OASL probe set 2),
iii. were altered only in the IVT protocol (BNIP3 probe set 2),
iv. match in IVT protocol and one of the dIVT protocols (SNK and Adlican).

All of the 15 differentially expressed genes tested, as determined by the microarray data using either protocol, produced similar results with real-time PCR (Table 9). Regulation factors were higher in six cases and lower in nine cases comparing microarray and real-time PCR results.

Table 9: Altered gene expression data for selected Affymetrix® U133A human genome chip probe sets. Listed are the fold changes (D = decrease, I = increase) of *C. pneumoniae*-infected HeLa-cells in the IFN-γ persistence model (96h CP+IFN-γ). All selected genes have signal log ratios greater than 1.32 or lower than -1.32 ($\alpha 1 = 0.05$; $\alpha 2 = 0.065$; $\tau = 0.015$) and represent calls in both samples (treatment versus mock at the corresponding time-point).

Gene Title	Gene Symbol	Accession No.	Gene Expression	
			Microarray	real-time PCR
BCL2/adenovirus E1B 19kDa interacting protein 3	BNIP3	NM_004052	D (3.27)	D (5.38)
BCL2/adenovirus E1B 19kDa interacting protein 3	BNIP3	NM_004052	D (3.14)	D (5.38)
carbonic anhydrase IX	CA9	NM_001216	D (14.93)	D (10.25)
dapper homolog 1	DACT1	NM_016651	D (4.08)	D (2.77)
Adlican	DKFZp564I1922	AF245505	D (3.18)	D (3.96)
dickkopf homolog 1 (Xenopus laevis)	DKK1	NM_012242	I (6.19)	I (8.45)
interferon-induced protein 44	IFI44	NM_006417	I (4.47)	I (4.05)
keratin 17	KRT17	NM_000422	D (3.18)	D (2.96)
keratin 17	KRT17	NM_000422	D (3.81)	D (2.96)
lysyl oxidase	LOX	NM_002317	D (2.87)	D (6.42)
N-myc downstream regulated gene 1	NDRG1	NM_006096	D (4.87)	D (8.27)
2'-5'-oligoadenylate synthetase-like	OASL	NM_198213	I (3.01)	I (5.62)
2'-5'-oligoadenylate synthetase-like	OASL	NM_198213	I (2.83)	I (5.62)
prostaglandin E receptor 4	PTGER4	NM_000958	I (5.66)	I (6.21)
serum-inducible kinase	SNK/PLK2	NM_006622	I (4.82)	I (2.91)

10.3 DEVELOPMENT OF REAL-TIME PCR IN VITRO DIAGNOSTICA FOR THE DETECTION OF *CHLAMYDIA TRACHOMATIS*

Pathogen diagnosis by the polymerase chain reaction (PCR) is based on the amplification of specific regions of the pathogen genome. In real-time PCR, the amplified product is detected by fluorescent dyes. These are usually linked to oligonucleotide probes that bind specifically to the amplified product. Monitoring the fluorescence intensities during the PCR run allows the detection and quantitation of the accumulating product without having to re-open the reaction tubes after the PCR run (Mackay, 2004). The newly developed *artus*™ *C. trachomatis PCR Kits* are CE-marked according to the EU directive and ISO certified.

10.3.1 Quantitative Assays

The *artus™ C. trachomatis LC/RG/TM PCR Kit* constitutes a ready-to-use system for the detection of *C. trachomatis* DNA using PCR in the *LightCycler®*, Rotor-Gene™ and ABI PRISM™ 7000/7700/7900 instruments. The *C. trachomatis Master* contains reagents and enzymes for the specific amplification of a 100 bp region of the *C. trachomatis* genome (*ompA* gene) and for the direct detection of the specific amplicon. In addition, the *artus™ C. trachomatis LC/RG/TM PCR Kit* contains a second heterologous amplification system to control the DNA isolation procedure and to check for possible PCR inhibition. This is detected as an *Internal Control* (*IC*) in a second fluorimeter channel. The detection limit of the analytical *C. trachomatis* PCR is not reduced. For this application, the *Internal Control* has to be added to the isolation at a ratio of 0.1 µl per 1 µl elution volume. To allow for the determination of the pathogen load, external positive controls (*C. trachomatis QS 1 - 4*) were generated that are based on a plasmid containing the *C. trachomatis* specific PCR amplification sequence. To generate a standard curve on the *LightCycler®* Instrument, all four *Quantitation Standards* are used and defined in the *Sample Loading Screen* as standards at the specified concentrations (see *LightCycler Operator's Manual*, Version 3.5, Chapter B, 2.4. Sample Data Entry). The PCR is prepared by addition of 2 µl magnesium solution to 13 µl master-mix and 5 µl template. On the Rotor-Gene™ 3000 and ABI PRISM™ SDS, all four *Quantitation Standards* should be defined in the menu window *Edit Samples* (see artus™ 3000 and ABI PRISM™ 7000/7700/7900HT SDS Software Manual). The PCR is prepared by addition of 15 µl master-mix to 10 µl template.

10.3.1.1 Analytical Sensitivity of the Quantitative C. trachomatis Assay

To determine the analytical sensitivity of the *artus™ C. trachomatis LC PCR Kit*, a standard dilution series was set up from 525 to nominal 0.1 *C. trachomatis* copies/µl and analyzed with the *artus™ C. trachomatis LC PCR Kit*. Testing was carried out on three different days on eight replicates. The results were determined by a probit analysis. The detection limit of the *artus™ C. trachomatis LC PCR Kit* is consistent at 4 copies/µl ($p = 0.05$), which means that there is a 95 % probability to detect 4 copies/µl.

To determine the analytical sensitivity of the *artus™ C. trachomatis RG PCR Kit*, a standard dilution series was set up from 10 to nominal 0.078 *C. trachomatis* copies/µl and analyzed with the *artus™ C. trachomatis RG PCR Kit*. Testing was carried out on three different days

on eight replicates. The results were determined by a probit analysis. The detection limit of the *artus™ C. trachomatis RG PCR Kit* is consistent at 0.5 copies/µl (p = 0.05).
To determine the analytical sensitivity of the *artus™ C. trachomatis TM PCR Kit*, a standard dilution series was set up from 100 to nominal 0.0625 *C. trachomatis* copies/µl and analyzed by the ABI PRISM™ 7000, 7700 and 7900HT Sequence Detection Systems with the help of the *artus™ C. trachomatis TM PCR Kit*. Testing for all instruments was carried out on three different days on eight replicates. The results were determined by a probit analysis. The detection limit of the *artus™ C. trachomatis TM PCR Kit* is consistent at 0.3 copies/µl (ABI PRISM™ 7000) and 0.2 copies/µl (ABI PRISM™ 7700/7900HT) (p = 0.05). This means that there is a 95 % probability that 0.3 copies/µl and 0.2 copies/µl will be detected, respectively.

10.3.1.2 Specificity of the quantitative C. trachomatis Assay

The primers and probes were checked for possible homologies to all sequences published in gene banks. Hence, the detectability of all relevant serovars has been ensured by database alignment and by a PCR run with the following serovars (Table 10):

Table 10: Testing of the specificity of the serovars.

Chlamydia strain	ATCC #	Serotype	Lot #
C. trachomatis	VR-571B	A	RB 64583:6
C. trachomatis	VR-573	B	RB 64583:6
C. trachomatis	VR-347 (prep 1)	Ba	RB 72171-26
C. trachomatis	VR-572	C	RB 64583:6
C. trachomatis	VR-885	D	RB 64583:6
C. trachomatis	VR-348B	E	RB 64583:6
C. trachomatis	VR-346	F	RB 64583:6
C. trachomatis	VR-878	G	RB 64583:6
C. trachomatis	VR-879	H	RB 64583:6
C. trachomatis	VR-880	I	RB 64583:6
C. trachomatis	VR-886	J	RB 64583:6
C. trachomatis	VR-887	K	RB 64583:6
C. trachomatis	VR-901B	LGV I	RB 64583:6
C. trachomatis	VR-902B	LGV II	RB 64583:6
C. trachomatis	VR-577	LGV II	RB 64583:6
C. trachomatis	VR-903	LGV III	75157183

Moreover, the specificity was validated with 100 different *C. trachomatis* negative urine samples and 30 negative swab samples. These did not generate any signals with the *C. trachomatis* specific primers and probes. To determine the specificity of the *artus*™ *C. trachomatis LC/RG/TM PCR Kit* the control group listed in Table 2 (Materials and Methods) has been tested for cross-reactivity. None of the tested pathogens was reactive.

10.3.1.3 Precision of the Quantitative C. trachomatis Assay

Precision data of the *artus*™ *C. trachomatis LC PCR Kit* were collected using a *C. trachomatis Quantitation Standard* diluted to a final concentration of 12 copies/µl (threefold concentration of the analytical sensitivity limit). Testing was performed with eight replicates. The precision data were calculated on basis of the CT values of the amplification curves (CT: threshold cycle, see Table 11). Based on these results, the overall statistical spread of any given sample with the mentioned concentration is 5.8 % and 1.93% for the detection of the *Internal Control*. These values are based on the totality of all single values of the determined variabilities.

Table 11: Precision data on basis of the CT values.

	CT mean	Standard deviation	Variance
Intra-assay variability	36.01	0.48	0.23
Inter-assay variability	38.31	2.56	6.57
Inter-batch variability	33.22	2.30	5.29
Total variance	35.86	2.08	4.33

Precision data of the *artus*™ *C. trachomatis RG PCR Kit* were collected using a *C. trachomatis Quantitation Standard* diluted to a final concentration of 10 copies/µl (QS 4). Testing was performed with eight replicates. The precision data were calculated on the basis of the CT values of the amplification curves (CT: threshold cycle, see Table 12). In addition, precision data for quantitative results in copies/µl were determined using the corresponding CT values. Based on these results, the overall statistical spread of any given sample with the mentioned concentration is 2.29 % (CT) or 12.58 % (conc.) and 1.05% for the detection of the

Internal Control (CT). These values are based on the totality of all single values of the determined variabilities.

Table 12: Precision data on basis of the CT values.

	Coefficient of variation [%]	Standard deviation	Variance
Intra-assay variability	0.50	0.13	0.02
Inter-assay variability	2.34	0.63	0.40
Inter-batch variability	1.92	0.51	0.26
Total variance	2.29	0.61	0.38

Precision data of the *artus™ C. trachomatis TM PCR Kit* were collected using the *Quantitation Standard* of the lowest concentration (*QS 4*; 10 copies/µl). Testing was performed with eight replicates. The precision data were calculated on basis of the CT values of the amplification curves (CT: threshold cycle, see Table 13). In addition, precision data for quantitative results in copies/µl were determined using the corresponding CT values. Based on these results, the overall statistical spread of any given sample with the mentioned concentration is 2.80 % (CT) or 13.41 % (conc.) and 2.46% for the detection of the *Internal Control* (CT). These values are based on the totality of all single values of the determined variabilities.

Table 13: Precision data on basis of the CT values.

	Coefficient of variation [%]	Standard deviation	Variance
Intra-assay variability	0.50	0.13	0.02
Inter-assay variability	2.34	0.63	0.40
Inter-batch variability	1.92	0.51	0.26
Total variance	2.29	0.61	0.38

10.3.1.4 Robustness of the Quantitative C. trachomatis Assay

The verification of the robustness allows the determination of the total failure rate of the *artus™ C. trachomatis LC/RG/TM PCR Kit.* 128 *C. trachomatis* negative samples of urine and 30 negative swab samples were spiked with 12 copies/µl (LC), 1.5 copies/µl (RG) or 1 copy/µl (TM) elution volume of *C. trachomatis* control DNA (threefold concentration of the analytical sensitivity limit). After extraction using the QIAamp Viral RNA Mini Kit, these samples were analyzed with the *artus™ C. trachomatis LC/RG/TM PCR Kit.* For all *C. trachomatis* samples, the failure rate was 0 %. In addition, the robustness of the *Internal Control* was assessed by purification and analysis of 96 *C. trachomatis* negative urine samples. The total failure rate was 0 %. Inhibitions were not observed. Thus, the robustness of the *artus™ C. trachomatis LC/RG/TM PCR Kit* is ≥ 99 %.

10.3.1.5 Diagnostic Evaluation of the Quantitative C. trachomatis Assay

The *artus™ C. trachomatis LC PCR Kit* was evaluated in one study (Eickhoff M *et al.*, 2003). 54 cervical swabs, 22 urethral swabs and 35 urine specimens (8 female, 27 male) were tested altogether. Comparative tests were carried out in a diagnostic laboratory using the routine procedure (in-house SYBR Green LightCycler® PCR) and by means of the COBAS® AMPLICOR® using the CT/NG PCR Kit. The samples were analyzed in duplicate. Samples showing discrepancies were determined four times. The capacity of the test was separately calculated for each type of sample. The sensitivity and the specificity were calculated with respect to the results of the comparative tests as well as to those differentiated according to the type of sample and the patient. The results are summarized in Table 14.

Table 14: Results of the comparative validation study.

	Number of samples	**Artus™ Kit** Positive samples	**COBAS AMPLICOR** (artus™/COBAS®)		**SYBR Green** (artus™/SYBR)	
			Sensitivity	**Specificity**	**Sensitivity**	**Specificity**
Swab Women	54	53.70%	27/27	25/27	29/29	25/25
Urine Women	8	37.50%	3/3	5/5	3/3	5/5
Swab Men	22	59.10%	13/15	7/7	13/13	9/9
Urine Men	27	37.00%	10/10	17/17	10/10	17/17
Total	**111**	**49.50%**	**53/55**	**54/56**	**55/55**	**56/56**

The *artus*™ *C. trachomatis TM* and *RG PCR Kit* in combination with the ABI PRISM™ 7000 SDS and the Rotor-Gene™ 3000 have been compared to the LCx *C. trachomatis* Assay (Abbott Laboratories, Abbott Park, IL, USA) and the APTIMA Combo 2™ *C. trachomatis* Assay (Gen-Probe Incorporated, San Diego, U.S.A.). For these purposes, 150 retrospective swab specimens (50 urethral, 50 cervical and 50 vulval swabs) as well as 100 retrospective urine specimens (50 male and 50 female specimens) have been tested. All specimens were prior analyzed with the LCx® and the APTIMA Combo 2™ Assay as part of a routine screening program. They were handled according to the manufacturer's instructions. Subsequently, the samples were stored at -20°C until the date of analysis with the *artus*™ *C. trachomatis RG* and *TM PCR Kit*. For purification, the QIAamp Viral RNA Mini kit was used. On retrospective, urine and swab specimens the *artus*™ *C. trachomatis RG PCR Kit* as well as the *artus*™ *C. trachomatis TM PCR Kit* showed a diagnostic sensitivity of 99.2 % and a specificity of 98.4 %, respectively. The inhibition rate was 0 %.

10.3.2 Qualitative Assays

The *artus*™ *C. trachomatis Plus LC* and *RG PCR Kit* constitutes a ready-to-use system for the detection of *C. trachomatis* DNA using PCR in the *LightCycler*® and Rotor-Gene™ instrument. The *C. trachomatis Plus Master* contains reagents and enzymes for the specific amplification of a 106 bp region of the *C. trachomatis* genome (*ompA* gene) and of a 111 bp region of the cryptical plasmid of *C. trachomatis*, and for the direct detection of the specific amplicon. In addition, the *artus*™ *C. trachomatis Plus PCR Kits* contain a second heterologous amplification system to control the DNA isolation procedure and to check for possible PCR inhibition. This is detected as an *Internal Control* (*IC*) in a second fluorimeter channel. The detection limit of the analytical *C. trachomatis* PCR is not reduced. For this application, the *Internal Control* has to be added to the isolation at a ratio of 0.1 µl per 1 µl elution volume. As a positive control, the *C. trachomatis* plasmid was generated based on the *C. trachomatis* specific cryptic plasmid PCR amplification sequence. The PCR is prepared by addition of 2 µl magnesium solution to 13 µl master-mix and 10 µl template. Examples of positive and negative PCR reactions are given in Figure 29 and Figure 30, respectively.

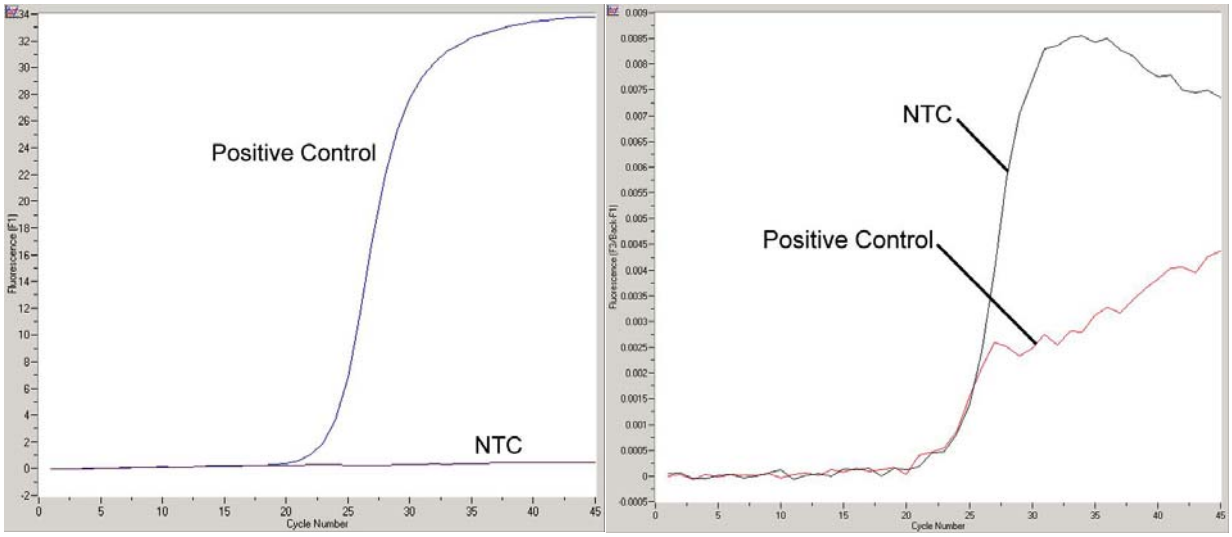

Figure 29: Detection of the *C. trachomatis Plus LC Positive Control* in fluorimeter channel F1 of **the *LightCycler® 1.1/1.2/1.5* Instrument** (left graph). Detection of the *Internal Control* (*IC*) in fluorimeter channel F3/Back-F1 of the *LightCycler® 1.1/1.2/1.5* Instrument with simultaneous amplification of the *C. trachomatis Plus LC Positive Control* (right graph). NTC: non-template control (negative control).

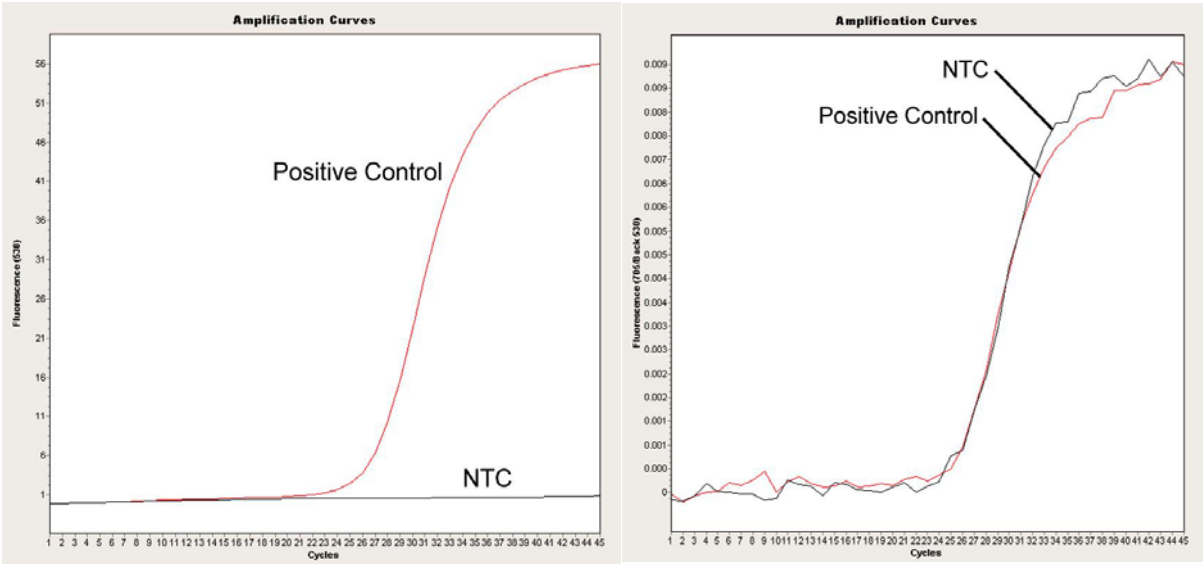

Figure 30: Detection of the *C. trachomatis Plus LC Positive Control* in fluorescence channel 530 of **the *LightCycler® 2.0* Instrument** (left side). Detection of the *Internal Control* (*IC*) in fluorescence channel 705/Back 530 of the *LightCycler® 2.0* Instrument with simultaneous amplification of the *C. trachomatis Plus LC Positive Control* (right side). NTC: non-template control (negative control).

10.3.2.1 Analytical Sensitivity of the Qualitative C. trachomatis Assay

The analytical detection limit as well as the analytical detection limit in consideration of the purification (sensitivity limits) were assessed for the artus™ *C. trachomatis Plus LC PCR Kit.* The analytical detection limit in consideration of the purification is determined using *C. trachomatis*-positive clinical specimens in combination with a particular extraction method. In contrast, the analytical detection limit is determined without clinical specimens and independent from the selected extraction method, using serovars of known concentration.

To determine the analytical sensitivity of the *artus™ C. trachomatis Plus LC PCR Kit*, a *C. trachomatis* serovar E dilution series was set up from 0.66 to nominal 0.002 *C. trachomatis* copies/µl and analyzed on the *LightCycler® 1.1/1.2/1.5* Instrument in combination with the *artus™ C. trachomatis Plus LC PCR Kit*. Testing was carried out on three different days on eight replicates. The results were determined by a probit analysis. The analytical detection limit of the *artus™ C. trachomatis Plus LC PCR Kit* in combination with the *LightCycler® 1.1/1.2/1.5* Instrument is consistently 0.1 copies/µl ($p = 0.05$). This means that there is a 95 % probability that 0.1 copies/µl will be detected. A graphical illustration of the probit analysis is shown in Figure 31.

The analytical sensitivity in consideration of the purification (QIAamp DNA Mini Kit) of the *artus™ C. trachomatis Plus LC PCR Kit* on the *LightCycler® 1.1/1.2/1.5* Instrument in combination was determined using a dilution series of a *C. trachomatis* serovar from 2.1 to nominal 0.00066 *C. trachomatis* copies/µl spiked in clinical swabs specimens. These were subjected to DNA extraction using the QIAamp DNA Mini Kit (extraction volume: 200 µl, elution volume: 100 µl). Each of the eight dilutions was analyzed with the *artus™ C. trachomatis Plus LC PCR Kit* on three different days on eight replicates. The results were determined by a probit analysis. The analytical detection limit in consideration of the purification of the *artus™ C. trachomatis Plus LC PCR Kit* in combination with the *LightCycler® 1.1/1.2/1.5* Instrument is consistently 0.4 copies/µl ($p = 0.05$). This means that there is a 95 % probability that 0.4 copies/µl will be detected.

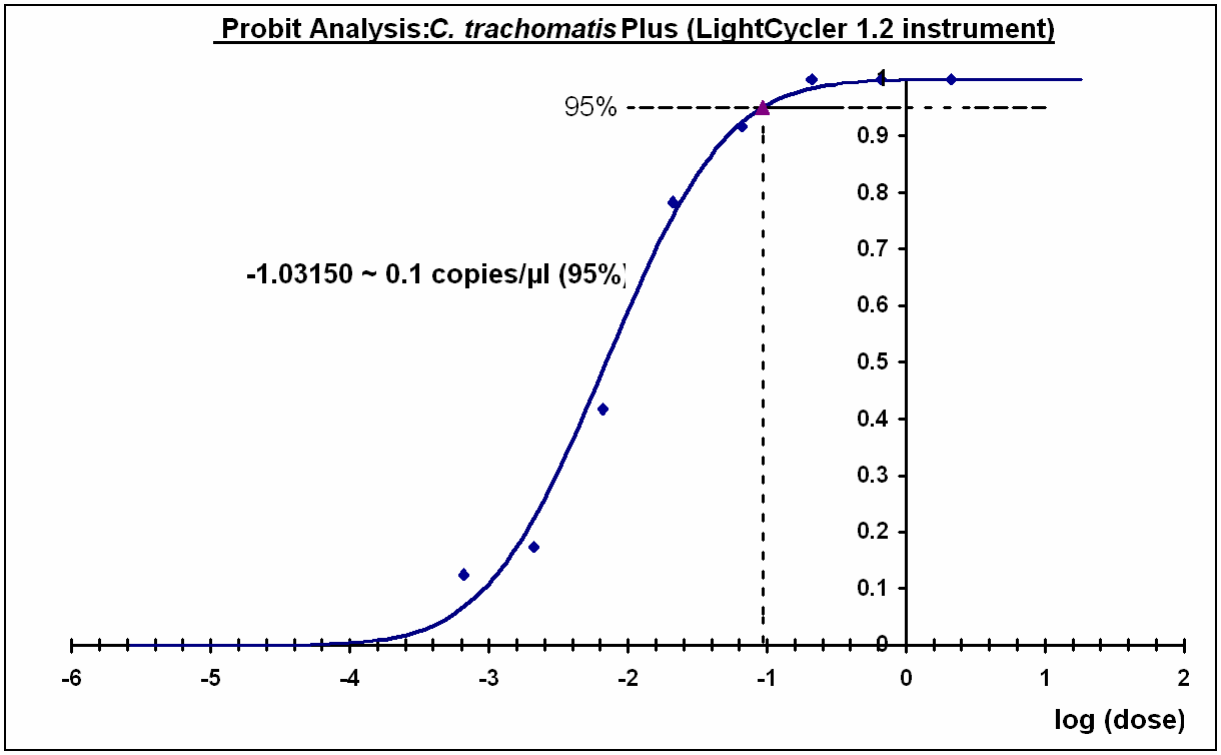

Figure 31: Analytical sensitivity of the *artus*™ *C. trachomatis Plus LC PCR Kit* on the *LightCycler*® *1.2* Instrument.

The analytical sensitivity in consideration of the purification (MagNA Pure DNA Isolation Kit, Roche Diagnostics) of the *artus*™ *C. trachomatis Plus LC PCR Kit* on the *LightCycler*® *1.1/1.2/1.5* Instrument in combination was determined using a dilution series of a *C. trachomatis* serovar E from 2.1 to nominal 0.00066 *C. trachomatis* copies/µl spiked in clinical swabs specimens. These were subjected to DNA extraction using the MagNA Pure DNA Isolation Kit (extraction volume: 100 µl, elution volume: 100 µl). Each of the eight dilutions was analyzed with the *artus*™ *C. trachomatis Plus LC PCR Kit* on three different days on eight replicates. The results were determined by a probit analysis. The analytical detection limit in consideration of the purification with the *LightCycler*® *1.1/1.2/1.5* Instrument is consistently 0.5 copies/µl (p = 0.05). This means that there is a 95 % probability that 0.55 copies/µl will be detected.

To determine the analytical sensitivity of the *artus*™ *C. trachomatis Plus LC PCR Kit*, a *C. trachomatis* serovar E dilution series was set up from 0.66 to nominal 0.002 *C. trachomatis* copies/µl and analyzed on the *LightCycler*® *2.0* Instrument in combination with the *artus*™ *C. trachomatis Plus LC PCR Kit*. Testing was carried out on three different days on eight replicates. The results were determined by a probit analysis. The analytical detection limit of the *artus*™ *C. trachomatis Plus LC PCR Kit* in combination with

the *LightCycler® 2.0* Instrument is consistently 0.12 copies/µl (p = 0.05). This means that there is a 95 % probability that 0.12 copies/µl will be detected.

The analytical sensitivity in consideration of the purification (QIAamp DNA Mini Kit) of the *artus™ C. trachomatis Plus LC PCR Kit* on the *LightCycler® 2.0* Instrument in combination was determined using a dilution series of a *C. trachomatis* serovar E from 2.1 to nominal 0.00066 *C. trachomatis* copies/µl spiked in clinical swabs specimens. These were subjected to DNA extraction using the QIAamp DNA Mini Kit (extraction volume: 200 µl, elution volume: 100 µl). Each of the eight dilutions was analyzed with the *artus™ C. trachomatis Plus LC PCR Kit* on three different days on eight replicates. The results were determined by a probit analysis. The analytical detection limit in consideration of the purification of the *artus™ C. trachomatis Plus LC PCR Kit* in combination with the *LightCycler® 2.0* Instrument is consistently 0.7 copies/µl (p = 0.05). This means that there is a 95 % probability that 0.7 copies/µl will be detected.

The analytical sensitivity in consideration of the purification (MagNA Pure DNA Isolation Kit) of the *artus™ C. trachomatis Plus LC PCR Kit* on the *LightCycler® 2.0* Instrument in combination was determined using a dilution series of a *C. trachomatis* serovar E from 2.1 to nominal 0.00066 *C. trachomatis* copies/µl spiked in clinical swabs specimens. These were subjected to DNA extraction using the MagNA Pure DNA Isolation Kit (extraction volume: 200 µl, elution volume: 100 µl). Each of the eight dilutions was analyzed with the *artus™ C. trachomatis Plus LC PCR Kit* on three different days on eight replicates. The results were determined by a probit analysis. The analytical detection limit in consideration of the purification with the *LightCycler® 2.0* Instrument is consistently 0.4 copies/µl (p = 0.05). This means that there is a 95 % probability that 0.4 copies/µl will be detected.

To determine the analytical sensitivity of the *artus™ C. trachomatis Plus RG PCR Kit*, a *C. trachomatis* serovar E dilution series has been set up from 6.6 to nominal 0.0006 *C. trachomatis* copies/µl and analyzed on the *artus™ 3000* or correspondingly the *Rotor-Gene™ 3000* in combination with the *artus™ C. trachomatis Plus RG PCR Kit*. Testing was carried out on three different days on eight replicates. The results were determined by a probit analysis. The analytical detection limit of the *artus™ C. trachomatis Plus RG PCR Kit* in combination with the *artus™ 3000* or correspondingly the *Rotor-Gene™ 3000* is consistently 0.2 copies/µl (p = 0.05). This means that there is a 95 % probability that 0.2 copies/µl will be detected.

The analytical sensitivity in consideration of the purification (QIAamp DNA Mini Kit) of the *artus™ C. trachomatis Plus RG PCR Kit* on the *Rotor-Gene™ 3000* was determined using a dilution series of a *C. trachomatis* serovar E from 6.6 to nominal 0.0006 *C. trachomatis* copies/µl spiked in clinical swabs specimens. These were subjected to DNA extraction using the QIAamp DNA Mini Kit (extraction volume: 200 µl, elution volume: 100 µl). Each of the eight dilutions was analyzed with the *artus™ C. trachomatis Plus RG PCR Kit* on three different days on eight replicates. The results were determined by a probit analysis. The analytical detection limit in consideration of the purification of the *artus™ C. trachomatis Plus RG PCR Kit* in combination with the *Rotor-Gene™ 3000* is consistently 0.6 copies/µl ($p = 0.05$). This means that there is a 95 % probability that 0.6 copies/µl will be detected.

10.3.2.2 Specificity of the Qualitative C. trachomatis Assay

The specificity of the *artus™ C. trachomatis Plus LC* and *RG PCR Kit* is first and foremost ensured by the selection of the primers and probes, as well as the selection of stringent reaction conditions. The primers and probes were checked for possible homologies to all in gene banks published sequences by sequence comparison analysis. The detectability of all relevant serovars has thus been ensured by a database alignment and by PCR run on the Rotor-Gene™ 3000 with the serovars shown in Table 10. Moreover, the specificity was validated with 100 different *C. trachomatis* negative swabs, 30 urine and 30 semen samples. These did not generate any signals with the *C. trachomatis* specific primers and probes, which are included in the *C. trachomatis Plus LC* and *RG Master*. To determine the specificity of the *artus™ C. trachomatis Plus LC* and *RG PCR Kit* the control group listed in Table 2 was tested for cross-reactivity. None of the tested pathogens were reactive.

10.3.2.3 Precision of the Qualitative C. trachomatis Assay

Precision data of the *artus™ C. trachomatis Plus LC PCR Kit* were collected using the *C. trachomatis* serovar E of the concentration that is next to the threefold cut-off value (2.1 copies/µl in consideration of the purification, 0.66 copies/µl without consideration of the purification). Testing was performed with eight replicates. The precision data were calculated on the basis of the CT values of the amplification curves (CT: threshold cycle, Table 15 and 16). Based on these results, the overall statistical spread of any given sample with the mentioned concentration is 3.95 % (CT), 3.89 % (CT) in consideration of the purification with the QIAamp DNA Mini Kit and 3.47 % (CT) in consideration of the purification with the

MagNA Pure DNA Isolation Kit, for the detection of the *Internal Control* 2.29 % (CT), 3.48 % (CT) in consideration of the purification with the QIAamp DNA Mini Kit and 3.30 % (CT) in consideration of the purification with the MagNA Pure DNA Isolation Kit. These values are based on the totality of all single values of the determined variabilities.

Table 15: Precision data on the basis of the CT values.

C. trachomatis serovar E 0.66 copies/µl	**Standard deviation**	**Variance**	**Coefficient of variation [%]**
Intra-assay variability	0.29	0.08	0.91
Inter-assay variability	0.74	0.55	2.41
Inter-batch variability	1.35	1.81	4.23
Total variance	1.16	1.35	3.95

Table 16: Precision data on the basis of the CT values.

C. trachomatis serovar E 2.10 copies/µl	**Standard deviation**	**Variance**	**Coefficient of variation [%]**
Intra-assay variability	0.14	0.02	0.46
Inter-assay variability	0.78	0.61	2.46
Inter-batch variability	1.11	1.23	3.33
Total variance	1.26	1.59	3.89

Precision data of the *artus*™ *C. trachomatis RG PC Kit* were collected using the *C. trachomatis* serovar E of the concentration that is next to the threefold cut-off value (2.1 copies/µl in consideration of the purification, 0.66 copies/µl without consideration of the purification). Testing was performed with eight replicates. The precision data were calculated on basis of the CT values of the amplification curves (CT: threshold cycle, see Table 17 and 18). Based on these results, the overall statistical distribution of any given sample with the mentioned concentration is 2.45 % (CT) and 1.87 % (CT) in consideration of the purification with the QIAamp DNA Mini Kit, for the detection of the *Internal Control* 3.34 % (CT) and 2.13 % (CT) in consideration of the purification with the QIAamp DNA Mini Kit. These values are based on the totality of all single values of the determined variabilities.

Table 17: Precision data on the basis of the CT values.

C. trachomatis serovar E 0.66 copies/µl	**Standard deviation**	**Variance**	**Coefficient of variation [%]**
Intra-assay variability	0.38	0.14	1.23
Inter-assay variability	0.58	0.33	1.90
Inter-batch variability	0.46	0.21	1.47
Total variance	0.64	0.41	2.45

Table 18: Precision data on the basis of the CT values.

C. trachomatis serovar E 2.10 copies/µl	**Standard deviation**	**Variance**	**Coefficient of variation [%]**
Intra-assay variability	0.33	0.11	1.06
Inter-assay variability	0.49	0.11	1.09
Inter-batch variability	0.58	0.34	1.83
Total variance	0.58	0.34	1.87

10.3.2.4 Robustness of the qualitative C. trachomatis Assay

The verification of the robustness allows the determination of the total failure rate of the *artus™ C. trachomatis Plus LC* and *RG PCR Kit.* 100 *C. trachomatis* negative samples of swabs, 30 of urine and 30 of semen were spiked with 2.1 copies/µl elution volume of *C. trachomatis* control DNA (approximately threefold concentration of the analytical sensitivity limit). After extraction using the QIAamp DNA Mini Kit (seminal and swabs samples), QIAamp Viral RNA Mini Kit (urine samples) and the MagNA Pure DNA Isolation Kit (urine, swabs and seminal samples) these samples were analyzed with the *artus™ C. trachomatis Plus LC* and *RG PCR Kit.* For all *C. trachomatis* samples, the failure rate was 0 %. In addition, the robustness of the *Internal Control* was assessed by purification and analysis of 100 *C. trachomatis* negative swabs, 30 urine and 30 semen samples. The total failure rate was 0 %. Inhibitions were not observed. Thus, the robustness of the *artus™ C. trachomatis Plus LC* and *RG PCR Kit* is ≥ 99 %.

10.3.2.5 Diagnostic Evaluation of the qualitative C. trachomatis Assay

The *artus™ C. trachomatis Plus LC* and *RG PCR Kit* has been evaluated in four studies.

Comparison of the artus™ *C. trachomatis* Plus assays with the COBAS Amplicor CT/NG Assay regarding the testing of swab and urine specimens

In comparison of the *artus™ C. trachomatis Plus LC* and *RG PCR Kit* with the COBAS Amplicor (CT/NG Assay, Roche Diagnostics, Mannheim, Germany), 107 retrospective swab and urine specimens were tested.

Diagnostic Sensitivity

In this study, the sensitivity of the *artus*™ *C. trachomatis Plus LC* and *RG PCR Kit* was 100% and 98 %, respectively. Inhibitions did not occur.

Diagnostic Specificity

The diagnostic specificity of the *artus*™ *C. trachomatis Plus LC* and *RG PCR Kit* was 100 %.

Table 19: Results of the comparative validation study (LightCycler (bold) and Rotor-Gene™ 3000 (inverse))

artus™ *C. trachomatis* Plus PCR Kits	SYBR Green I/COBAS Amplicor +		SYBR Green I/COBAS Amplicor -	
+	**49**	*47*	**0**	*1*
-	**0**	*1*	**58**	*58*

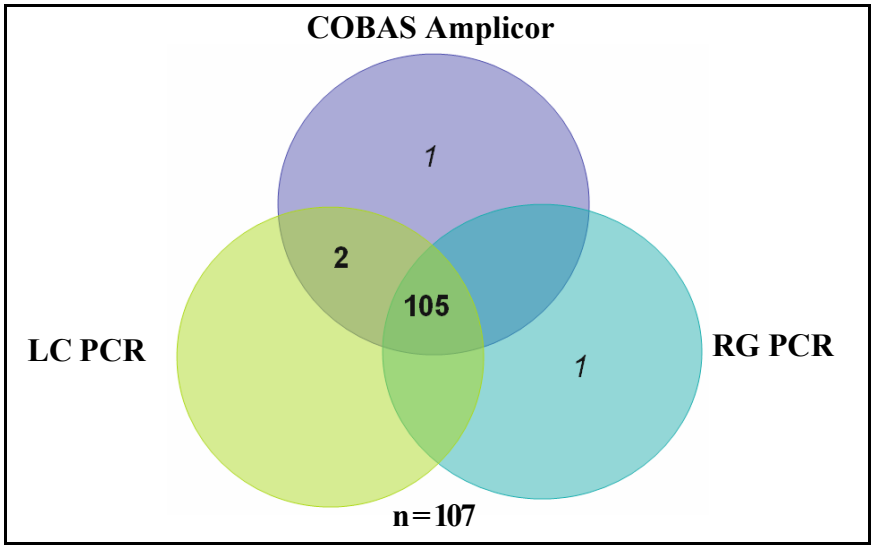

Figure 32: The Venn Diagram shows a correlation of 100% of the COBAS Amplicor CT/NG assay to the *artus™ C. trachomatis Plus LC PCR Kit* and 98.13% to the *artus™ C. trachomatis Plus RG PCR Kit.*

Comparison of the artus™ *C. trachomatis* Plus assays with the COBAS Amplicor CT/NG Assay regarding the testing of semen specimen

In comparison of the *artus™ C. trachomatis Plus LC* and *RG PCR Kit* with the COBAS Amplicor (CT/NG Assay, Roche Diagnostics, Mannheim, Germany), 65 prospective semen specimen were tested.

Diagnostic Sensitivity

For 65 tested retrospective semen specimen, a 100% correlation of the *artus™ C. trachomatis Plus LC* and *RG PCR Kit* compared to the COBAS Amplicor Assay was observed. The inhibition rate was 0 %.

Diagnostic Specificity

The diagnostic specificity of artus^{TM} *C. trachomatis Plus LC* and *RG Kit* is 100 %.

Table 20: Results of the comparative validation study (LightCycler (bold) and Rotor-Gene™ 3000 (inverse))

artus™ *C. trachomatis* Plus PCR Kits	COBAS Amplicor (IVF clinic) +		COBAS Amplicor (IVF clinic) -	
+	**16**	*16*	**0**	*0*
-	**0**	*0*	49	*49*

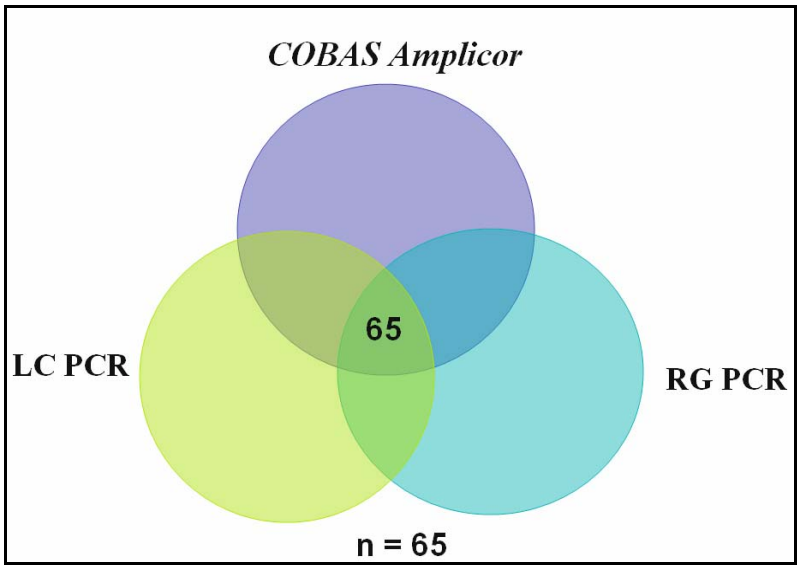

Figure 33: The Venn Diagram shows a correlation of 100% of the COBAS Amplicor CT/NG assay to the *artus™ C. trachomatis Plus LC* and *RG PCR Kit*.

Comparison of the artus™ *C. trachomatis* Plus assays with the LCx and Aptima Combo 2 Assay regarding the testing of swab and urine specimens

In comparison of the *artus™ C. trachomatis Plus LC* and *RG PCR Kit* with a LCR – ligase chain reaction (LCx® CT Assay, Abbott Laboratories, Abbott Park, USA) and a TMA (transcription mediated amplification [APTIMA Combo 2 Assay, Gen-Probe Incorporated, San Diego, USA]), 234 retrospective swab and urine specimens were tested.

Diagnostic Sensitivity

In this study, the correlation of the LCR (LCx® CT Assay) and Aptima® Combo 2™ Assay with the *artus™ C. trachomatis Plus LC PCR Kit* was 99% and with the *artus™ C. trachomatis Plus RG PCR Kit* 98 % for retrospective swab and urine specimens.

Diagnostic Specificity

The diagnostic specificity of the *artus™ C. trachomatis Plus LC PCR Kit* was 100% and of the *artus™ C. trachomatis Plus RG PCR Kit* 99 %.

Table 21: Results of the comparative validation study (LightCycler (bold) and Rotor-Gene™ 3000 (inverse))

artus™ *C. trachomatis* Plus PCR Kits	LCx/Aptima Combo 2 +		LCx/Aptima Combo 2 -	
+	**107**	*104*	**0***	*1**
-	**1**	*2*	**126**	*127*

*Two artus™ positive samples were removed from analysis due to low sample material for re-testing

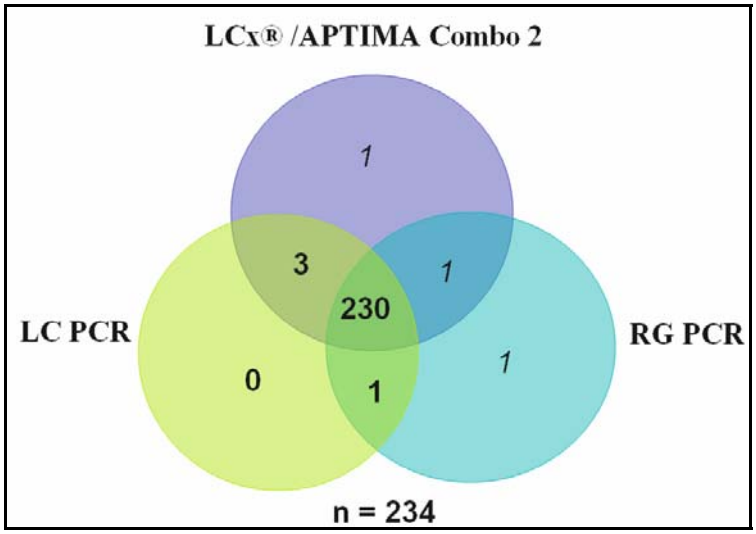

Figure 34: The Venn Diagram shows a total correlation of 98% of the LCx/Aptima Combo 2 assay to the *artus™ C. trachomatis Plus PCR Kit.*

Testing of clinical eye swabs

100 previously tested eye swabs have been tested retrospectively with the *artus™ C. trachomatis Plus RG PCR Kit*.

Diagnostic Sensitivity

For the 100 tested retrospective eye swabs, the diagnostic sensitivity of the *artus™ C. trachomatis Plus LC* and *RG PCR Kit* was 100 %.

Diagnostic Specificity

The diagnostic specificity of the *artus*™ *C. trachomatis Plus RG PCR Kit* was 100 %.

Table 22: Results of the comparative validation study (LightCycler (bold) and Rotor-Gene™ 3000 (inverse))

artus™ *C. trachomatis* Plus PCR Kits	In house assay (Klinikum Krefeld, Germany) +		In house assay (Klinikum Krefeld, Germany) -	
+	**5**	*5*	**0**	0
-	**0**	*0*	**95**	*95*

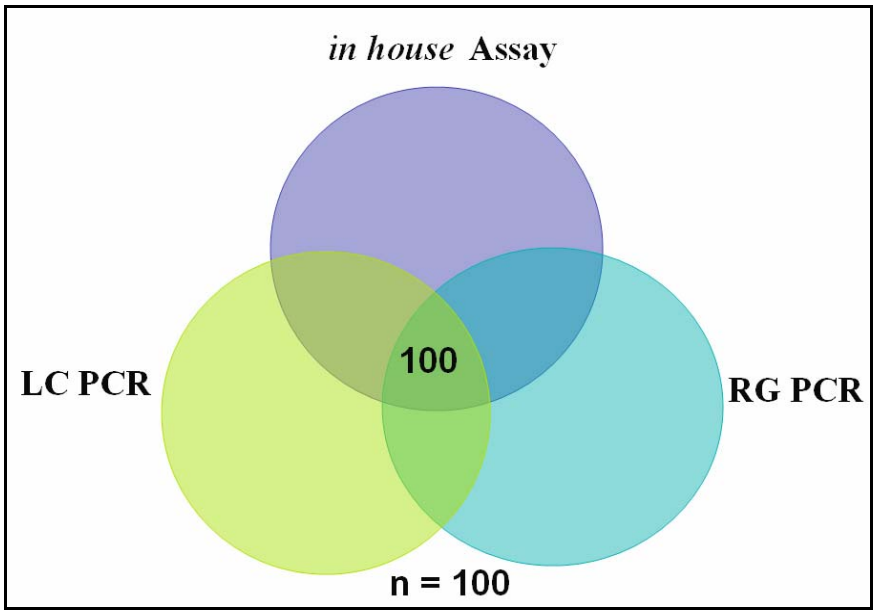

Figure 35: The Venn Diagram shows a total correlation of 100% of the in house assay to the *artus™ C. trachomatis Plus PCR Kit*.

10.4 DEVELOPMENT OF A REAL-TIME PCR IN VITRO DIAGNOSTICUM FOR THE DETECTION OF *CHLAMYDIA PNEUMONIAE*

The new *artus™ C. pneumoniae TM PCR Kit* was developed to allow for quantitation of bacterial load from cell culture or clinical specimens.

The *artus™ C. pneumoniae TM PCR Kit* constitutes a ready-to-use system for the detection of *C. pneumoniae* DNA using PCR in the ABI PRISM™ 7000 SDS instrument. The *C. pneumoniae Master* contains reagents and enzymes for the specific amplification of an 85 bp region of the *C. pneumoniae* genome (*ompA* gene), and for the direct detection of the specific amplicon. In addition, the kit contains a second heterologous amplification system to control the DNA isolation procedure and to check for possible PCR inhibition. This is detected as an *Internal Control* (*IC*) in a second fluorimeter channel. The detection limit of the analytical *C. pneumoniae* PCR is not reduced. For this application, the *Internal Control* has to be added to the isolation at a ratio of 0.1 µl per 1 µl elution volume. To allow the determination of the pathogen load, external positive controls (*C. pneumoniae QS 1 - 4*) were generated that are based on a plasmid containing the *C. pneumoniae* specific PCR amplification sequence. The PCR is prepared by addition of 15 µl master-mix to 10 µl template.

10.4.1 Analytical Sensitivity of the qualitative *C. pneumoniae* Assay

To determine the analytical sensitivity of the *artus™ C. pneumoniae TM PCR Kit*, a standard dilution series has been set up from 10 to nominal 0.0125 *C. pneumoniae* copies/µl and analyzed on the ABI PRISM™ 7000 SDS. Testing was carried out on three different days on eight replicates. The results were determined by a probit analysis. The detection limit of the *artus™ C. pneumoniae TM PCR Kit* is consistently 0.9 copies/µl ($p = 0.05$). This means that there is a 95 % probability that 0.9 copies/µl will be detected.

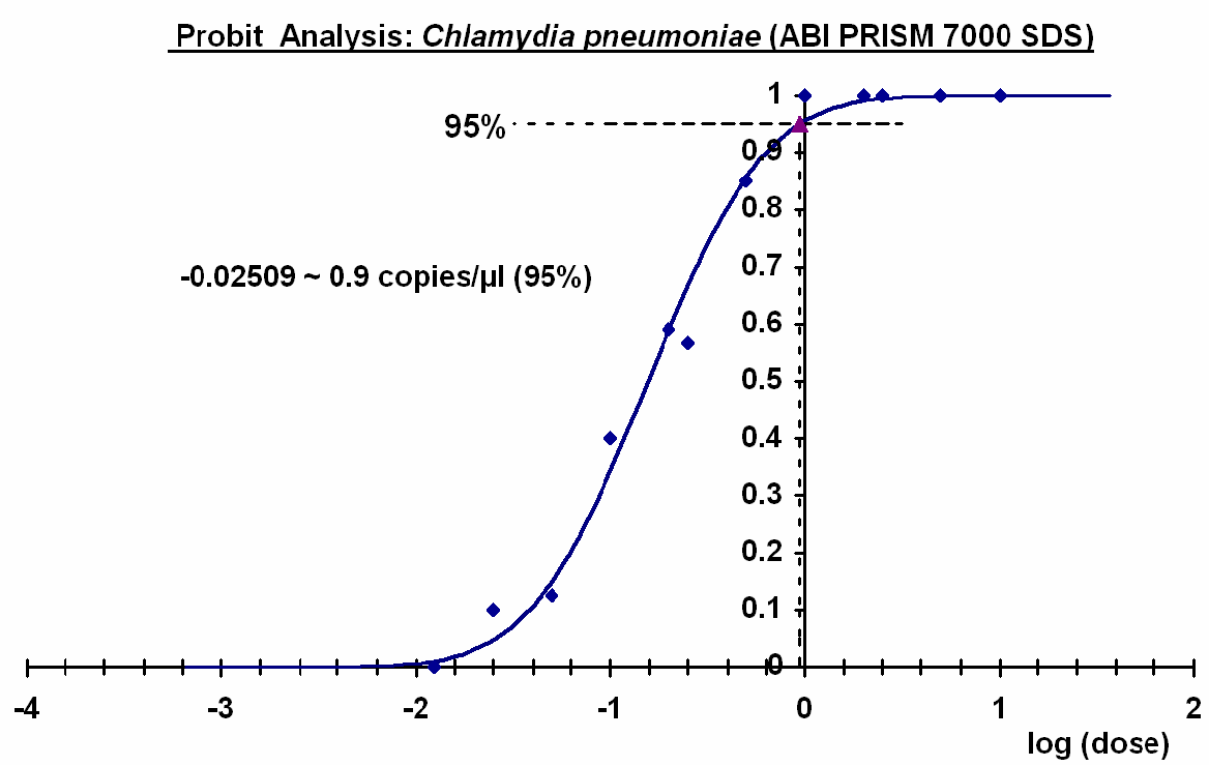

Figure 36: Analytical sensitivity of the artus™ *C. pneumoniae* TM PCR Kit

10.4.2 Specificity of the qualitative *C. pneumoniae* Assay

The primers and probes were checked for possible homologies to all sequences published in gene banks. To determine the specificity of the *artus™ C. pneumoniae TM PCR Kit*, the control group listed in Table 23 was tested for cross-reactivity. None of the tested pathogens has been reactive.

Table 23: Testing of the specificity of *C. pneumoniae*

Control group	Reference Stocks	Number	Serovar
Acinetobacter spp.	DSM	586	
Bordetella pertussis	DSMZ	5571	
C. pneumoniae	ATCC	VR2282	
C. pneumoniae	ATCC	VR1310	
C. psittaci	ATCC	Borg	
C. trachomatis	ATCC	VR-571B, -573, -347	A, B, Ba
C. trachomatis	ATCC	VR-572, -885 -348B, -346, -878, -879, -880, -886, -887	C- K
C. trachomatis	ATCC	VR-901B	(LGV I)
C. trachomatis	ATCC	VR-902B, VR-577	(LGV II)
C. trachomatis	ATCC	VR-903	(LGV III)
Candida albicans	DSM	1386	
Candida glabrata	DSM	11226	
Corynebacterium diphtheriae	DSMZ	44123	
Corynebacterium jeikeium	DSMZ	7171	
Eikenella corrodens	DSMZ	8340	
Enterococcus faecium	DSMZ	20477	
Escherichia coli	DSM	30083	
Gardnerella vaginalis	DSM	4944	
Haemophilus influenzae	DSM	4690	
Haemophilus parainfluenzae	DSMZ	8978	
Herpes simplex 1 and 2	-	-	
Klebsiella pneumoniae	DSM	30104	
Lactobacillus acidophilus	DSMZ	20079	
Mycobacterium bovis subsp. bovis	DSMZ	43990	
Mycobacterium tuberculosis	ATCC	25177	
Neisseria gonorrhoeae	DSM	9188	
Neisseria meningitidis	DSMZ	9188	
Peptostreptococcus productus	DSM	2950	
Prevotella denticola	DSMZ	20614	
Proteus mirabilis	NCTC	8309	
Pseudomonas aeruginosa	DSMZ	50071	
Salmonella typhimurium		BgVV-No	
Staphylococcus aureus	DSM	20372	
Staphylococcus epidermidis	DSMZ	1798	
Stenotrophomonas maltophilia	DSMZ	50170	
Streptococcus agalactiae	DSM	6784	
Streptococcus pneumoniae	DSMZ	20566	
Streptococcus pyogenes	DSM	20565	

11. Discussion

11.1 HOST-CELL RESPONSES INDUCED BY *CHLAMYDIA PNEUMONIAE* DURING PERSISTENCE IN THE IFN-γ MODEL

During the last years, it became apparent that *Chlamydia* can switch in cell culture and in the living organism to a metabolically and morphologically altered, persistent form (Hogan *et al.*, 2004). Thus, chlamydial persistence has recently become a central issue of chlamydial research.

In evolution, intracellular *Chlamydia* had to adapt to their host-cells: usually productive infection leads to destruction of host-cells, which is essential for the release of new elementary bodies. However, this effect must be balanced with host-cell survival. Taking into account these biological phenomena, chlamydial infections often stay undetected since they only cause mild symptoms; typically, chlamydial diseases show a subacute or chronic course. The best example for such a disease caused by persisting *Chlamydia* is reactive arthritis by *C. trachomatis* (Zeidler *et al.*, 2004; Whittum-Hudson *et al.*, 1999; Gerard *et al.*, 1998). Persistence may also play a role in the context of diseases caused or at least modified by *C. pneumoniae*.

On the one hand, a persistent state might be the result because the "wrong" host-cell-type is infected; if irreversible, persistence means a "dead-end" for the bacteria. On the other hand, if the persisting state is reversible or if productive infection is only slowed down and not completely interrupted, chlamydial persistence will provide a save haven for the long-time survival of the pathogen. Regardless of the fate of the persisting *Chlamydia*, persistent infection has a strong potential to influence the pathogenesis of the host-cell.

To gain insight into the biology of persistence and its implications, cell-culture models can provide valuable information: experimental conditions are optimally defined, high rates of relatively synchronized infection can be achieved, and signaling pathways can be easily dissected. Thus, the molecular interaction between *Chlamydia* and their host-cells can be investigated in a very sensitive system. Additionally, due to relatively strong cell responses and relatively low variations, screening methods such as microarrays can be employed more easily. Nevertheless, the culture models cannot replace animal models or the analysis of human tissue. However, they can facilitate the design of such studies; in particular, they can aid selection of good candidates for specific *in situ* investigations on a rational basis. For example, up-regulation of Egr-1 by *Chlamydia* was first identified by microarray and RT-PCR in HeLa-cells (Hess *et al.*, 2001). Meanwhile, this was confirmed for *C. pneumoniae* in vascular tissue (Rupp *et al.*, 2005).

As recently shown, at least two different types of responses exist at later time-points (day 4 or 7) in host-cells persistently infected – depending on the mode of the induction of persistence (Peters *et al.*, 2005). It is unclear, which of these models resembles the situation in the living organism the closest. However, it is just as well possible that these models and the different response patterns represent different *in vivo* situations. The IFN-γ model of induction of persistence is most frequently used because of several advantages compared to other models. For instance, in mice, IFN-γ plays a central role in the defense against *C. pneumoniae* (Netea *et al.*, 2004; Rothfuchs *et al.*, 2004b; Rothfuchs *et al.*, 2004a; Rothfuchs *et al.*, 2001; Geng *et al.*, 2000; Rottenberg *et al.*, 2000; Vuola *et al.*, 2000; Rottenberg *et al.*, 1999). The Penicillin G model leads to similar host-cell responses that can be induced by various conditions. In the IFN-γ model, persistence is clearly reversible as aberrant bodies can be efficiently re-activated into the productive cycle.

11.1.1 Screening of host-cell gene regulation by microarrays

In a former study (Peters *et al.*, 2005), only a few genes known to be up-regulated in productive infection were investigated. At a late time-point of IFN-γ-induced persistence, the regulation of these genes was no longer affected by *C. pneumoniae*. This experimental part of this thesis was conducted to explore whether *C. pneumoniae* silences host-cell responses in general, or whether a new expression pattern appears, which might ameliorate the survival of the bacteria and might also influence the pathogenesis. To identify such a putative modified expression pattern in persistence, a broad and sensitive screening method had to be used. Thus, microarrays were applied consisting of more than 20,000 human gene probe sets and a high MOI of *C. pneumoniae*. Gene expression at an early time-point (24h) of persistent infection was compared to the corresponding time-point of productive infection. Moreover, a relative late time-point of persistent infection was included (day 4), which most probably resembles the situation found in long-time *in situ* infection.

The screening was performed by analyzing each sample in duplicate. Pearson correlation revealed high reproducibility of the array results indicating the appropriateness of the broad screening method. Nevertheless, a second method, such as real-time PCR, should definitively be used for confirming the analysis since some probe sets on the arrays are expected to be based on wrong sequence information. After stringent filter analysis, 66 differentially expressed genes were identified. Using less stringent conditions, up to 100-times more altered

genes were discovered but concomitantly, the risk of obtaining false positive results increases. Therefore, the more stringent filter conditions are preferred due to higher specificity.

When the IFN-γ model is used for persistence study, tryptophan depletion through activation of the host tryptophan-degrading enzyme, indoleamine 2,3-dioxygenase (IDO), is expected (Pantoja *et al.*, 2000). Absolute analysis of microarrays revealed an absence of IDO 24h after productive *C. pneumoniae* infection. Thus, the Th1-dominated immune response seems not to be activated after this time of infection. After IFN-γ addition, IDO was detected in all sample types (mock-infected and *C. pneumoniae*-infected). Interestingly, signal intensities decrease about 10-fold when comparing 24h and 96h persistent infection. As long as IFN-γ is added to the cell culture, IDO seems to be activated. However, artificial activation of this enzyme is only possible for limited time periods, most probably reflecting the *in vivo* situation.

11.1.2 Determination of *C. pneumoniae* ompA cDNA and of bacterial load by real-time PCR

The bacterial load differed no more than 3-fold between the samples, whereby no chlamydial contamination of the mock samples took place (Fig. 11). The analysis of *C. pneumoniae* DNA and cDNA showed the success of the IFN-γ-induced persistence. In the presence of the cytokine, only a slight increase occurred in bacterial DNA from 24h to 96h. Moreover, cDNA levels decreased from 24h to 96h post infection and due to persistence induction caused by a modified bacterial metabolism and arrest of bacterial replication as previously described (Beatty *et al.*, 1994b). Therefore, the bacterial load measurement by real-time PCR is an excellent alternative to the frequently used immunofluorescence for monitoring a successful induction of persistence induction. Immunofluorescence staining of all sample types was performed by the department of Medical Microbiology, Medical School Hannover (Hannover, Germany) to ensure persistence induction. In addition, the used persistence model was optimized in the department of Medical Microbiology until less than 0.1% infectious EBs were produced within 24h. The IFN-γ model was analyzed in detail for the occurrence of infectious EBs in persistence and reactivation over a period of 10 days (Peters *et al.*, 2005). Therefore, the results obtained in this *in vitro* experiment enabled the drawing of conclusions for *in vivo* situations.

11.1.3 Suitable endogenous controls for the analysis of *C. pneumoniae*-induced host-cell responses

Before semiquantitative real-time PCRs (two-step RT-PCRs) for 19 HeLa-cell genes were performed (Table 3), which were regulated during infection with *C. pneumoniae* as shown by microarrays (Affymetrix® U133A chips), suitable endogenous controls were selected. Suzuki *et al*. (2000) reviewed the problem of choosing suitable endogenous controls. The authors recommend caution in the use of GAPDH as an endogenous control since it has been shown that its expression may be up-regulated in proliferating cells. They recommend β-actin as an alternative reference gene (Suzuki *et al.*, 2000). The use of GAPDH is severely criticized by others (Aerts *et al.*, 2004; Dheda *et al.*, 2004; Bustin, 2000). It is a particularly unpopular choice in cancer research because of its increased expression in aggressive cancers (Goidin *et al.*, 2001). Surveys of tumor cell lines or tissues reported inconsistent results with GAPDH, while beta-glucuronidase (GUS) and 18S rRNA were the best choices for this target (Aerts *et al.*, 2004). Care should be taken when 18S rRNA is used as an endogenous control since it is a ribosomal RNA species (not mRNA) and therefore may not always reflect the regulation effects of the overall cellular mRNA population.

Real-time PCR is an optimal method for gene expression analyses, but the selection of the endogenous control is critical for the interpretation of the data. Selection must be performed for each experiment to avoid erroneous conclusions. Hence, it is desirable to choose controls whose expression will remain constant under the experimental conditions designed for the target gene (Schmittgen and Zakrajsek, 2000).

18S rRNA, TBP and GUS had the most stable expression in the tested samples assuming that the control genes are not co-regulated (Table 4 and Figure 12). Moreover, the three similarly expressed genes are members of different gene families and underlie different transcription mechanisms. The conclusion can be drawn that these genes remain unregulated after *C. pneumoniae* infection and IFN-γ induction. Since the chosen mRNA species should be proportional to the amount of input RNA and 18S rRNA should not be used alone (see above), it was decided to use a combination of various endogenous controls as recommended by different research groups (Schmid *et al.*, 2003; Vandesompele *et al.*, 2002). Parallel normalization of the three endogenous controls improved the accuracy of the expression level measurements by compensating for small variations.

11.1.4 Host-cell gene expression profiling during active and persistent *C. pneumoniae* infection by real-time PCR and Northern blot analysis

Antimicrobial therapy, effective in treatment of acute infections, may not be able to resolve the persistent infection associated with the chronic conditions. Therefore, a recent line of research aims at a strategy for preventing or controlling chlamydial infections. Immune intervention could such a strategy but would require an understanding of the immunity mechanisms in the various stages of *C. pneumoniae* infection. After addition of IFN-γ, which simulates part of the Th1-dominated immune response to *C. pneumoniae* infection, the bacterium stops to replicate due to tryptophan depletion. However, the bacterium is not eliminated but instead enters a persistent state as part of its defense strategy.

The present host-cell gene expression profiling was conducted to investigate whether *C. pneumoniae* silences the responses of host-cells as previously observed for individual genes, or whether other changes in the expression of host-cell genes can be uncovered during persistence, which might ameliorate the survival of the bacteria and influence the pathogenesis. The latter hypothesis of a modified expression pattern of persistently infected cells was confirmed. The gene expression analysis of the 19 chosen genes showed two groups of gene regulation. The first group contained seven permanently up-regulated genes (DKK1, CYR61, RAI3, OASL, IFI44, PLK2 and PTGER4). The second group consisted of nine permanently down-regulated genes (Adlican, BNIP3, CA9, CTH, Insig1, DACT1, LOX, NDRG1 and HEY1). KRT17 could be placed into both groups showing an increase 24h after chlamydial productive infection and 24h after IFN-γ-induced persistent infection as well as a decrease 96h after persistence.

The observed induced changes in the mRNA-level (most likely, in host-cell transcription) reflect key responses and pathways of the infected cells: a) inhibition of apoptosis by up-regulation of anti-apoptotic and down-regulation of pro-apoptotic host-cell genes, b) changes in the cell cycle supporting its arrest, and c) changes in the lipid metabolism most likely participating in the composition of the inclusion membrane and mimicry (see Figure 37 for a model of *C. pneumoniae* host-cell interactions).

The interferon-induced 2'-5'-oligoadenylate synthetase (OASL) was permanently activated in infected HeLa-cells (Fig. 16). Overexpressed OASL up-regulates the anti-apoptotic genes Bcl-2 and Bcl-x_L promoting cell survival. Also, the activation of the wnt inhibitor dickkopf-1 (DKK1, Fig. 15) and the down-regulation of the lectin-like oxidized low-density lipoprotein scavenger receptor gene (LOX-1, Fig. 17) support cell survival. LOX-1, a receptor for oxidized low-density lipoprotein, activates pro-apoptotic genes like Bad and the Bcl-2 nineteen kilodalton interacting protein 3 (BNIP3) by the nuclear factor-kappa B (NF-kappa B) signaling pathway. Thus, the observed down-regulation of the death factor BNIP3 (Fig. 17), which has shown to be a key transcriptional target for NF-kappa B (Baetz *et al.*, 2005), results from down-regulation of LOX-1. Interestingly LOX-1 has shown to play a critical role in atherosclerosis providing a potential functional link between persistent infection with *C. pneumoniae* and atherosclerosis (Nakajima *et al.*, 2006; Vohra *et al.*, 2006). Regulation of the cell cycle by p53 is known to be controlled by various mechanisms (Balint and Vousden, 2001; Vogelstein *et al.*, 2000). A common feature to regulate p53 activity is the control of p53 protein stability. One key molecule in this process is HDM2 which directs the nuclear export and degradation of p53 in a ubiquitin-dependent way (Haupt *et al.*, 1997). Hairy/E(spl)-related with YRPW motif 1 (HEY1) activates p53 through transcriptional modulation of HDM2 expression. During *C. pneumoniae* infection, HEY1 was down regulated (Fig. 18). This decreased expression of HEY1 should lead to the activation of HDM2 and thus, inhibit p53-induced apoptosis. Recently, Wu and colleagues (Wu *et al.*, 2005) revealed the retinoic acid-induced protein 3 (RAI3) as a novel p53 transcriptional target functioning as an anti-apoptotic gene. The activation of other anti-apoptotic mechanisms is already known to occur in productive infection (Fischer *et al.*, 2004; Fan *et al.*, 1998). Thus, up-regulation of anti-apoptotic RAI3 (Fig. 15) seems also to be part of *C. pneumoniae* strategies for long time survival.

Another *C. pneumoniae* strategy during persistent infection seems to bring about cell cycle arrest. When DNA is damaged, the p53 target gene Polo-like kinase 2 (PLK2/SNK), arrests the cell cycle. Its permanent activation by *C. pneumoniae* (Fig. 16) may lead to a halt in the cell cycle near the G1-to-S transition. At 96h of persistent *C. pneumoniae* infection, Dapper homolog 1 (DACT1; also called LOC51339), an inhibitor of the wnt/beta-catenin signaling pathway, was down-regulated (Fig. 17). This should lead to β-catenin activation, up-regulation of c-myc and thereby down-regulation of the p53 inhibitor N-myc downstream regulated (NDRG1, Fig. 17) linking chlamydial infection again to inhibition of apoptosis and cell cycle arrest.

The permanently activated matrix protein Cysteine-rich 61 (CYR61/CCN1, Fig. 15) is an immediate-early response gene that is involved in similar signaling pathways: up-regulation of CYR61 activates β-catenin and the downstream-regulated c-myc. Thus, permanent activation of Cyr61 (together with down-regulation of DACT1 and decrease of NDRG1) by *C. pneumoniae* may activate a p53 pathway involving p21 and p130 activation, which leads to cell cycle arrest. In addition, it was shown that Cyr61 promotes cell survival (Todorovicc *et al.*, 2005); (Jin *et al.*, 2005). Hyperoxia induces Cyr61 expression in a variety of pulmonary cells and in lung tissue *in vivo*. Cyr61-overexpressing cells induce the Akt pathway and thereby protect against cell death.

For *C. pneumoniae* persistent infection of HeLa-cells, carbonic anhydrase 9 protein (CA9) may play a role in host-cell defense mechanisms. Dorai and colleagues have recently found that the intracellular domain of the CA9 protein seems to be involved in the Akt pathway (Dorai *et al.*, 2005). Down-regulation of CA9 will lead to down-regulation of anti-apoptotic genes (Bcl-2 and Bcl-x_L) and the activation of pro-apoptotic genes (Bad) and thereby cell death. CA9 catalyzes the reversible hydratation of CO_2 (Tripp *et al.*, 2001; Pastorek *et al.*, 1994). CA9 possesses cell surface enzyme activity which functions to convert CO_2 that has diffused to the extracellular space back into bicarbonate and protons. This enables the chloride-anion exchanger on the cell membrane to transport these newly generated HCO_3^- anions back into the cytoplasm. Thus, the function of membrane bound CA9 would contribute to extracellular acidose, which in turn leads to the activation of cell surface proteases, the release of growth factors, and suppression of the immune function of effector T-cells. In contrast, by down regulation of CA9 the immune function should be stimulated by *C. pneumoniae* (Fig. 17).

In addition, persisting *C. pneumoniae* seem to interact with the host-cell metabolism, e.g. the down-regulation of protein metabolism (Adlican, Fig. 17) or cystein biosynthesis (CTH, Fig. 18). Two differentially expressed genes, prostaglandin E receptor 4 (PTGER4, Fig. 16) and insulin-induced gene 1 (Insig1, Fig. 17), are involved in host-cell lipid synthesis. For *C. trachomatis*, it was shown that the lipid metabolism required for chlamydial growth contributes to Chlamydia-induced proinflammatory interleukin-8 production (Fukuda *et al.*, 2005). They found that *C. trachomatis* LGV II up-regulated PTGER4, a cell surface receptor for prostaglandin E2 (PGE2), in cervical epithelial HeLa 229 cells. It can be assumed that the permanent up-regulation of PTGER4 during *C. pneumoniae* infection, as shown in this

experimental work, leads simultaneously to interleukin-8 production and inflammation. In addition, up-regulation of interferon-induced, hepatitis C-associated microtubular aggregate 44kD protein (IFI44, Fig. 16) – a cytosceletal protein activated as response to stress or pathogen infection – seems to participate in inflammation processes. Insig1 is a protein of the endoplasmatic reticulum (ER) that blocks proteolytic activation of sterol regulatory element-binding proteins (SREBPs), membrane-bound transcription factors that activate synthesis of cholesterol and fatty acids. Thus, down-regulation of Insig1 during *C. pneumoniae* infection might lead to activation of lipid synthesis. Reduction of Insig1 can result from an inhibition of protein synthesis mediated by hypotonic stress (Harding *et al.*, 1999).

Only the cytosceletal protein keratin 17 (KRT17) showed a variable gene expression from increase to decrease during *C. pneumoniae* infection in this study (confirmed by Northern blot, Fig. 23). It is possible that KRT17 is involved in chlamydial lipid mimicry of their inclusion. Chlamydial inclusions are not effected by lysosomal fusion due to integration of host-cell lipids into their inclusion membrane. These host-cell lipids and specific chlamydial proteins protect chlamydial inclusion against the lysosome defense mechanism. KRT17 seems to contribute to the changes of the cytoskeleton by *C. pneumoniae* infection. Twenty-four hours after infection KRT17 is up-regulated. Thus, intracellular transport may be altered to internalize host-cell lipids into the inclusion membrane. Ninety-six hours after infection, lipid mimicry is accomplished. There is no longer a need to alter intracellular transport. In contrast, host-cell activity has to be reduced to provide long-term survival reflected in down-regulation of KRT17.

To ensure that results obtained with a MOI of 30 provide information for more physiological conditions, real-time PCR analysis for some of the genes were repeated using a MOI 3 of *C. pneumoniae* for infection. This modified experiment essentially revealed the same type of functional responses as described above, however, as expected, showing a smaller factor of regulation (Fig. 21). These results clearly indicated that experiments using MOI 30 of *C. pneumoniae* infection reflect changes of host-cell gene expression comparable to more physiological conditions.

The two genes HASPA1-A and HSPA1-B could not be confirmed to be differentially regulated using three different real-time PCRs (Fig. 20). The third PCR target region was the same as used by Affymetrix® for microarray analysis. Therefore, a Northern blot analysis was performed on HSPA1-A/B, CYR61 and KRT17 in mock- and *C. pneumoniae*-infected

HeLa-cells (MOI 30) in the IFN-γ persistence model. For normalization, RNA measurement prior to membrane blotting as well as the endogenous control TBP was used. Comparison of both normalization methods improved the conclusion that TBP is indeed unregulated and therefore, in combination with GUS and 18S rRNA best fitted as an endogenous control (Table 5). The results of altered gene expression obtained by real-time PCR were confirmed using Northern blotting with only one exception (CYR61). This confirmed that at least two different methods for gene expression studies should be employed. Real-time PCR seems to be more reliable than microarray analysis. In addition, it is a very sensitive method, which may explain the divergent results between Northern blot and real-time PCR. One reason, why HSPA1 altered gene expression could not be confirmed by neither real-time PCR nor Northern blotting, may be a sequence mismatch in one of the Affymetrix® HG-U133A probe sets for these genes.

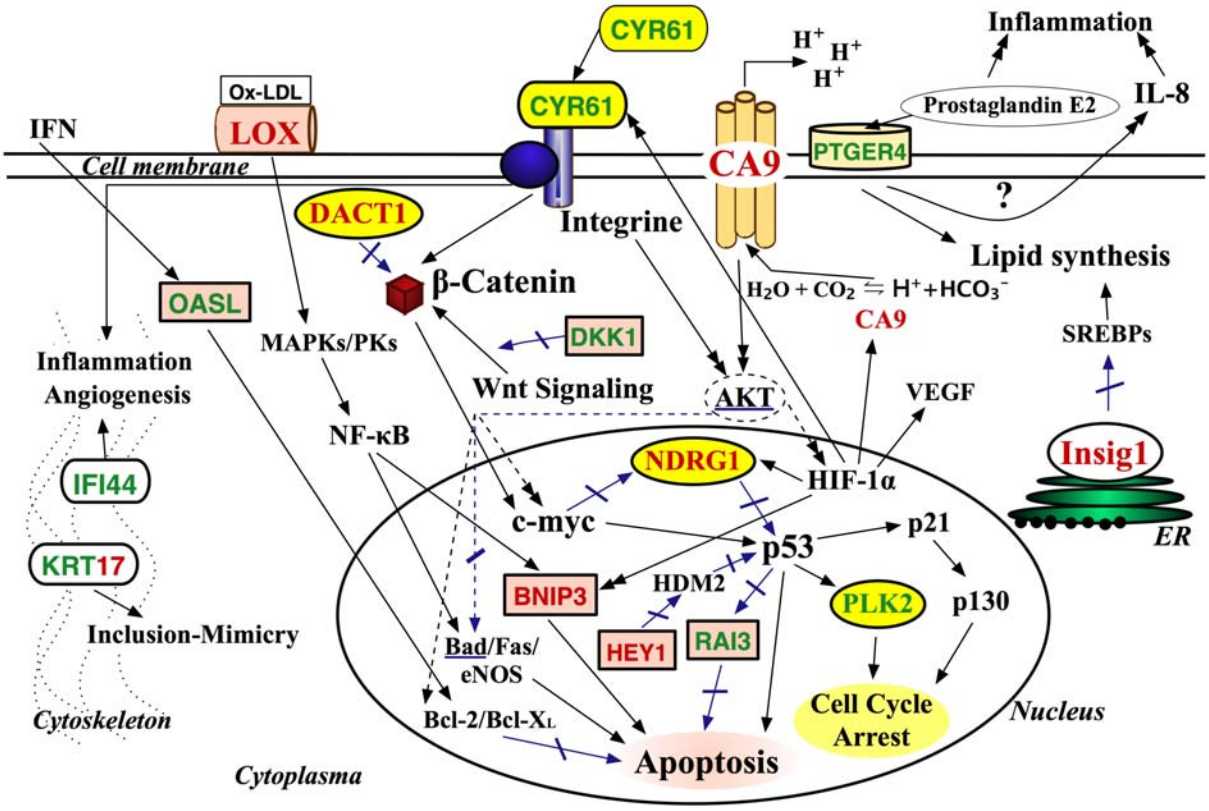

Figure 37: Predicted model of *C. pneumoniae* host-cell interaction. All analyzed host-cell genes that were up-regulated during persistent *C. pneumoniae* infection in HeLa-cells (IFN-γ model) are indicated in green. All host-cell genes which were down-regulated are indicated in red. Black arrows symbolize positive gene regulations; blue arrows symbolize negative feedback controls. The observed *C. pneumoniae*-induced regulations are linked to anti-apoptosis, cell-cycle arrest, and modifications of the lipid metabolism.

The results clearly show that *C. pneumoniae*-induced host-cell responses are not simply shut down at later time points of persistent infection. On the contrary, genes related to apoptosis, cell-cycle arrest, or host-cell metabolism are regulated by *C. pneumoniae*. As intracellular pathogens, *C. pneumoniae* rely on host-cells for all aspects of their survival. As such, the molecules participating in interactions with the host could be attractive targets for therapeutic intervention, in particular in persistence where antibiotic drugs are ineffective. The results of this gene expression study have cast light on host-pathogen relationships that are essential for chlamydial survival. In conclusion, the identified pattern of host-cell responses may reflect a general strategy of *C. pneumoniae* to permit long-time survival during persistence. Using this knowledge, strategically interfering with essential interactions between *C. pneumoniae* and the host-cell, like apoptosis inhibition or cell cycle arrest, could be exploited to develop an innovative and potentially more relevant arsenal of therapeutic compounds.

11.2 aRNA AMPLIFICATION

Targets for hybridization to high-density oligonucleotide arrays were prepared by two different protocols and subsequently compared. Samples from two different human cell types, a normal (mock-infected) and an IFN-γ-induced persistent *C. pneumoniae*-infected HeLa-cell, were used for target preparation by the two different methods (IVT and dIVT) of two independent experiments and hybridized to HG-U133A GeneChips. The results of these experiments suggest the following conclusions: i.) To generate a meaningful gene expression pattern *in vivo*, it is essential to isolate RNA from either an infected (persistent or productive) or a normal cell. RNA amplification methods have shown to be very well suited to generate the microgram quantities of RNA required to perform microarray experiments with an average increase of 5,532-fold (from 10 ng to 55.32 µg). The smaller amount of sample required for dIVT protocol (250 times less than IVT protocol) makes it a highly desirable method when changing from *in vitro* models to *in vivo* models in *C. pneumoniae* gene expression studies. ii.) The used RNA amplification technique enables the comparison of samples that contain divergent amounts of input RNA because size reductions of amplified RNAs were avoided resulting in low microarray backgrounds and high percentages of detection p values lower than 0.01 (see Table 22). iii.) aRNA amplification technology has proved to be a powerful approach for *C. pneumoniae* gene expression profiling *in vivo* with a mean Pearson coefficient of 0.95 comparing IVT versus dIVT samples. Several studies have reported an increase in the number of detectable genes when combining amplification techniques with microarrays (Nygaard *et al.*, 2003; Wang *et al.*, 2003; Hu *et al.*, 2002; Puskas

et al., 2002). Hu *et al.* (2002) suggested that the increase was due primarily to improvements in the signal intensity of low abundance genes, raising them above the noise level on the arrays. Although fewer differentially expressed genes were discovered in the IVT protocol, most were detectable for differential expression at a lower threshold by both protocols. Hence, the basis of differentially expressed genes in both protocols is identical.

Overall the results show that the data generated by the two IVT methods identified the same genes to be differentially expressed at suitable noise level settings. The usage of aRNA amplification will allow changing from *in vitro* to *in vivo* persistence models where sample amounts are limiting. This will advance our knowledge of persistence processes and how *Chlamydiaceae* participate in the pathogenesis of chronic diseases. Even after two or more rounds of RNA amplification the same major genes affected by chlamydial persistence can be identified stressing the suitability of linear RNA amplification methodology for *C. pneumoniae* gene expression studies *in vivo*. These major genes may lead to new potential drug targets and at the end to chlamydicidal drugs that are effective against persistent infection.

11.3 DEVELOPMENT OF REAL-TIME PCR *IN VITRO* DIAGNOSTICA FOR THE DETECTION OF *C. TRACHOMATIS*

The genome of the obligate intracellular bacterium *Chlamydia trachomatis* consists of a circular chromosome and a conserved cryptic plasmid, which is present in multiple copies (5-10) in the organism. The plasmid has great practical importance as the preferred target for nucleic acid amplification technologies. The use of this multi-copy gene improves the possibility to detect infected patients. However, a few isolates of *C. trachomatis* have been described, which do not contain the plasmid (Miyashita *et al.*, 2001; Matsumoto *et al.*, 1998; Stothard *et al.*, 1998; Farencena *et al.*, 1997; An and Olive, 1994). At the same time it could be shown that the cryptic plasmid is not necessary for the survival and the replication of *Chlamydia*.

Historically, *Chlamydia* detection methods have included cell culture in the McCoy cell line, direct staining with the Papanicolaou cell line, and direct immunofluorescence and immunoassays, e.g. ELISAs. Cell culture was once regarded as the gold standard for *C. trachomatis* diagnosis. However, the sensitivity of cell culture compared with expanded standard tests is at best 75-80% and probably nearer 55-65%. Serological detection methods are also available, but these are not species-specific and, therefore, often produce meaningless

results. More current methods of diagnosing and detecting *C. trachomatis*, which are based on nucleic acid amplification techniques, allow routine diagnostic testing and do not require invasive sample collection. Examples of two nucleic acid amplification-based diagnostic assays include the Roche COBAS® Amplicor *C. trachomatis* system and the Becton Dickinson Microbiology Systems BD Probe Tec ET. Both of these assays are based upon detecting the *C. trachomatis* cryptic plasmid.

One aim of this thesis was the development of quantitative as well as qualitative CE-marked *in vitro* diagnostic assays detecting *C. trachomatis* DNA from swab, urine and sperm samples by real-time PCR. The newly developed assays should also meet the need for an accurate, reliable, and easy-to-use diagnostic assay, capable of detecting all *C. trachomatis*, including those that do not contain the cryptic plasmid.

The newly developed diagnostic tests are able to sensitively detect *Chlamydiaceae* during all stages of their developmental life cycle. All of the developed quantitative PCRs allow for monitoring the bacterial load and therefore chlamydicidal drug therapy.

In 2005, in cooperation with a hospital in India, DNA of 176 patient samples was extracted using the QIAamp DNA Mini Kit. For amplification and detection, the *artus*™ *C. trachomatis Plus RG PCR Kit* was used on the Rotor-Gene™ 3000 instrument. In one patient sample, *C. trachomatis* was repeatedly detected using the *ompA*-specific primers, but it was not detected using primers specific for the cryptic plasmid, as shown in Figure 38. The cryptic plasmid-based PCR reaction is approximately 10-fold more sensitive compared to the *ompA*-based assay. Therefore, the negative result is not due to lower sensitivity. So a risk of getting false negative results by using only plasmid-based diagnostic assays exists. Therefore, an assay, which based on the cryptic plasmid as well as on the *ompA* gene, should be used.

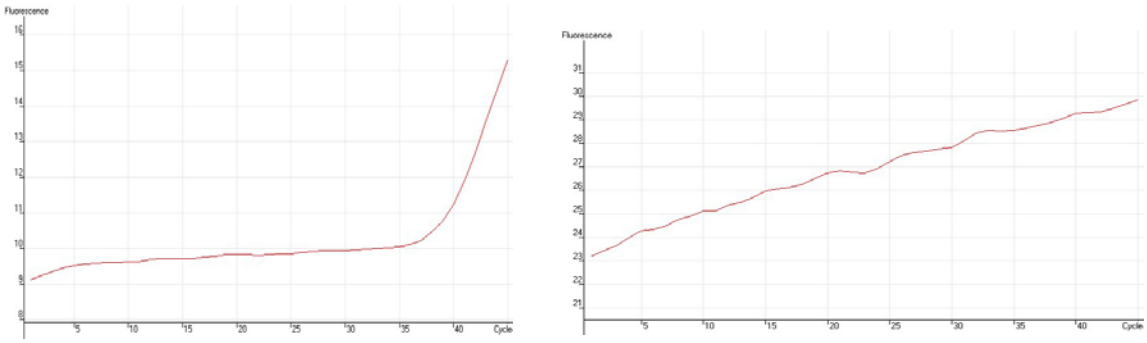

Figure 38: Detection of *C. trachomatis* DNA. In patient sample RT115 *C. trachomatis* DNA was repeatedly detected by using the *ompA*-based *artus*™ *C. trachomatis RG PCR Kit* (left side). In the same runs the patient sample was *C. trachomatis* negative using the *artus*™ *C. trachomatis Plus RG PCR Kit* as a cryptic plasmid-based detection assay by removal of the *ompA* primers and probes (right side).

All of the developed qualitative real-time PCRs provide methods and reagents for detecting *C. trachomatis* based upon detection of *C. trachomatis* genome and cryptic plasmid nucleic acid sequences. The existence of bacteria lacking the cryptic plasmid is known since several years, therefore it is irresponsible to use assays for the detection of *Chlamydia trachomatis* that consciously ignore this fact and rely only on the cryptic plasmid. The simultaneous detection of two sequences, as used in the *artus*™ *C. trachomatis Plus PCR Kits*, improves complementation and accuracy in detecting *Chlamydia*. It is thought that in the coming years, *Chlamydia* lacking the cryptic plasmid will increasingly appear, as most commercially available nucleic acid amplification-based detection systems are based on detection of the cryptic plasmid. This artificial selection leads to an advantage for *Chlamydia* lacking the plasmid by remaining undetected, untreated and therefore multiplying themselves.

The detection of rRNA represents an alternative. This target however entails an increased risk of unspecific detections, because 16S rRNA is present in all bacteria and the variable domains show a high degree of homology within bacteria families. Another disadvantage is that the target-RNA in patient sample degrades faster than DNA. For this reason, the probability to detect the pathogen in difficult sample material (e.g. sperm specimens) characterized by high inhibitory substances and low pathogen material, is low using a RNA target than a DNA target. Therefore, the *artus*™ *C. trachomatis Plus PCR Kits* have a unique combination of *C. trachomatis* specific primers and probes that enables high sensitive detection of chlamydial DNA from various sample materials and high specificity by using a combined *ompA*- and cryptic plasmid-based PCR.

With the developed CE-marked qualitative *C. trachomatis* real-time PCR assays laboratory physicians no longer need to implement mostly *in-house* confirmation-PCRs that are necessary if commercial test systems are used, which are based on the cryptic plasmid. Soon due to changes of the IVD guidelines these *in-house* assays will no longer be allowed. Then the only possibility for a responsible diagnostic is the use of a certified detection system that considers the fact of the appearance of plasmid-free variants and enables its sensitive and specific detection. Alternative methods like ELISA or cell culture can barely provide this.

11.4 DEVELOPMENT OF A REAL-TIME PCR *IN VITRO* DIAGNOSTICUM FOR THE DETECTION OF *C. PNEUMONIAE*

The diagnostic testing for chlamydial infection has changed in the past few years. New highly sensitive tests based on nucleic acid amplification technology (NAAT) have been developed to create new opportunities for innovative screening programs. Effective screening for these agents can facilitate prompt treatment and prevent its sequels. In this thesis, NAAT was used by developing the *artus*™ *C. pneumoniae TM PCR Kit* to determine the bacterial load in each *C. pneumoniae*-infected HeLa-cell sample. The developed real-time PCR assay is a powerful and very accurate tool to measure chlamydial DNA as well as cDNA. It allows controlling for successful persistence induction, for contamination of mock-infected control samples and to assure comparable results of *C. pneumoniae*-infected samples by knowing the bacterial load in each sample. Therefore, the *artus*™ *C. pneumoniae TM PCR Kit* is best adapted for the use in therapy monitoring, chlamydial gene expression studies, and an alternative to frequently used immunofluorescence.

12. References

ABI (1997) Relative Quantitation of Gene Expression. In *ABI PRISM 7700 Sequence Detection System, User Bulletin* Applied Biosystems, pp. 1-36.

Aerts, J.L., Gonzales, M.I. and Topalian, S.L. (2004) Selection of appropriate control genes to assess expression of tumor antigens using real-time RT-PCR. *Biotechniques*. **36**: 84-86, 88, 90-81.

Affymetrix (2001) Affymetrix Microarray Suite User's Guide. In Santa Clara, CA: Affymetrix.

Ahmad, A., Dawson, C.R., Yoneda, C., Togni, B. and Schachter, J. (1977) Resistance to reinfection with a chlamydial agent (guinea pig inclusion conjunctivitis agent). *Invest Ophthalmol Vis Sci*. **16**: 549-553.

An, Q. and Olive, D.M. (1994) Molecular cloning and nucleic acid sequencing of Chlamydia trachomatis 16S rRNA genes from patient samples lacking the cryptic plasmid. *Mol Cell Probes*. **8**: 429-435.

Anand, V. and Gupta, S. (2001) Antibiotic therapy in coronary heart disease--where do we currently stand? *Cardiovasc Drugs Ther*. **15**: 209-210.

Anderson, I.E., Baxter, S.I., Dunbar, S., Rae, A.G., Philips, H.L., Clarkson, M.J. and Herring, A.J. (1996) Analyses of the genomes of chlamydial isolates from ruminants and pigs support the adoption of the new species Chlamydia pecorum. *Int J Syst Bacteriol*. **46**: 245-251.

Appleyard, W.T., Aitken, I.D. and Anderson, I. (1983) Outbreak of chlamydial abortion in goats. *Vet Rec*. **113**: 63.

Baetz, D., Regula, K.M., Ens, K., Shaw, J., Kothari, S., Yurkova, N. and Kirshenbaum, L.A. (2005) Nuclear factor-kappaB-mediated cell survival involves transcriptional silencing of the mitochondrial death gene BNIP3 in ventricular myocytes. *Circulation*. **112**: 3777-3785.

Baker, J.A. (1944) Virus causing pneumonia in cats and producing elementary bodies. *J Exp Med*. **79**: 159.

Balin, B.J., Gerard, H.C., Arking, E.J., Appelt, D.M., Branigan, P.J., Abrams, J.T., *et al* (1998) Identification and localization of Chlamydia pneumoniae in the Alzheimer's brain. *Med Microbiol Immunol (Berl)*. **187**: 23-42.

Balint, E.E. and Vousden, K.H. (2001) Activation and activities of the p53 tumour suppressor protein. *Br J Cancer*. **85**: 1813-1823.

Bannantine, J.P., Griffiths, R.S., Viratyosin, W., Brown, W.J. and Rockey, D.D. (2000) A secondary structure motif predictive of protein localization to the chlamydial inclusion membrane. *Cell Microbiol*. **2**: 35-47.

Barbour, A.G., Amano, K., Hackstadt, T., Perry, L. and Caldwell, H.D. (1982) Chlamydia trachomatis has penicillin-binding proteins but not detectable muramic acid. *J Bacteriol*. **151**: 420-428.

Baugh, L.R., Hill, A.A., Brown, E.L. and Hunter, C.P. (2001) Quantitative analysis of mRNA amplification by in vitro transcription. *Nucl. Acids Res.* **29**: E29.

Beatty, W.L., Byrne, G.I. and Morrison, R.P. (1993) Morphologic and antigenic characterization of interferon gamma-mediated persistent Chlamydia trachomatis infection in vitro. *Proc Natl Acad Sci U S A*. **90**: 3998-4002.

Beatty, W.L., Byrne, G.I. and Morrison, R.P. (1994a) Repeated and persistent infection with Chlamydia and the development of chronic inflammation and disease. *Trends Microbiol*. **2**: 94-98.

Beatty, W.L., Morrison, R.P. and Byrne, G.I. (1995) Reactivation of persistent Chlamydia trachomatis infection in cell culture. *Infect Immun*. **63**: 199-205.

Beatty, W.L., Belanger, T.A., Desai, A.A., Morrison, R.P. and Byrne, G.I. (1994b) Tryptophan depletion as a mechanism of gamma interferon-mediated chlamydial persistence. *Infect Immun*. **62**: 3705-3711.

Bedson, S. (1950) Primary atypical pneumonia. *British Medical Journal*. **4695**: 1461-1463.

Bedson, S. and Gostling, J. (1954) A study of the mode of multiplication of psittacosis virus. *British Journal of Experimental Pathology*. **35**: 299-308.

Belland, R.J., Nelson, D.E., Virok, D., Crane, D.D., Hogan, D., Sturdevant, D., *et al* (2003) Transcriptome analysis of chlamydial growth during IFN-gamma-mediated persistence and reactivation. *Proc Natl Acad Sci U S A*. **100**: 15971-15976.

Birkelund, S., Lundemose, A.G. and Christiansen, G. (1989) Immunoelectron microscopy of lipopolysaccharide in Chlamydia trachomatis. *Infect Immun*. **57**: 3250-3253.

Black, C.M., Tharpe, J.A. and Russell, H. (1992) Distinguishing Chlamydia species by restriction analysis of the major outer membrane protein gene. *Mol Cell Probes*. **6**: 395-400.

Blythe, M.J., Katz, B.P., Batteiger, B.E., Ganser, J.A. and Jones, R.B. (1992) Recurrent genitourinary chlamydial infections in sexually active female adolescents. *J Pediatr*. **121**: 487-493.

Bonner, R.F., Emmert-Buck, M., Cole, K., Pohida, T., Chuaqui, R., Goldstein, S. and Liotta, L.A. (1997) Laser capture microdissection: molecular analysis of tissue. *Science*. **278**: 1481,1483.

Brade, H., Brade, L. and Nano, F.E. (1987) Chemical and serological investigations on the genus-specific lipopolysaccharide epitope of Chlamydia. *Proc Natl Acad Sci U S A*. **84**: 2508-2512.

Brunham, R.C. and Peeling, R.W. (1994) Chlamydia trachomatis antigens: role in immunity and pathogenesis. *Infect Agents Dis*. **3**: 218-233.

Burgess, J.K. and Hazelton, R.H. (2000) New developments in the analysis of gene expression. *Redox Rep*. **5**: 63-73.

Bustin, S.A. (2000) Absolute quantification of mRNA using real-time reverse transcription polymerase chain reaction assays. *J Mol Endocrinol*. **25**: 169-193.

Byrne, G.I. and Krueger, D.A. (1983) Lymphokine-mediated inhibition of Chlamydia replication in mouse fibroblasts is neutralized by anti-gamma interferon immunoglobulin. *Infect Immun*. **42**: 1152-1158.

Byrne, G.I., Lehmann, L.K. and Landry, G.J. (1986) Induction of tryptophan catabolism is the mechanism for gamma-interferon-mediated inhibition of intracellular Chlamydia psittaci replication in T24 cells. *Infect Immun*. **53**: 347-351.

Caldwell, H.D., Kromhout, J. and Schachter, J. (1981) Purification and partial characterization of the major outer membrane protein of Chlamydia trachomatis. *Infect Immun*. **31**: 1161-1176.

Caldwell, H.D., Wood, H., Crane, D., Bailey, R., Jones, R.B., Mabey, D., *et al* (2003) Polymorphisms in Chlamydia trachomatis tryptophan synthase genes differentiate between genital and ocular isolates. *J Clin Invest*. **111**: 1757-1769.

Cockram, F.A. and Jackson, A.R. (1981) Keratoconjunctivitis of the koala, Phascolarctos cinereus, caused by Chlamydia psittaci. *J Wildl Dis*. **17**: 497-504.

Coles, A.M., Reynolds, D.J., Harper, A., Devitt, A. and Pearce, J.H. (1993) Low-nutrient induction of abnormal chlamydial development: a novel component of chlamydial pathogenesis? *FEMS Microbiol Lett*. **106**: 193-200.

Coombes, B.K. and Mahony, J.B. (2001) cDNA array analysis of altered gene expression in human endothelial cells in response to Chlamydia pneumoniae infection. *Infect Immun*. **69**: 1420-1427.

Craven, R.A. and Banks, R.E. (2001) Laser capture microdissection and proteomics: possibilities and limitation. *Proteomics*. **1**: 1200-1204.

Danilition, S.L., Maclean, I.W., Peeling, R., Winston, S. and Brunham, R.C. (1990) The 75-kilodalton protein of Chlamydia trachomatis: a member of the heat shock protein 70 family? *Infect Immun*. **58**: 189-196.

Dheda, K., Huggett, J.F., Bustin, S.A., Johnson, M.A., Rook, G. and Zumla, A. (2004) Validation of housekeeping genes for normalizing RNA expression in real-time PCR. *Biotechniques*. **37**: 112-114, 116, 118-119.

Dorai, T., Sawczuk, I.S., Pastorek, J., Wiernik, P.H. and Dutcher, J.P. (2005) The role of carbonic anhydrase IX overexpression in kidney cancer. *EurJ Cancer*. **41**: 2935-2947.

Eb, F., Orfila, J. and Lefebvre, J.F. (1976) Ultrastructural study of the development of the agent of ewe's abortion. *Journal of Ultrastructure Research*. **56**: 177-185.

Eberwine, J., Yeh, H., Miyashiro, K., Cao, Y., Nair, S., Finnell, R., *et al* (1992) Analysis of gene expression in single live neurons. *Proc Natl Acad Sci U S A*. **89**: 3010-3014.

Eickhoff M, Laue T, Ruckes T, Cramer SO, Krupp G and Tiemann C. (2003) Ultra-rapid detection of Chlamydia trachomatis by real-time PCR in the LightCycler using SYBR green technology or 5'-nuclease probes. *Clin Lab*. **49**: 217-225.

Everett, K.D. and Andersen, A.A. (1997) The ribosomal intergenic spacer and domain I of the 23S rRNA gene are phylogenetic markers for Chlamydia spp. *Int J Syst Bacteriol*. **47**: 461-473.

Everett, K.D., Bush, R.M. and Andersen, A.A. (1999) Emended description of the order Chlamydiales, proposal of Parachlamydiaceae fam. nov. and Simkaniaceae fam. nov., each containing one monotypic genus, revised taxonomy of the family Chlamydiaceae, including a new genus and five new species, and standards for the identification of organisms. *Int J Syst Bacteriol*. **49 Pt 2**: 415-440.

Fan, T., Lu, H., Hu, H., Shi, L., McClarty, G.A., Nance, D.M., *et al* (1998) Inhibition of apoptosis in chlamydia-infected cells: blockade of mitochondrial cytochrome c release and caspase activation. *J Exp Med*. **187**: 487-496.

Farencena, A., Comanducci, M., Donati, M., Ratti, G. and Cevenini, R. (1997) Characterization of a new isolate of Chlamydia trachomatis which lacks the common plasmid and has properties of biovar trachoma. *Infect Immun*. **65**: 2965-2969.

Fehlner-Gardiner, C., Roshick, C., Carlson, J.H., Hughes, S., Belland, R.J., Caldwell, H.D. and McClarty, G. (2002) Molecular basis defining human Chlamydia trachomatis tissue tropism. A possible role for tryptophan synthase. *J Biol Chem*. **277**: 26893-26903.

Fischer, S.F., Vier, J., Kirschnek, S., Klos, A., Hess, S., Ying, S. and Hacker, G. (2004) Chlamydia inhibit host cell apoptosis by degradation of proapoptotic BH3-only proteins. *J Exp Med*. **200**: 905-916.

Fox, A., Rogers, J.C., Gilbart, J., Morgan, S., Davis, C.H., Knight, S. and Wyrick, P.B. (1990) Muramic acid is not detectable in Chlamydia psittaci or Chlamydia trachomatis by gas chromatography-mass spectrometry. *Infect Immun*. **58**: 835-837.

Frost, E.H., Deslandes, S., Veilleux, S. and Bourgaux-Ramoisy, D. (1991) Typing Chlamydia trachomatis by detection of restriction fragment length polymorphism in the gene encoding the major outer membrane protein. *J Infect Dis*. **163**: 1103-1107.

Fukuda, E.Y., Lad, S.P., Mikolon, D.P., Iacobelli-Martinez, M. and Li, E. (2005) Activation of lipid metabolism contributes to interleukin-8 production during Chlamydia trachomatis infection of cervical epithelial cells. *Infect Immun*. **73**: 4017-4024.

Fukushi, H. and Hirai, K. (1992) Proposal of Chlamydia pecorum sp. nov. for Chlamydia strains derived from ruminants. *Int J Syst Bacteriol*. **42**: 306-308.

Gaillard, E.T., Hargis, A.M., Prieur, D.J., Evermann, J.F. and Dhillon, A.S. (1984) Pathogenesis of feline gastric chlamydial infection. *Am J Vet Res*. **45**: 2314-2321.

Geng, Y., Berencsi, K., Gyulai, Z., Valyi-Nagy, T., Gonczol, E. and Trinchieri, G. (2000) Roles of interleukin-12 and gamma interferon in murine Chlamydia pneumoniae infection. *Infect Immun*. **68**: 2245-2253.

Gerard, H.C., Branigan, P.J., Schumacher, H.R., Jr. and Hudson, A.P. (1998) Synovial Chlamydia trachomatis in patients with reactive arthritis/Reiter's syndrome are viable but show aberrant gene expression. *J Rheumatol*. **25**: 734-742.

Gieffers, J., Rupp, J., Gebert, A., Solbach, W. and Klinger, M. (2004) First-choice antibiotics at subinhibitory concentrations induce persistence of Chlamydia pneumoniae. *Antimicrob Agents Chemother*. **48**: 1402-1405.

Gieffers, J., Fullgraf, H., Jahn, J., Klinger, M., Dalhoff, K., Katus, H.A., *et al* (2001) Chlamydia pneumoniae infection in circulating human monocytes is refractory to antibiotic treatment. *Circulation*. **103**: 351-356.

Girjes, A.A., Ellis, W.A., Lavin, M.F. and Carrick, F.N. (1993a) Immuno-dot blot as a rapid diagnostic method for detection of chlamydial infection in koalas (Phasolarctos cinereus). *Vet Rec*. **133**: 136-141.

Girjes, A.A., Hugall, A., Graham, D.M., McCaul, T.F. and Lavin, M.F. (1993b) Comparison of type I and type II Chlamydia psittaci strains infecting koalas (Phascolarctos cinereus). *Vet Microbiol*. **37**: 65-83.

Goidin, D., Mamessier, A., Staquet, M.J., Schmitt, D. and Berthier-Vergnes, O. (2001) Ribosomal 18S RNA prevails over glyceraldehyde-3-phosphate dehydrogenase and beta-actin genes as internal standard for quantitative comparison of mRNA levels in invasive and noninvasive human melanoma cell subpopulations. *Anal Biochem*. **295**: 17-21.

Gordon, F.B., Dressler, H.R. and Quan, A.L. (1966) Observations on guinea pig inclusion conjunctivitis agent. *J Infect Dis*. **116**: 203-207.

Grayston, J.T. (1989a) Chlamydia pneumoniae, strain TWAR. *Chest*. **95**: 664-669.

Grayston, J.T. (2000) Background and current knowledge of Chlamydia pneumoniae and atherosclerosis. *J Infect Dis*. **181 Suppl 3**: S402-410.

Grayston, J.T., Alexander, E.R., Kenny, G.E., Clarke, E.R., Fremont, J.C. and Maccoll, W.A. (1965) Mycoplasma Pneumoniae Infections. Clinical and Epidemiologic Studies. *Jama*. **191**: 369-374.

Grayston, J.T., C.-C. Kuo, L. A. Campbell and S.-P. Wang (1989b) *Chlamydia pneumoniae* sp. nov. for *Chlamydia* sp. strain TWAR. *Int. J. Syst. Bacteriol.* **39**: 88–90.

Grieg, J.R. (1936) Enzootic abortion in ewes. A preliminary note. *Vet Rec*. **48**: 1225-1232.

Hahn, D.L., Dodge, R.W. and Golubjatnikov, R. (1991) Association of Chlamydia pneumoniae (strain TWAR) infection with wheezing, asthmatic bronchitis, and adult-onset asthma. *Jama*. **266**: 225-230.

Halberstaedter, L. and Prowazek, S.v. (1907) Über Zelleinschlüsse parasitärer Natur beim Trachom. *Arb.GesundhAmt.* **26**: 44-47.

Hammerschlag, M.R. (2003) Advances in the management of Chlamydia pneumoniae infections. *Expert Rev Anti Infect Ther*. **1**: 493-503.

Hammerschlag, M.R., Chirgwin, K., Roblin, P.M., Gelling, M., Dumornay, W., Mandel, L., *et al* (1992) Persistent infection with Chlamydia pneumoniae following acute respiratory illness. *Clin Infect Dis*. **14**: 178-182.

Harding, H.P., Zhang, Y. and Ron, D. (1999) Protein translation and folding are coupled by an endoplasmic-reticulum-resident kinase. *Nature*. **397**: 271-274.

Hartley, J.C., Stevenson, S., Robinson, A.J., Littlewood, J.D., Carder, C., Cartledge, J., *et al* (2001) Conjunctivitis due to Chlamydophila felis (Chlamydia psittaci feline pneumonitis agent) acquired from a cat: case report with molecular characterization of isolates from the patient and cat. *J Infect*. **43**: 7-11.

Haupt, Y., Maya, R., Kazaz, A. and Oren, M. (1997) Mdm2 promotes the rapid degradation of p53. *Nature*. **387**: 296-299.

Herring, A.J., Anderson, I.E., McClenaghan, M., Inglis, N.F., Williams, H., Matheson, B.A., *et al* (1987) Restriction endonuclease analysis of DNA from two isolates of Chlamydia psittaci obtained from human abortions. *Br Med J (Clin Res Ed)*. **295**: 1239.

Hess, S., Rheinheimer, C., Tidow, F., Bartling, G., Kaps, C., Lauber, J., *et al* (2001) The reprogrammed host: Chlamydia trachomatis-induced up-regulation of glycoprotein 130 cytokines, transcription factors, and antiapoptotic genes. *Arthritis Rheum*. **44**: 2392-2401.

Hess, S., Peters, J., Bartling, G., Rheinheimer, C., Hegde, P., Magid-Slav, M., *et al* (2003) More than just innate immunity: comparative analysis of Chlamydophila pneumoniae and Chlamydia trachomatis effects on host-cell gene regulation. *Cell Microbiol*. **5**: 785-795.

Hoelzle, L.E., Steinhausen, G. and Wittenbrink, M.M. (2000) PCR-based detection of chlamydial infection in swine and subsequent PCR-coupled genotyping of chlamydial omp1-gene amplicons by DNA-hybridization, RFLP-analysis and nucleotide sequence analysis. *Epidemiol Infect*. **125**: 427-439.

Hogan, R.J., Mathews, S.A., Kutlin, A., Hammerschlag, M.R. and Timms, P. (2003) Differential expression of genes encoding membrane proteins between acute and continuous Chlamydia pneumoniae infections. *Microb Pathog*. **34**: 11-16.

Hogan, R.J., Mathews, S.A., Mukhopadhyay, S., Summersgill, J.T. and Timms, P. (2004) Chlamydial persistence: beyond the biphasic paradigm. *Infect Immun*. **72**: 1843-1855.

Hu, L., Wang, J., Baggerly, K., Wang, H., Fuller, G.N., Hamilton, S.R., *et al* (2002) Obtaining reliable information from minute amounts of RNA using cDNA microarrays. *BMC Genomics*. **3**: 16.

Igietseme, J.U., Uriri, I.M., Kumar, S.N., Ananaba, G.A., Ojior, O.O., Momodu, I.A., *et al* (1998) Route of infection that induces a high intensity of gamma interferon-secreting T cells in the genital tract produces optimal protection against Chlamydia trachomatis infection in mice. *Infect Immun*. **66**: 4030-4035.

Ingalls, R.R. and Golenbock, D.T. (1995) CD11c/CD18, a transmembrane signaling receptor for lipopolysaccharide. *J Exp Med*. **181**: 1473-1479.

Inman, R.D., Whittum-Hudson, J.A., Schumacher, H.R. and Hudson, A.P. (2000) Chlamydia and associated arthritis. *Curr Opin Rheumatol*. **12**: 254-262.

Jain, K.K., Mathur, G.P. and Srivastava, J.R. (1975) Malignancy in childhood: A clinico-pathological study of 45 cases. *Indian J Pediatr*. **42**: 61-66.

Jin, Y., Kim, H.P., Ifedigbo, E., Lau, L.F. and Choi, A.M. (2005) Cyr61 protects against hyperoxia-induced cell death via Akt pathway in pulmonary epithelial cells. *Am J Respir Cell Mol Biol*. **33**: 297-302.

Jones, B.R., Collier, L.H. and Smith, C.H. (1959) Isolation of virus from inclusion blenorrhoea. *Lancet*: 902-905.

Jones, M.L., Gaston, J.S. and Pearce, J.H. (2001) Induction of abnormal Chlamydia trachomatis by exposure to interferon-gamma or amino acid deprivation and comparative antigenic analysis. *Microb Pathog*. **30**: 299-309.

Jorgensen, D.M. (1997) Gestational psittacosis in a Montana sheep rancher. *Emerg Infect Dis*. **3**: 191-194.

Kalman, S., Mitchell, W., Marathe, R., Lammel, C., Fan, J., Hyman, R.W., *et al* (1999) Comparative genomes of Chlamydia pneumoniae and C. trachomatis. *Nat Genet*. **21**: 385-389.

Kaltenboeck, B. and Storz, J. (1992) Biological properties and genetic analysis of the ompA locus in chlamydiae isolated from swine. *Am J Vet Res*. **53**: 1482-1487.

Kaltenboeck, B., Kousoulas, K.G. and Storz, J. (1992) Two-step polymerase chain reactions and restriction endonuclease analyses detect and differentiate ompA DNA of Chlamydia spp. *J Clin Microbiol*. **30**: 1098-1104.

Kazdan, J.J., Schachter, J. and Okumoto, M. (1967) Inclusion conjunctivitis in the guinea pig. *Am J Ophthal*. **64**: 116-124.

Kikuta, L.C., Puolakkainen, M., Kuo, C.C. and Campbell, L.A. (1991) Isolation and sequence analysis of the Chlamydia pneumoniae GroE operon. *Infect Immun*. **59**: 4665-4669.

Knudsen, K., Madsen, A.S., Mygind, P., Christiansen, G. and Birkelund, S. (1999) Identification of two novel genes encoding 97- to 99-kilodalton outer membrane proteins of Chlamydia pneumoniae. *Infect Immun*. **67**: 375-383.

Koehler, J.E., Birkelund, S. and Stephens, R.S. (1992) Overexpression and surface localization of the Chlamydia trachomatis major outer membrane protein in Escherichia coli. *Mol Microbiol*. **6**: 1087-1094.

Kornak, J.M., Kuo, C.C. and Campbell, L.A. (1991) Sequence analysis of the gene encoding the Chlamydia pneumoniae DnaK protein homolog. *Infect Immun*. **59**: 721-725.

Kuo, C.C., Jackson, L.A., Campbell, L.A. and Grayston, J.T. (1995) Chlamydia pneumoniae (TWAR). *Clin Microbiol Rev*. **8**: 451-461.

Kuo, C.C., Shor, A., Campbell, L.A., Fukushi, H., Patton, D.L. and Grayston, J.T. (1993) Demonstration of Chlamydia pneumoniae in atherosclerotic lesions of coronary arteries. *J Infect Dis*. **167**: 841-849.

Lennart J., Andersen AA. and Rockey DD. (2001) Growth and development of tetracycline-resistant Chlamydia suis. *Antimicrob Agents Chemother*. **45**: 2198-2203.

Lietman, T., Brooks, D., Moncada, J., Schachter, J., Dawson, C. and Dean, D. (1998) Chronic follicular conjunctivitis associated with Chlamydia psittaci or Chlamydia pneumoniae. *Clin Infect Dis*. **26**: 1335-1340.

Lin, S.L. (2003) Single-cell cDNA library construction using cycling aRNA amplification. *Methods Mol Biol*. **221**: 117-127.

Louis, C., Nicolas, G., Eb, F., Lefebvre, J.F. and Orfila, J. (1980) Modifications of the envelope of Chlamydia psittaci during its developmental cycle: freeze-fracture study of complementary replicas. *J Bacteriol*. **141**: 868-875.

Lukacova, M., Baumann, M., Brade, L., Mamat, U. and Brade, H. (1994) Lipopolysaccharide smooth-rough phase variation in bacteria of the genus Chlamydia. *Infect Immun*. **62**: 2270-2276.

Mackay, I. (2004) Real-time PCR in the microbiology laboratory. *Clin Microbiol Infect*. **10**: 190-212.

Mare, C.J. (1994) Mammalian chlamydiosis. In *Handbook of Zoonoses.* Beran, G.W. (ed.) Boca Raton, Fl., U.S.A.: CRC Press, pp. 403-415.

Matsumoto, A. (1973) Fine structures of cell envelopes of Chlamydia organisms as revealed by freeze-etching and negative staining techniques. *J Bacteriol*. **116**: 1355-1363.

Matsumoto, A. (1982) Surface projections of Chlamydia psittaci elementary bodies as revealed by freeze-deep-etching. *J Bacteriol*. **151**: 1040-1042.

Matsumoto, A. and Manire, G.P. (1970) Electron microscopic observations on the effects of penicillin on the morphology of Chlamydia psittaci. *J Bacteriol*. **101**: 278-285.

Matsumoto, A., Izutsu, H., Miyashita, N. and Ohuchi, M. (1998) Plaque Formation by and Plaque Cloning of Chlamydia trachomatis Biovar Trachoma. *J Clin Microbiol*. **36**: 3013-3019.

McCauley, E.H. and Tieken, E.L. (1968) Psittacosis-lymphogranuloma venereum agent isolated during an abortion epizootic in goats. *J. Am. Vet. Med. Assoc*. **152**: 1758-1765.

McColl, K.A., Martin, R.W., Gleeson, L.J., Handasyde, K.A. and Lee, A.K. (1984) Chlamydia infection and infertility in the female koala (Phascolarctos cinereus). *Vet Rec*. **115**: 655.

McKinlay, A.W., White, N., Buxton, D., Inglis, J.M., Johnson, F.W., Kurtz, J.B. and Brettle, R.P. (1985) Severe Chlamydia psittaci sepsis in pregnancy. *Q J Med*. **57**: 689-696.

Melgosa, M.P., Kuo, C.C. and Campbell, L.A. (1993) Outer membrane complex proteins of Chlamydia pneumoniae. *FEMS Microbiol Lett*. **112**: 199-204.

Miyashita, N., Matsumoto, A., Fukano, H., Niki, Y. and Matsushima, T. (2001) The 7.5-kb common plasmid is unrelated to the drug susceptibility of Chlamydia trachomatis. *J Infect Chemother*. **7**: 113-116.

Moazed, T.C., Kuo, C.C., Grayston, J.T. and Campbell, L.A. (1998) Evidence of systemic dissemination of Chlamydia pneumoniae via macrophages in the mouse. *J Infect Dis*. **177**: 1322-1325.

Molestina, R.E., Miller, R.D., Lentsch, A.B., Ramirez, J.A. and Summersgill, J.T. (2000) Requirement for NF-kappaB in transcriptional activation of monocyte chemotactic protein 1 by Chlamydia pneumoniae in human endothelial cells. *Infect Immun*. **68**: 4282-4288.

Molestina, R.E., Klein, J.B., Miller, R.D., Pierce, W.H., Ramirez, J.A. and Summersgill, J.T. (2002) Proteomic analysis of differentially expressed Chlamydia pneumoniae genes during persistent infection of HEp-2 cells. *Infect Immun*. **70**: 2976-2981.

Morrison, R.P., Belland, R.J., Lyng, K. and Caldwell, H.D. (1989) Chlamydial disease pathogenesis. The 57-kD chlamydial hypersensitivity antigen is a stress response protein. *J Exp Med*. **170**: 1271-1283.

Moulder, J.W. (1966) The relation of the psittacosis group (Chlamydiae) to bacteria and viruses. *Annu Rev Microbiol*. **20**: 107-130.

Moulder, J.W. (1991) Interaction of chlamydiae and host cells in vitro. *Microbiol Rev*. **55**: 143-190.

Mount, D.T., Bigazzi, P.E. and Barron, A.L. (1973) Experimental genital infection of male guinea pigs with the agent of guinea pig inclusion conjunctivitis and transmission to females. *Infect Immun*. **8**: 925-930.

Murray, E.S. (1964) Guinea Pig Inclusion Conjunctivitis Virus. I. Isolation and Identification as a Member of the Psittacosis-Lymphogranuloma-Trachoma Group. *J Infect Dis*. **114**: 1-12.

Nakajima, K., Nakano, T. and Tanaka, A. (2006) The oxidative modification hypothesis of atherosclerosis: The comparison of atherogenic effects on oxidized LDL and remnant lipoproteins in plasma. *Clin Chim Acta*.

Netea, M.G., Kullberg, B.J., Jacobs, L.E., Verver-Jansen, T.J., van der Ven-Jongekrijg, J., Galama, J.M., *et al* (2004) Chlamydia pneumoniae stimulates IFN-gamma synthesis through MyD88-dependent, TLR2- and TLR4-independent induction of IL-18 release. *J Immunol*. **173**: 1477-1482.

Nurminen, M., Leinonen, M., Saikku, P. and Makela, P.H. (1983) The genus-specific antigen of Chlamydia: resemblance to the lipopolysaccharide of enteric bacteria. *Science*. **220**: 1279-1281.

Nygaard, V., Loland, A., Holden, M., Langaas, M., Rue, H., Liu, F., *et al* (2003) Effects of mRNA amplification on gene expression ratios in cDNA experiments estimated by analysis of variance. *BMC Genomics*. **4**: 11.

Omori, T., Morimoto, K., Harada, Y., Inaba, S., Ishi, I. and Matumoto, M. (1957) Miyagawanella: psittacosis-lymphogramloma group of viruses. I. Excretion of goat pneumonia virus in faeces. *Jap. J. Exp. Med.* **27**: 131-143.

Ostler, H.B., Schachter, J. and Dawson, C.R. (1969) Acute follicular conjunctivitis of epizootic origin. Feline pneumontis. *Arch Ophthalmol*. **82**: 587-591.

Page, L.A. (1966) Revision of the family *Chlamydiaceae* Rake (*Rickettsiales*): unification of the psittacosis-lymphogranuloma venereum- trachoma group of organisms in the genus *Chlamydia* Jones, Rake and Stearns, 1945. *Int. J. Syst. Bacteriol.* **16**: 223-252.

Page, L.A. (1968) Proposal for the recognition of two species in the genus *Chlamydia* Jones, Rake, and Stearns, 1945. *Int. J. Syst. Bacteriol.* **18**: 51-66.

Pantoja, L.G., Miller, R.D., Ramirez, J.A., Molestina, R.E. and Summersgill, J.T. (2000) Inhibition of Chlamydia pneumoniae replication in human aortic smooth muscle cells by gamma interferon-induced indoleamine 2, 3-dioxygenase activity. *Infect Immun*. **68**: 6478-6481.

Pantoja, L.G., Miller, R.D., Ramirez, J.A., Molestina, R.E. and Summersgill, J.T. (2001) Characterization of Chlamydia pneumoniae persistence in HEp-2 cells treated with gamma interferon. *Infect Immun*. **69**: 7927-7932.

Pastorek, J., Pastorekova, S., Callebaut, I., Mornon, J.P., Zelnik, V., Opavsky, R., *et al* (1994) Cloning and characterization of MN, a human tumor-associated protein with a domain homologous to carbonic anhydrase and a putative helix-loop-helix DNA binding segment. *Oncogene*. **9**: 2877-2888.

Patnode, D., S.-P. Wang, and J. T. Grayston. (1990) Persistence of *Chlamydia pneumoniae*, strain TWAR, microimmunofluorescent antibody. In *Seventh International Symposium on Human Chlamydial Infections*. W. R. Bowie, H.D.C., R. P. Jones, P.-A. Mårdh, G. L. Ridgway, J. Schachter, W. E. Stamm, and M. E. Ward (ed.): Cambridge University Press, Cambridge, United Kingdom, pp. 406–409.

Perez-Martinez, J.A. and Storz, J. (1985) Antigenic diversity of Chlamydia psittaci of mammalian origin determined by microimmunofluorescence. *Infect Immun*. **50**: 905-910.

Peters, J., Hess, S., Endlich, K., Thalmann, J., Holzberg, D., Kracht, M., *et al* (2005) Silencing or permanent activation: host-cell responses in models of persistent Chlamydia pneumoniae infection. *Cellular Microbiology*. **7**: 1099-1108.

Pickett, M.A., Ward, M.E. and Clarke, I.N. (1988) High-level expression and epitope localization of the major outer membrane protein of Chlamydia trachomatis serovar L1. *Mol Microbiol*. **2**: 681-685.

Poirier, G.M., Pyati, J., Wan, J.S. and Erlander, M.G. (1997) Screening differentially expressed cDNA clones obtained by differential display using amplified RNA. *Nucleic Acids Res*. **25**: 913-914.

Pospischil, A., Thoma, R., Hilbe, M., Grest, P., Zimmermann, D. and Gebbers, J.O. (2002) Abortion in humans caused by Chlamydophila abortus (Chlamydia psittaci serovar 1). *Schweiz Arch Tierheilkd.* **144**: 463-466.

Puskas, L.G., Zvara, A., Hackler, L., Jr. and Van Hummelen, P. (2002) RNA amplification results in reproducible microarray data with slight ratio bias. *Biotechniques*. **32**: 1330-1334, 1336, 1338, 1340.

Ramsey, D.T. (2000) Feline chlamydia and calicivirus infections. *Vet Clin North Am Small Anim Pract*. **30**: 1015-1028.

Regan, R.J., Dathan, J.R. and Treharne, J.D. (1979) Infective endocarditis with glomerulonephritis associated with cat chlamydia (C. psittaci) infection. *Br Heart J*. **42**: 349-352.

Rockey, D.D., Heinzen, R.A. and Hackstadt, T. (1995) Cloning and characterization of a Chlamydia psittaci gene coding for a protein localized in the inclusion membrane of infected cells. *Mol Microbiol*. **15**: 617-626.

Rockey, D.D., Viratyosin, W., Bannantine, J.P., Suchland, R.J. and Stamm, W.E. (2002) Diversity within inc genes of clinical Chlamydia trachomatis variant isolates that occupy non-fusogenic inclusions. *Microbiology*. **148**: 2497-2505.

Rodolakis, A. and Souriau, A. (1989) Variations in the virulence of strains of Chlamydia psittaci for pregnant ewes. *Vet Rec*. **125**: 87-90.

Rodolakis, A., Bernard, F. and Lantier, F. (1989) Mouse models for evaluation of virulence of Chlamydia psittaci isolated from ruminants. *Res Vet Sci*. **46**: 34-39.

Rothermel, C.D., Rubin, B.Y. and Murray, H.W. (1983) Gamma-interferon is the factor in lymphokine that activates human macrophages to inhibit intracellular Chlamydia psittaci replication. *J Immunol*. **131**: 2542-2544.

Rothfuchs, A.G., Trumstedt, C., Wigzell, H. and Rottenberg, M.E. (2004a) Intracellular bacterial infection-induced IFN-gamma is critically but not solely dependent on Toll-like receptor 4-myeloid differentiation factor 88-IFN-alpha beta-STAT1 signaling. *J Immunol*. **172**: 6345-6353.

Rothfuchs, A.G., Kreuger, M.R., Wigzell, H. and Rottenberg, M.E. (2004b) Macrophages, CD4+ or CD8+ cells are each sufficient for protection against Chlamydia pneumoniae infection through their ability to secrete IFN-gamma. *J Immunol*. **172**: 2407-2415.

Rothfuchs, A.G., Gigliotti, D., Palmblad, K., Andersson, U., Wigzell, H. and Rottenberg, M.E. (2001) IFN-alpha beta-dependent, IFN-gamma secretion by bone marrow-derived macrophages controls an intracellular bacterial infection. *J Immunol*. **167**: 6453-6461.

Rottenberg, M.E., Gigliotti Rothfuchs, A.C., Gigliotti, D., Svanholm, C., Bandholtz, L. and Wigzell, H. (1999) Role of innate and adaptive immunity in the outcome of primary infection with Chlamydia pneumoniae, as analyzed in genetically modified mice. *J Immunol*. **162**: 2829-2836.

Rottenberg, M.E., Gigliotti Rothfuchs, A., Gigliotti, D., Ceausu, M., Une, C., Levitsky, V. and Wigzell, H. (2000) Regulation and role of IFN-gamma in the innate resistance to infection with Chlamydia pneumoniae. *J Immunol*. **164**: 4812-4818.

Rupp, J., Hellwig-Burgel, T., Wobbe, V., Seitzer, U., Brandt, E. and Maass, M. (2005) Chlamydia pneumoniae infection promotes a proliferative phenotype in the vasculature through Egr-1 activation in vitro and in vivo. *Proc Natl Acad Sci U S A*. **102**: 3447-3452.

Saikku, P., Leinonen, M., Mattila, K., Ekman, M.R., Nieminen, M.S., Makela, P.H., *et al* (1988) Serological evidence of an association of a novel Chlamydia, TWAR, with chronic coronary heart disease and acute myocardial infarction. *Lancet*. **2**: 983-986.

Sakash, J.B., Byrne, G.I., Lichtman, A. and Libby, P. (2002) Cytokines induce indoleamine 2,3-dioxygenase expression in human atheroma-asociated cells: implications for persistent Chlamydophila pneumoniae infection. *Infect Immun*. **70**: 3959-3961.

Sayada, C., Denamur, E., Orfila, J., Catalan, F. and Elion, J. (1991) Rapid genotyping of the Chlamydia trachomatis major outer membrane protein by the polymerase chain reaction. *FEMS Microbiol Lett*. **67**: 73-78.

Schachter, J. (1989) Chlamydial infections--past, present, future. *J Am Vet Med Assoc*. **195**: 1501-1506.

Schachter, J., Ostler, H.B. and Meyer, K.F. (1969) Human infection with the agent of feline pneumonitis. *Lancet*. **1**: 1063-1065.

Schachter, J., Stephens, R.S., Timms, P., Kuo, C., Bavoil, P.M., Birkelund, S., *et al* (2001) Radical changes to chlamydial taxonomy are not necessary just yet. *Int J Syst Evol Microbiol*. **51**: 249, 251-243.

Schmid, H., Cohen, C.D., Henger, A., Irrgang, S., Schlondorff, D. and Kretzler, M. (2003) Validation of endogenous controls for gene expression analysis in microdissected human renal biopsies. *Kidney Int*. **64**: 356-360.

Schmittgen, T.D. and Zakrajsek, B.A. (2000) Effect of experimental treatment on housekeeping gene expression: validation by real-time, quantitative RT-PCR. *J Biochem Biophys Methods*. **46**: 69-81.

Shemer, Y. and Sarov, I. (1985) Inhibition of growth of Chlamydia trachomatis by human gamma interferon. *Infect Immun*. **48**: 592-596.

Shi, Y. and Tokunaga, O. (2004) Chlamydia pneumoniae (C. pneumoniae) infection upregulates atherosclerosis-related gene expression in human umbilical vein endothelial cells (HUVECs). *Atherosclerosis*. **177**: 245-253.

Simone, N.L., Bonner, R.F., Gillespie, J.W., Emmert-Buck, M.R. and Liotta, L.A. (1998) Laser-capture microdissection: opening the microscopic frontier to molecular analysis. *Trends Genet*. **14**: 272-276.

Spears, P. and Storz, J. (1979) Biotyping of Chlamydia psittaci based on inclusion morphology and response to diethylaminoethyl-dextran and cycloheximide. *Infect Immun*. **24**: 224-232.

Stamm, W.E. (2000) Potential for antimicrobial resistance in Chlamydia pneumoniae. *J Infect Dis*. **181 Suppl 3**: S456-459.

Stamp, J.T., McEwen, A.D., Watt, J.A.A. and Nisbet, D.I. (1950) Enzootic abortion in ewes. I. Transmission of the disease. *Vet Rec*. **62**: 251-254.

Stephens, R.S., Kalman, S., Lammel, C., Fan, J., Marathe, R., Aravind, L., *et al* (1998) Genome sequence of an obligate intracellular pathogen of humans: Chlamydia trachomatis. *Science*. **282**: 754-759.

Storz, J. (1964) Superinfection of pregnant ewes latently infected with a psittacosis-lymphogranuloma agent. *Cornell Vet*. **53**: 469-480.

Storz, J. (1971) Intestinal chlamydial infections of ruminants. In *Chlamydia and Chlamydia-Induced Diseases.* Thomas, C.C. (ed.) Springfield, Illinois, U.S.A, pp. 146-154.

Storz, J., Baghian, A. and Kousoulas, K.G. (1994) Advances in detection and differentiation of chlamydiae from animals. In *Chlamydial Infections, Proceedings of the Eighth International Symposium on Human Chlamydial Infections*.

Storz, J., Shupe, J.L., James, L.F. and Smart, R.A. (1963) Polyarthritis of Sheep in the Intermountain Region Caused by a Psittacosis-Lymphogranuloma Agent. *Am J Vet Res*. **24**: 1201-1206.

Stothard, D.R., Williams, J.A., Van Der Pol, B. and Jones, R.B. (1998) Identification of a Chlamydia trachomatis serovar E urogenital isolate which lacks the cryptic plasmid. *Infect Immun*. **66**: 6010-6013.

Subtil, A., Delevoye, C., Balana, M.E., Tastevin, L., Perrinet, S. and Dautry-Varsat, A. (2005) A directed screen for chlamydial proteins secreted by a type III mechanism identifies a translocated protein and numerous other new candidates. *Mol Microbiol*. **56**: 1636-1647.

Suchland, R.J., Rockey, D.D., Bannantine, J.P. and Stamm, W.E. (2000) Isolates of Chlamydia trachomatis that occupy nonfusogenic inclusions lack IncA, a protein localized to the inclusion membrane. *Infect Immun*. **68**: 360-367.

Summersgill, J.T., Sahney, N.N., Gaydos, C.A., Quinn, T.C. and Ramirez, J.A. (1995) Inhibition of Chlamydia pneumoniae growth in HEp-2 cells pretreated with gamma interferon and tumor necrosis factor alpha. *Infect Immun*. **63**: 2801-2803.

Suzuki, T., Higgins, P.J. and Crawford, D.R. (2000) Control selection for RNA quantitation. *Biotechniques*. **29**: 332-337.

T'ang, E.-F., Chang, H.-L., Huang, Y.-T. and Wang, K.-C. (1957) Trachoma virus in chick embryo. *National Medical Journal of China*. **43**: 81-85.

Thomson, N.R., Yeats, C., Bell, K., Holden, M.T., Bentley, S.D., Livingstone, M., *et al* (2005) The Chlamydophila abortus genome sequence reveals an array of variable proteins that contribute to interspecies variation. *Genome Res*. **15**: 629-640.

Todorovicc, V., Chen, C.C., Hay, N. and Lau, L.F. (2005) The matrix protein CCN1 (CYR61) induces apoptosis in fibroblasts. *J Cell Biol*. **171**: 559-568.

Toh, H., Miura, K., Shirai, M. and Hattori, M. (2003) In silico inference of inclusion membrane protein family in obligate intracellular parasites chlamydiae. *DNA Res*. **10**: 9-17.

Tripp, B.C., Smith, K. and Ferry, J.G. (2001) Carbonic anhydrase: new insights for an ancient enzyme. *J Biol Chem*. **276**: 48615-48618.

Trogan, E. and Fisher, E.A. (2005) Laser capture microdissection for analysis of macrophage gene expression from atherosclerotic lesions. *Methods Mol Biol*. **293**: 221-231.

Van Gelder, R.N., von Zastrow, M.E., Yool, A., Dement, W.C., Barchas, J.D. and Eberwine, J.H. (1990) Amplified RNA synthesized from limited quantities of heterogeneous cDNA. *Proc Natl Acad Sci U S A*. **87**: 1663-1667.

Vandesompele, J., De Preter, K., Pattyn, F., Poppe, B., Van Roy, N., De Paepe, A. and Speleman, F. (2002) Accurate normalization of real-time quantitative RT-PCR data by geometric averaging of multiple internal control genes. *Genome Biol*. **3**: RESEARCH0034.

Villemonteix, P., Agius, G., Ducroz, B., Rouffineau, J., Plocoste, V., Castets, M. and Magnin, G. (1990) Pregnancy complicated by severe Chlamydia psittaci infection acquired from a goat flock: a case report. *Eur J Obstet Gynecol Reprod Biol*. **37**: 91-94.

Virok, D., Loboda, A., Kari, L., Nebozhyn, M., Chang, C., Nichols, C., *et al* (2003) Infection of U937 monocytic cells with Chlamydia pneumoniae induces extensive changes in host cell gene expression. *J Infect Dis*. **188**: 1310-1321.

Vogelstein, B., Lane, D. and Levine, A.J. (2000) Surfing the p53 network. *Nature*. **408**: 307-310.

Vohra, R.S., Murphy, J.E., Walker, J.H., Ponnambalam, S. and Homer-Vanniasinkam, S. (2006) Atherosclerosis and the Lectin-like OXidized Low-Density Lipoprotein Scavenger Receptor. *Trends Cardiovasc Med*. **16**: 60-64.

Vuola, J.M., Puurula, V., Anttila, M., Makela, P.H. and Rautonen, N. (2000) Acquired immunity to Chlamydia pneumoniae is dependent on gamma interferon in two mouse strains that initially differ in this respect after primary challenge. *Infect Immun*. **68**: 960-964.

Wang, J., Hu, L., Hamilton, S.R., Coombes, K.R. and Zhang, W. (2003) RNA amplification strategies for cDNA microarray experiments. *Biotechniques*. **34**: 394-400.

Wang, S.-P., and J. T. Grayston (1990) Population prevalence of antibody to *Chlamydia pneumoniae,* strain TWAR. In *Seventh International Symposium on Human Chlamydial Infections*. W. R. Bowie, H.D.C., R. P. Jones, P.-A. Mårdh, G. L. Ridgway, J. Schachter, W. E. Stamm, and M. E. Ward (ed.): Cambridge University Press, Cambridge, United Kingdom, pp. 402–405.

Weinstock, H., Dean, D. and Bolan, G. (1994) Chlamydia trachomatis infections. *Infect Dis Clin North Am*. **8**: 797-819.

Whittum-Hudson, J.A., Gerard, H.C., Clayburne, G., Schumacher, H.R. and Hudson, A.P. (1999) A non-invasive murine model of chlamydia-induced reactive arthritis. *Rev Rhum Engl Ed*. **66**: 50S-55S; discussion 56S.

Wilson, M.R. (1963) Isolation of psittacosis-lymphogranuloma venereum group viruses from the faeces of clinically normal cattle in Britain. . *Vet Rec*. **74**: 1430-1431.

Wolf, K., Fischer, E. and Hackstadt, T. (2000) Ultrastructural analysis of developmental events in Chlamydia pneumoniae-infected cells. *Infect Immun*. **68**: 2379-2385.

Worm, H.C., Wirnsberger, G.H., Mauric, A. and Holzer, H. (2004) High prevalence of Chlamydia pneumoniae infection in cyclosporin A-induced post-transplant gingival overgrowth tissue and evidence for the possibility of persistent infection despite short-term treatment with azithromycin. *Nephrol Dial Transplant*. **19**: 1890-1894.

Wu, Q., Ding, W., Mirza, A., Van Arsdale, T., Wei, I., Bishop, W.R.*, et al* (2005) Integrative genomics revealed RAI3 is a cell growth-promoting gene and a novel P53 transcriptional target. *J Biol Chem*. **280**: 12935-12943.

Yang, J., Hooper, W.C., Phillips, D.J., Tondella, M.L. and Talkington, D.F. (2003) Induction of proinflammatory cytokines in human lung epithelial cells during Chlamydia pneumoniae infection. *Infect Immun*. **71**: 614-620.

Zeidler, H., Kuipers, J. and Kohler, L. (2004) Chlamydia-induced arthritis. *Curr Opin Rheumatol*. **16**: 380-392.

13. Supplement

13.1 TABLE S1: RESULTS OF AFFYMETRIX® U133A HUMAN GENOME CHIP COMPARISON ANALYSIS.

The mRNA expression of 66 genes was up- or down-regulated in *C. pneumoniae* productive-infected cells or during IFN-γ-induced persistence in comparison to mock-infected HeLa-cells. All of these 66 genes had signal log ratios greater 1.32 or lower -1.32 and present calls in both samples (treatment versus mock at the corresponding time-point).

Probeset	Gene	Signal Log Ratio
207761_s_at	gb:NM_014033.1 /DEF=Homo sapiens DKFZP586A0522 protein (DKFZP586A0522)	-1.55; -2.19
201626_at	NM_005542: insulin induced gene 1 isoform 1 // NM_198336: isoform 2 // NM_198337: isoform 3	-1.98;-1.67
201627_s_at	gb:NM_005542.1 /DEF=Homo sapiens insulin induced gene 1 (INSIG1)	-1.59;-1.94
218858_at	gb:NM_022783.1 /DEF=Homo sapiens hypothetical protein FLJ12428 (FLJ12428)	-1.42;-1.96
205199_at	gb:NM_001216.1 /DEF=Homo sapiens carbonic anhydrase IX (CA9)	-3.96;-2.99
204298_s_at	NM_002317 // lysyl oxidase preproprotein	-1.7;-1.86
209596_at	gb:AF245505.1 /DEF=Homo sapiens Adlican	-1.79;-1.67
215446_s_at	gb:L16895 /DEF=Human lysyl oxidase (LOX) gene	-2.06;-1.84
212236_x_at	gb:Z19574 /DEF=H.sapiens gene for cytokeratin 17 =Hs.2785 keratin 17	-1.8;-1.95
205157_s_at	gb:NM_000422.1 /DEF=Homo sapiens keratin 17 (KRT17)	-1.68;-2.42
219179_at	gb:NM_016651.2 /DEF=Homo sapiens heptacellular carcinoma novel gene-3 protein (LOC51339)	-1.53;-1.34
221478_at	gb:AL132665.1 /DEF=Homo sapiens mRNA	-1.48;-1.36
201848_s_at	gb:U15174.1 /DEF=Homo sapiens BCL2adenovirus E1B 19kD-interacting protein 3 (BNIP3)	-1.59;-1.71
200632_s_at	gb:NM_006096.1 /DEF=Homo sapiens N-myc downstream regulated (NDRG1)	-2.82;-2.02
210512_s_at	gb:AF022375.1 /DEF=Homo sapiens vascular endothelial growth factor	-1.97;-1.42
203439_s_at	gb:BC000658.1 /DEF=Homo sapiens, stanniocalcin 2	-1.57;-1.44
203574_at	gb:NM_005384.1 /DEF=Homo sapiens nuclear factor, interleukin 3 regulated (NFIL3)	-1.61;-1.4
205194_at	gb:NM_004577.1 /DEF=Homo sapiens phosphoserine phosphatase (PSPH)	-2.26;-1.85
204201_s_at	NM_080683 // protein tyrosine phosphatase, non-receptor type 13 isoform 1 // isoform 2 //isoform 3 // isoform 4 //	-1.72;-1.7
203438_at	gb:AI435828 /FEA=EST /DB_XREF=gi:4305913 /DB_XREF=est:th79e05.x1 /UG=Hs.155223 stanniocalcin 2	-1.37;-1.35
217168_s_at	NM_014685 // homocysteine-inducible, endoplasmic reticulum stress-inducible, ubiquitin-like domain member 1	-1.81;-1.41
218145_at	gb:NM_021158.1 /DEF=Homo sapiens protein kinase domains containing protein similar to phosphoprotein C8FW (LOC57761)	-1.62;-1.82

206085_s_at	gb:NM_001902.1 /DEF=Homo sapiens cystathionase (cystathionine gamma-lyase) (CTH)	-2.17;-1.52
209610_s_at	NM_003038 // solute carrier family 1, member 4 (glutamateneutral amino acid transporter)	-1.77;-1.56
205047_s_at	gb:NM_001673.1 /DEF=Homo sapiens asparagine synthetase (ASNS)	-2.19;-2.17
217127_at	gb:AL354872 /DEF=Human DNA sequence from clone RP11-42O15 on chromosome 1. Contains the CTH gene for two isoforms of cystathionase (cystathionine gamma-lyase) and a CHORD containing protein 1 (CHP1) pseudogene	-2.51;-1.95
202308_at	gb:NM_004176.1 /DEF=Homo sapiens sterol regulatory element binding transcription factor 1 (SREBF1)	-1.43;-1.52
204284_at	Hs.303090 protein phosphatase 1, regulatory (inhibitor) subunit 5 /FL=gb:NM_005398.1,NM_005398 // protein phosphatase 1, regulatory (inhibitor)	-1.86;-1.51
222303_at	UG=Hs.292477 ESTs,AY216265 // Homo sapiens ETS2 intronic transcript 1	-1.48;-1.47
219764_at	gb:NM_007197.1 /DEF=Homo sapiens frizzled (Drosophila) homolog 10 (FZD10)	-1.57;-1.42
44783_s_at	NM_012258 // hairy/enhancer-of-split related with YRPW motif 1	-2.07;-1.88_-2.29;-2.51
204698_at	gb:NM_002201.2 /DEF=Homo sapiens interferon stimulated gene (20kD) (ISG20)	1.76;1.91
204747_at	gb:NM_001549.1 /DEF=Homo sapiens interferon-induced protein with tetratricopeptide repeats 4 (IFIT4)	1.41;1.7
205552_s_at	gb:NM_002534.1 /DEF=Homo sapiens 2,5-oligoadenylate synthetase 1 (40-46 kD) (OAS1)	1.79;1.71
218943_s_at	gb:NM_014314.1 /DEF=Homo sapiens RNA helicase (RIG-I), DEAD/H (Asp-Glu-Ala-Asp/His) box polypeptide RIG-I	1.92;1.94
210163_at	gb:AF030514.1 /DEF=Homo sapiens interferon stimulated T-cell alpha chemoattractant	1.93;1.75
204952_at	gb:NM_014400.1 /DEF=Homo sapiens GPI-anchored metastasis-associated protein homolog (C4.4A)	2.54;2.43
205660_at	gb:NM_003733.1 /DEF=Homo sapiens 2-5oligoadenylate synthetase-like (OASL)	2.38;2.46
202581_at	gb:NM_005346.2 /DEF=Homo sapiens heat shock 70kD protein 1B (HSPA1B)	3.77;3.17
201324_at	gb:NM_001423.1 /DEF=Homo sapiens epithelial membrane protein 1 (EMP1)	1.53;1.57
200799_at	gb:NM_005345.3 /DEF=Homo sapiens heat shock 70kD protein 1A (HSPA1A)	3.37;2.86
200800_s_at	gb:NM_005345.3 /DEF=Homo sapiens heat shock 70kD protein 1A (HSPA1A)	3.85;3.56
213051_at	NM_020119 // zinc finger antiviral protein isoform 1	1.77;2.06
219863_at	gb:NM_016323.1 /DEF=Homo sapiens cyclin-E binding protein 1 (LOC51191)	1.34;2.21
205483_s_at	gb:NM_005101.1 /DEF=Homo sapiens interferon-stimulated protein, 15 kDa (ISG15)	1.89;1.78

210797_s_at	gb:AF063612.1 /DEF=Homo sapiens 2-5oligoadenylate synthetase-related protein p30 (OASL)	2.48;2.64
214453_s_at	Consensus includes gb:NM_006417.1 /DEF=Homo sapiens interferon-induced, hepatitis C-associated microtubular aggregate protein (44kD) (MTAP44)	2.44;2.31
211122_s_at	gb:AF002985.1 /DEF=Homo sapiens putative alpha chemokine (H174)	1.51;2.02
214059_at	gb:BE049439 /FEA=EST /DB_XREF=gi:8366494 /DB_XREF=est:xw86e11.x1 interferon-induced, hepatitis C-associated microtubular aggregate protein (44kD)	1.7;2.13
203153_at	gb:NM_001548.1 /DEF=Homo sapiens interferon-induced protein with tetratricopeptide repeats 1 (IFIT1)	2.09;2.05
216804_s_at	gb:AK027217.1 Homo sapiens cDNA: NM_006457 // LIM protein (similar to rat protein kinase C-binding enigma)	1.44;1.48
220104_at	gb:NM_020119.1 /DEF=Homo sapiens hypothetical protein FLB6421 (FLB6421), NM_024625 // zinc finger antiviral protein isoform 2	1.66;1.92
201939_at	gb:NM_006622.1 /DEF=Homo sapiens serum-inducible kinase (SNK), gb:AF223574.1,NM_006622: polo-like kinase 2 (PLK2)	1.89;2.27
204897_at	gb:AA897516 /Hs.199248 prostaglandin E receptor 4 (subtype EP4) ,NM_000958 // prostaglandin E receptor 4, subtype EP4	1.46;1.95
201694_s_at	gb:NM_001964.1 /DEF=Homo sapiens early growth response 1 (EGR1)	2.3;1.73
210764_s_at	gb:AF003114.1 /DEF=Homo sapiens CYR61, Hs.8867 cysteine-rich, angiogenic inducer, 61	2.52;2.04
208892_s_at	gb:BC003143.1 /DEF=Homo sapiens, dual specificity phosphatase 6	1.8;1.6
202644_s_at	gb:NM_006290.1 /DEF=Homo sapiens tumor necrosis factor, alpha-induced protein 3 (TNFAIP3)	1.39;1.98
209101_at	gb:M92934.1 /DEF=Human connective tissue growth factor	2.38;1.98
217997_at	AF220656 // Homo sapiens apoptosis-associated nuclear protein PHLDA1 (PHLDA1)	1.81;1.7
204420_at	NM_005438 // FOS-like antigen 1	1.73;1.77
204948_s_at	gb:NM_013409.1 /DEF=Homo sapiens follistatin (FST)	1.38;1.66
207345_at	gb:NM_006350.2 /DEF=Homo sapiens follistatin (FST)	1.55;1.42
203108_at	gb:NM_003979.2 /DEF=Homo sapiens retinoic acid induced 3 (RAI3)	1.91;1.42_1.46;1.77
206924_at	gb:NM_000641.1 /DEF=Homo sapiens interleukin 11 (IL11)	2.38;2.45_1.58;1.52
204602_at	gb:NM_012242.1 /DEF=Homo sapiens dickkopf (Xenopus laevis) homolog 1 (DKK1)	1.99;2.08_1.81;2.02

13.2 TABLE S2: ALTERED GENE EXPRESSION DATA FOR SELECTED AFFYMETRIX® HG-U133A PROBE SETS.

All of these 19 genes were selected for real-time two-step RT-PCR analysis. Expression changes between two arrays are designated as "fold change" (treatment versus mock at the corresponding time-point). Depicted are the mean fold changes (D = decrease, I = increase) of two independent microarray experiments of *C. pneumoniae*-infected HeLa-cells (24h Cpn = productive infection) in the IFN-γ persistence model (24h and 96h Cpn+IFN-γ). All selected genes had signal log ratios greater 1.32 or lower -1.32 ($\alpha 1 = 0.05$; $\alpha 2 = 0.065$; $\tau = 0.015$) and present calls in both samples.

Gene	Probe Set	Accession Number	Mean Fold Change (n = 2) 24h Cpn	24h Cpn+IFN-γ	96h Cpn+IFN-γ
Homo sapiens 2'-5'oligoadenylate synthetase-like (OASL)	205660_at	NM_198213		I (5.35)	
Homo sapiens 2'-5'oligoadenylate synthetase-like (OASL)	210797_s_at	NM_198213		I (5.90)	
Homo sapiens Adlican	209596_at	AF245505.1			D (3.32)
Homo sapiens BCL2 adenovirus E1B 19kD-interacting protein 3 (BNIP3)	221478_at	NM_004052			D (2.68)
Homo sapiens BCL2 adenovirus E1B 19kD-interacting protein 3 (BNIP3)	201848_s_at	NM_004052			D (3.14)
Homo sapiens carbonic anhydrase IX (CA9)	205199_at	NM_001216			D (11.12)

Homo sapiens cystathionase (cystathionine gamma-lyase) (CTH)	206085_s_at	NM_001902		D (3.59)	
Homo sapiens cystathionase (cystathionine gamma-lyase) (CTH)	217127_at	NM_001902		D (4.69)	
Homo sapiens cysteine-rich, angiogenic inducer, 61 (CYR61)	210764_s_at	AF003114.1	I (4.86)		
Homo sapiens Dapper homolog 1 (DACT1)	219179_at	NM_016651			D (2.70)
Homo sapiens dickkopf (Xenopus laevis) homolog 1 (DKK1)	204602_at	NM_012242	I (4.10)		I (3.77)
Homo sapiens hairy/enhancer-of-split related with YRPW motif 1 (HEY1)	44783_s_at	NM_012258	D (3.93)	D (5.28)	
Homo sapiens heat shock 70kD protein 1A (HSPA1A)	200799_at	NM_005345		I (8.66)	

Homo sapiens heat shock 70kD protein 1A (HSPA1A)	200800_s_at	NM_005345		I (13.04)	
Homo sapiens heat shock 70kD protein 1B (HSPA1B)	202581_at	NM_005346		I (11.08)	
Homo sapiens insulin induced gene 1 (INSIG1)	201626_at	NM_005542	D (3.54)		
Homo sapiens insulin induced gene 1 (INSIG1)	201627_s_at	NM_005542	D (3.40)		
Homo sapiens interferon-induced, hepatitis C-associated microtubular aggregate protein (44kD) (MTAP44 or IFI44)	214453_s_at	NM_006417		I (5.19)	
Homo sapiens interferon-induced, hepatitis C-associated microtubular aggregate protein (44kD) (MTAP44 or IFI44)	214059_at	NM_006417		I (3.77)	
Homo sapiens keratin 17 (KRT17)	212236_x_at	NM_000422			D (3.67)

Homo sapiens keratin 17 (KRT17)	205157_s_at	NM_000422			D (4.14)
Homo sapiens lysyl oxidase (LOX) gene	215446_s_at	L16895			D (3.86)
Homo sapiens N-myc downstream regulated (NDRG1)	200632_s_at	NM_006096			D (5.35)
Homo sapiens prostaglandin E receptor 4 (subtype EP4) (PTGER4)	204897_at	NM_000958			I (3.26)
Homo sapiens retinoic acid induced 3 (RAI3)	203108_at	NM_003979	I (3.17)	I (3.06)	
Homo sapiens serum-inducible kinase (SNK) or polo-like kinase 2 (PLK2)	201939_at	NM_006622			I (4.23)

13.3 TABLE S3: TAQMAN PRIMER AND PROBE SEQUENCES.

Primers and probes were designed using the Primer Express® software (version 1.0; Applied Biosystems). TaqMan probes were labeled at the 5' end with the reporter dye molecule FAM (emission wavelength, 518 nm) and at the 3' end with the black hole quencher dye BHQ1.

Gene	Forward Primer	Reverse Primer	TaqMan Probe
Dapper homolog 1 (DACT1)	ACC TGA GAC TGG ATG TAG AAA AGA CA	GGA TCC TGA AGC CCC ATC A	CAG ACA GTC GGC CTA GCT CAG GGT TTT ATG
BCL2 adenovirus E1B 19kD-interacting protein 3 (BNIP3)	TGG ACG GAG TAG CTC CAA GAG	CAA TGC TAT GGG TAT CTG TTT CAG A	CCT CGC TCG CAG ACA CCA CAA G
2'-5'-oligoadenylate synthetase-like (OASL)	TGG AGC TGG TGG CGT TTC	GCT TTG CCA CAT GGT TTT CC	AGC CAA GCA TCA CAA AGA TGT TCT GA
Heat shock 70kDa protein 1B (HSPA1B)	GCG TGA TGA CTG CCC TGA T	CGC CCT CGT ACA CCT GGA T	ATC CCC ACC AAG CAG ACG CAG ATC TT
Heat shock 70kD protein 1A (HSPA1A)	CCA CCA AGC AGA CGC AGA T	AAG CGC CCC AAC AGA TTG T	CCT ACT CCG ACA ACC AAC CCG GG
Insulin induced gene 1 (Insig1)	TCG ACA GTC ACC TCG GAG AAC	CAA TTT AGC ACT GGC GTG GTT	AAG AGA GAA TGG GCC AGT GTC ATG CG
Keratin 17 (KRT17)	GAG CCG CAT CCT CAA CGA	TCG CGG TTC AGT TCC TCT GT	AGG ATG CCG AGG ATT GGT TCT TCA GC
Cysteine-rich, angiogenic inducer, 61 (CYR61)	CAG GAC GGC CTC CTT GGT A	TTC AGT GAG CTG CCT TTT CCA	CGA GGT GGA GTT GAC GAG AAA CAA TG
TATA-Box binding protein (TBP)	TTC GGA GAG TTC TGG GAT TGT A	TGG ACT GTT CTT CAC TCT TGG C	CCG TGG TTC GTG GCT CTC TTA TCC TCA
β-glucuronidase (GUS)	GAA AAT ATG TGG TTG GAG AGC TCA TT	CCG AGT GAA GAT CCC CTT TTT A	CCA GCA CTC TCG TCG GTG ACT GAC TGT TCA
18S rRNA	ACG GCT ACC ACA TCC AAG GA	CCA ATT ACA GGG CCT CGA AA	CAG GCG CGC AAA TTA CCC ACT CC

13.4 TABLE S4: TAQMAN PRE-DEVELOPED ASSAY REAGENTS (APPLIED BIOSYSTEMS)

Gene	Assay Number
Carbonic anhydrase IX (CA9)	Hs00154208_m1
N-myc downstream regulated (NDRG1)	Hs00608389_m1
Adlican	Hs00377849_m1
Lysyl oxidase (LOX)	Hs00184700_m1
Hairy/enhancer-of-split related with YRPW motif 1 (HEY1)	Hs00232618_m1
Retinoic acid induced 3 (RAI3)	Hs00173681_m1
Dickkopf (Xenopus laevis) homolog 1 (DKK1)	Hs00183740_m1
Serum-inducible kinase (SNK) or polo-like kinase 2 (PLK2)	Hs00198320_m1
prostaglandin E receptor 4 (PTGER4)	Hs00168761_m1
cystathionase (cystathionine gamma-lyase, CTH)	Hs00542276_m1
interferon-induced, hepatitis C-associated microtubular aggregate protein (44kD) (MTAP44 or IFI44)	Hs00197427_m1

13.5 FIGURE S1: RESULT OF BLAST ANALYSIS

Blast analysis of the sequenced real-time HSPA1-PCR-product based on the Affymetrix probe target region was performed using the online tool on http://www.ncbi.nlm.nih.gov/BLAST

Homo sapiens heat shock 70kDa protein 1B (HSPA1B), mRNA

Length = 2512; Score = 228 bits (115), Expect = 7e-58; Identities = 115/115 (100%)

Strand = Plus / Minus

```
Query: 1    ttggcgtccagccacgagatgacctcttgacacttgtccagaaccttcttcttgtccgcc 60
            ||||||||||||||||||||||||||||||||||||||||||||||||||||||||||||
Sbjct: 1955 ttggcgtccagccacgagatgacctcttgacacttgtccagaaccttcttcttgtccgcc 1896

Query: 61   tcgctgatcttgcccttgagcccctcatcctccacggcgctcttcatgttgaagg 115
            |||||||||||||||||||||||||||||||||||||||||||||||||||||||
Sbjct: 1895 tcgctgatcttgcccttgagcccctcatcctccacggcgctcttcatgttgaagg 1841
```

Ich will mich fügen
und halten still
und mich begnügen:
"Wie Gott es will."

Ich will nicht fragen:
"Warum dies mir?"
Du wirst mich tragen,
mein Gott, zu Dir.

Und mag zerbrechen
die ganze Welt,
So darf ich sprechen:
"Wie's Gott gefällt."

Ich bin geborgen,
oh sel'ger Stand,
so heut wie morgen
in Gottes Hand.

(Gerhard Fritzsche)